

RICE UNIVERSITY

Multiscale Strategies for Cartilage Repair

by

Sriram Venkata Eleswarapu

A THESIS SUBMITTED
IN PARTIAL FULFILLMENT OF THE
REQUIREMENTS FOR THE DEGREE

Doctor of Philosophy

APPROVED, THESIS COMMITTEE:


Kyriacos Athanasiou, Ph.D., Thesis Director
Distinguished Professor
Department of Biomedical Engineering
University of California, Davis


Antonios Mikos, Ph.D., Committee Chair
Louis Calder Professor
Department of Bioengineering
Rice University


Jun Lou, Ph.D.
Assistant Professor
Department of Mechanical Engineering
Rice University

HOUSTON, TEXAS
OCTOBER 2011

Abstract

Multiscale Strategies for Cartilage Repair

by

Sriram Venkata Eleswarapu

This thesis uses a multiscale approach to identify and manipulate physiologic and *in vitro* developmental milieus towards the functional repair of articular cartilage. The overarching goals of this work are to improve knowledge of cartilage physiology and to enhance functional engineering of biologic cartilage replacements. Towards this end, assessment and modulation of cartilage phenotype were undertaken at multiple levels of complexity: gene transcription, cytoskeletal architecture, ion channels, single cells, extracellular matrix, intact tissue, and the whole joint.

The first part of this thesis focused on probing cartilage phenotype at the single cell level. A quantitative single cell gene expression assay was developed and used to quantify cell-to-cell variability and the chondrocyte response to growth factors. Next, the viscoelastic compressive properties of single chondrocytes were measured and compared to cytoskeleton organization before and after growth factor exposure. It was found that growth factors increased matrix gene expression and induced cell stiffening in a time- and cartilage zone-dependent manner.

The second part of this thesis investigated the modulation of the chondrocyte microenvironment for enhanced cartilage tissue engineering. Tissue

constructs were grown *in vitro* using a chondrocyte self-assembly process. In one study, it was found that TRPV4 ion channel activation significantly increased cartilage matrix production and improved tensile properties in self-assembled constructs. In a second study, constructs were exposed to static or dynamic application of hypo-osmotic and hyper-osmotic stress. Static application of hyper-osmotic stress was found to improve construct compressive and tensile properties, and their corresponding biochemical mediators, significantly. A third study showed that treatment of constructs with ribose, an agent used for non-enzymatic glycation, produced enhanced tissue mechanics and biochemistry in a time-dependent manner.

The third part of this thesis describes efforts to improve the potential clinical translatability of *in vitro* cartilage repair strategies. A technique was developed to decellularize xenogenic self-assembled constructs. Decellularization resulted in histologic and biochemical cell depletion with maintenance of tissue mechanical properties. Additionally, a comprehensive characterization of the major tissues of the immature knee joint revealed and reinforced important structure-function relationships that will inform future cartilage repair strategies.

The total body of work contained in this thesis contributes significantly both to a basic understanding of cartilage physiology as well as to evolving strategies for cartilage repair. This thesis advances the field of cartilage tissue engineering by examining chondrocyte phenotype, the cell and tissue microenvironment, and avenues for clinical translation.

Acknowledgments

The body of work presented in this document represents only a fraction of the journey it concludes. I have been lucky during the course of this journey to have the support of wonderful mentors, colleagues, friends, and family. I am thankful to all who have stood by me during this time of tremendous personal and academic growth.

I would first like to thank Dr. Kyriacos Athanasiou for his invaluable mentorship over the past decade. He has provided me with countless opportunities to mature as an individual and as a scientist, and I am forever grateful for his support and encouragement. I look forward to the next stage of our friendship.

I would also like to thank the other members of my thesis committee, Dr. Tony Mikos and Dr. Jun Lou. Dr. Mikos' achievements have inspired me ever since my first days as an undergraduate at Rice University, and I am grateful to call him a teacher and mentor. I am thankful to Dr. Lou for serving on my committee and supporting my graduate education even while I relocated to California to complete my research.

During my years in the lab, I have been fortunate to work with outstanding colleagues and true friends. Chief among them is Donald Responde, who has been both a good friend and a scientific partner in crime. It has been a pleasure working alongside Donald over these last few years, and I am grateful that we were able to share our frustrations and celebrate our successes together. I am also thankful to have a friend in Dena Wiltz. Though she stayed in Texas when

Donald and I moved to California, she has always been a vital part of my graduate school experience.

I learned a great deal from the guidance and support of those who preceded me as graduate students in the lab. This thesis is a testament to their generosity. Dr. Jerry Hu provided important insight on my early research projects in the laboratory. I would like to thank Drs. Adrian Shieh and Nic Leipzig for their scientific contributions to the single cell project, and Dr. Benjamin Elder for pursuing decellularization and inviting me to collaborate with him. Thanks also to Drs. Roman Natoli and Chris Revell, who were important sounding boards as I worked to master the self-assembly process and learn the complex functional assays that dominate the majority of this thesis. I am also grateful for opportunities to talk shop and develop scientific ideas with Drs. Eugene Koay, Vince Willard, Johannah Sanchez-Adams, and Dan Huey.

I am thankful to a number of people at the University of California, Davis, for their collaboration and friendship. Drs. Hari Reddi and Leigh Griffiths have been important advisors. Dr. Grayson DuRaine is one of the most resourceful and persistent scientists I have ever met. Maelene Wong has been a good friend and an exemplar of good laboratory technique. Thanks also to Pasha Hadidi and Justin Chen for fruitful scientific discussions.

I am fortunate to be a student in the Medical Scientist Training Program at Baylor College of Medicine. I would like to thank Dr. Sharon Plon, Dr. Xander Wehrens, Kathy Crawford, Vanessa Hatfield, and Krista Defalco from the program for their strong continued support as I pursue my career goals as a

physician-scientist. Thanks also to the other members of my MD/PhD cohort, in particular Joe Doherty and Dr. David Simons, for their friendship during this long slog through medical and graduate school.

I am lucky to have friends who have been sources of great relief from the demands of research. There are too many to name individually, but I am especially thankful to Dr. Matt Oertli, who has been like a brother to me since we first met in college. I am glad he moved to California for residency; these past two years have been a worthy recapitulation of our time as college roommates. I also want to thank Rosey Hall for her support and encouragement, as well as Eric Rosenquist and Daniel Lenhoff for serving as intellectual foils on every subject under the sun. I am forever grateful for their friendship. Also, though it might be considered slightly unorthodox, I would be remiss not to mention Ira Glass, Terry Gross, Jad Abumrad, and Robert Krulwich: they kept me sane and functioning during countless several-night stretches of working (and sleeping) in the lab.

Finally, I am nothing without the love and support of my family. I owe all my accomplishments to them. Thanks to Dad, Mom, Shree, Anil, Rajosri, and Loveraj for everything.

Table of Contents

Abstract	ii
Acknowledgments	iv
Table of Contents	vii
List of Figures	xi
List of Tables	xii
Introduction	1
Motivation	2
Global objective	2
<i>Specific aim 1</i>	3
<i>Specific aim 2</i>	3
<i>Specific aim 3</i>	4
Overview of thesis chapters.....	6
Chapter 1. Articular cartilage structure, function, and disease	10
Abstract.....	11
Articular cartilage composition	11
Tissue organization.....	12
Material properties and mechanical function	13
Pathophysiology of osteoarthritis	14
Clinical and economic burden.....	16
Tissue engineering of articular cartilage	17
Chapter 2. Gene expression of single articular chondrocytes	19
Abstract.....	20
Introduction	21
Materials and methods	24
<i>Tissue harvest and cell seeding</i>	24
<i>Growth factor treatment</i>	25
<i>Single chondrocyte isolation</i>	25
<i>RNA isolation and real-time RT-PCR</i>	26
<i>Evaluation of GAPDH as a housekeeping gene</i>	27
<i>Relative abundance</i>	28
<i>Statistics</i>	28
Results	29
<i>Phase I: Influence of cartilage zone and seeding time</i>	29
<i>Phase II: Effects of seeding time and IGF-I on middle/deep cells</i>	30
Discussion.....	31

Chapter 3. Effects of growth factors on the biomechanics and cytoskeleton of single chondrocytes	44
Abstract.....	45
Introduction	46
Materials and methods	50
<i>Cell culture</i>	<i>50</i>
<i>Growth factor treatment</i>	<i>51</i>
<i>Single cell creep testing</i>	<i>51</i>
<i>Determination of single chondrocyte material properties</i>	<i>52</i>
<i>Fluorescence microscopy: F-actin staining</i>	<i>54</i>
<i>Gene expression of β-Actin</i>	<i>55</i>
<i>Data/statistical analysis</i>	<i>57</i>
Results	57
<i>Viscoelastic properties</i>	<i>57</i>
<i>Actin staining/fluorescent intensity</i>	<i>59</i>
<i>β-actin gene expression</i>	<i>60</i>
Discussion.....	61
Chapter 4. TRPV4 channel activation improves the tensile properties of self-assembled cartilage.....	75
Abstract.....	76
Introduction	77
Materials and methods	80
<i>Chondrogenic medium</i>	<i>80</i>
<i>Chondrocyte isolation.....</i>	<i>81</i>
<i>Preparation of agarose wells for construct self-assembly.....</i>	<i>81</i>
<i>Self-assembly of cartilage constructs.....</i>	<i>81</i>
<i>Phase I: Evaluation of time windows for TRPV4 activation.....</i>	<i>82</i>
<i>Phase II: TRPV4 activation versus Na⁺/K⁺ pump inhibition</i>	<i>82</i>
<i>Gross morphology and specimen portioning.....</i>	<i>83</i>
<i>Biochemical analysis.....</i>	<i>84</i>
<i>Tensile testing</i>	<i>84</i>
<i>Creep indentation testing</i>	<i>85</i>
<i>Statistical analysis.....</i>	<i>85</i>
Results	86
<i>Phase I: Evaluation of time windows for TRPV4 activation.....</i>	<i>86</i>
<i>Phase II: TRPV4 activation versus Na⁺/K⁺ pump inhibition</i>	<i>87</i>
Discussion.....	89
Chapter 5. Osmotic loading of self-assembled articular cartilage	99
Abstract.....	100
Introduction	101
Materials and methods	103
<i>Medium formulations.....</i>	<i>103</i>
<i>Chondrocyte isolation.....</i>	<i>104</i>
<i>Preparation of agarose wells for construct self-assembly.....</i>	<i>104</i>
<i>Self-assembly and osmotic loading of cartilage constructs.....</i>	<i>105</i>

<i>Gross morphology and histology</i>	106
<i>Quantitative biochemistry</i>	106
<i>Creep indentation testing</i>	107
<i>Tensile testing</i>	107
<i>Statistical analysis</i>	108
Results.....	109
<i>Gross appearance and histology</i>	109
<i>Quantitative biochemistry</i>	109
<i>Biomechanical evaluation</i>	110
<i>Correlation analysis</i>	110
Discussion.....	111
Chapter 6. Temporal assessment of ribose treatment on self-assembled cartilage	123
Abstract.....	124
Introduction.....	125
Materials and methods.....	128
<i>Media formulations</i>	128
<i>Chondrocyte isolation</i>	129
<i>Preparation of agarose wells for construct self-assembly</i>	129
<i>Self-assembly and culture of cartilage constructs</i>	130
<i>Gross morphology and histology</i>	131
<i>Quantitative biochemistry</i>	131
<i>Creep indentation testing</i>	132
<i>Tensile testing</i>	132
<i>Statistical analysis</i>	133
Results.....	133
<i>Gross appearance and histology</i>	133
<i>Quantitative biochemistry</i>	134
<i>Biomechanics</i>	135
Discussion.....	136
Chapter 7. Decellularization of tissue engineered cartilage	145
Abstract.....	146
Introduction.....	147
Materials and methods.....	149
<i>Chondrocyte isolation and seeding</i>	149
<i>Decellularization phase I</i>	150
<i>Decellularization phase II</i>	151
<i>Histology</i>	151
<i>Quantitative biochemistry</i>	151
<i>Indentation testing</i>	152
<i>Tensile testing</i>	152
<i>Statistical analysis</i>	153
Results.....	153
<i>Gross appearance and histology</i>	153
<i>Quantitative biochemistry</i>	154

<i>Biomechanical evaluation</i>	156
Discussion.....	157
Chapter 8. Structure-function relationships in the immature knee joint....	173
Abstract.....	174
Introduction	175
Materials and methods	179
<i>Tissue harvest and specimen preparation</i>	179
<i>Histology</i>	180
<i>Quantitative biochemistry</i>	180
<i>High performance liquid chromatography (HPLC)</i>	181
<i>Tensile testing</i>	181
<i>Statistical analysis</i>	182
Results	182
<i>Histology</i>	182
<i>Collagen content</i>	183
<i>Pyridinoline crosslink content</i>	183
<i>Tensile properties</i>	184
Discussion.....	185
Conclusions	194
Context.....	195
Chondrocyte physiology	195
Cellular microenvironment and self-assembly	200
Improving clinical translatability	205
Significance	209
References	210

List of Figures

Figure 1-1. Multiscale strategies for cartilage repair	5
Figure 2-1. Single cell approach.....	38
Figure 2-2. Phase I GAPDH mRNA abundance.....	39
Figure 2-3. Phase I superficial zone gene expression results	40
Figure 2-4. Phase I middle/deep zone gene expression results	41
Figure 2-5. Phase II gene expression results	42
Figure 3-1. Viscoelastic creep response of a single chondrocyte	68
Figure 3-2. Viscoelastic properties of single articular chondrocytes	69
Figure 3-3. Fluorescence images of each treatment group (100X).....	70
Figure 3-4. Fluorescence intensity of F-actin	71
Figure 3-5. β -actin mRNA abundance.....	72
Figure 3-6. Mechanical and growth factor stimulation in single cells	73
Figure 4-1. Phase I tensile properties of cartilage constructs	96
Figure 4-2. Phase II gross morphology of tissue engineered constructs	97
Figure 4-3. Phase II tensile properties of cartilage constructs	98
Figure 5-1. Gross morphology and histology of self-assembled constructs	120
Figure 5-2. GAG content and compressive stiffness of constructs	121
Figure 5-3. Collagen and tensile properties of self-assembled constructs	122
Figure 6-1. Gross morphology and histology of self-assembled constructs	141
Figure 6-2. GAG content and compressive stiffness of constructs	142
Figure 6-3. Collagen and tensile properties of self-assembled constructs	143
Figure 7-1. Histology for Phase I.....	167
Figure 7-2. Histology for Phase II.....	168
Figure 7-3. DNA content of constructs following decellularization in phase I....	169
Figure 7-4. DNA content of constructs following decellularization in phase II...	170
Figure 7-5. Construct properties following decellularization in phase I	171
Figure 7-6. Construct properties following decellularization in phase II	172
Figure 8-1. Continuum of knee joint connective tissues	190
Figure 8-2. Histology of representative joint tissues.....	191
Figure 8-3. Collagen and pyridinoline content of joint tissues	192
Figure 8-4. Tensile properties of joint tissues.....	193

List of Tables

Table 2-1. Sequences for real-time RT-PCR target genes	43
Table 3-1. Experimental design.....	74
Table 4-1. Growth metrics of tissue engineered constructs.	94
Table 4-2. Biochemical content of tissue engineered constructs.	95
Table 5-1. Growth metrics of self-assembled constructs	117
Table 5-2. Biochemical analysis of self-assembled constructs	118
Table 5-3. Pairwise correlations between biomechanics and biochemistry	119
Table 6-1. Growth metrics and biochemical content of constructs.....	144
Table 7-1. Phase I Construct wet weight and thickness values	163
Table 7-2. Phase II construct wet weight and thickness values	164
Table 7-3. Values for Poisson ratio and permeability from Phase I	165
Table 7-4. Values of Poisson ratio and permeability from Phase II.....	166

Introduction

The Fabric of Joints in the Human Body is a Subject so much the more entertaining, as it must strike every one that considers it attentively with an Idea of fine mechanical Composition. Wherever the Motion of one Bone upon another is requisite, there we find an excellent Apparatus for rendering that Motion safe and free... the articulating Cartilages...

... If we consult the standard Chirurgical Writers from Hippocrates down to the present Age, we shall find, that an ulcerated Cartilage is universally allowed to be a very troublesome Disease; that it admits of a Cure with more Difficulty than carious Bone; and that, when destroyed, it is not recovered.

William Hunter (1718-1783)

Of the Structure and Diseases of Articulating Cartilages [115]

Motivation

Nearly three centuries have passed since the pioneering anatomist and surgeon William Hunter marveled at the structure-function relationships of articular cartilage and remarked on the vexing problem of cartilage disease. To this day, articular cartilage degeneration remains an irreversible process that leads inexorably to pain and disability and contributes substantially to soaring health care costs among a rapidly aging population. There is tremendous clinical need for suitable replacements for damaged cartilage, and the field of tissue engineering aspires to address this challenge. The studies documented in this thesis are motivated by a need to improve our understanding of cartilage physiology, as well as to develop strategies to improve the functional engineering of biologic cartilage replacements.

Global objective

The overall objective of the work described in this thesis was to use a multiscale approach to identify and manipulate physiologic and *in vitro* developmental milieus towards the functional repair of articular cartilage. It was hypothesized that phenotypic assessment or modulation at multiple levels of complexity – i.e., gene transcription, cytoskeletal architecture, ion channels, single cells, the extracellular matrix, intact tissue, and the whole joint – would reveal salient intervention targets in the development of strategies for cartilage repair. To evaluate this global hypothesis, three specific aims were employed (Figure 1-1).

Specific aim 1

The first specific aim was to probe cartilage phenotype at the single cell level. A single cell gene expression assay was developed to examine the effects of attachment time, chondral zone, and growth factors on articular chondrocytes. Fluorescent staining and unconfined compression were also performed to determine how growth factors affect intracellular organization and chondrocyte material properties. It was hypothesized that chondrocytes would exhibit zone- and time-dependent phenotypic changes detectable at the single cell level in response to growth factor exposure.

Specific aim 2

The second specific aim was to modulate the chondrocyte microenvironment for enhanced cartilage tissue engineering. Three-dimensional tissue constructs were engineered *in vitro* from articular chondrocytes using a self-assembly process. These self-assembled constructs served as a model system to evaluate the effects of biochemical and biophysical stimuli on engineered cartilage. Ion channel activation, osmotic stress, and non-enzymatic glycation were evaluated separately to determine whether self-assembled constructs would respond with increased matrix biosynthesis and improvements in compressive and tensile properties. It was hypothesized that exposure to these biochemical and biophysical stimuli during *in vitro* tissue development would enhance extracellular matrix production and mechanical integrity in engineered constructs.

Specific aim 3

The third specific aim was to improve the potential clinical translatability of *in vitro* cartilage repair strategies. The first goal of this specific aim was to establish an optimal method for the decellularization of xenogenic cartilage. Decellularization techniques were tested on self-assembled constructs in an effort to rid the tissue of antigenic nuclear material. It was hypothesized that an optimal decellularization regimen could be identified that would not compromise tissue mechanical properties. The second goal of this specific aim was to conduct a comprehensive characterization of the whole knee joint to establish benchmarks for future repair strategies that must necessarily engage not just the surfaces of joints, but also the fibrocartilage, tendon, and ligament tissues that act in concert to support the kinematics of the normal joint. This study involved a thorough assessment of the tensile properties, collagen content, and pyridinoline crosslink abundance of all the major connective tissues of the immature knee joint. It was hypothesized that a precise elucidation of tissue composition would unveil important structure-function relationships to be applied in future tissue engineering efforts.

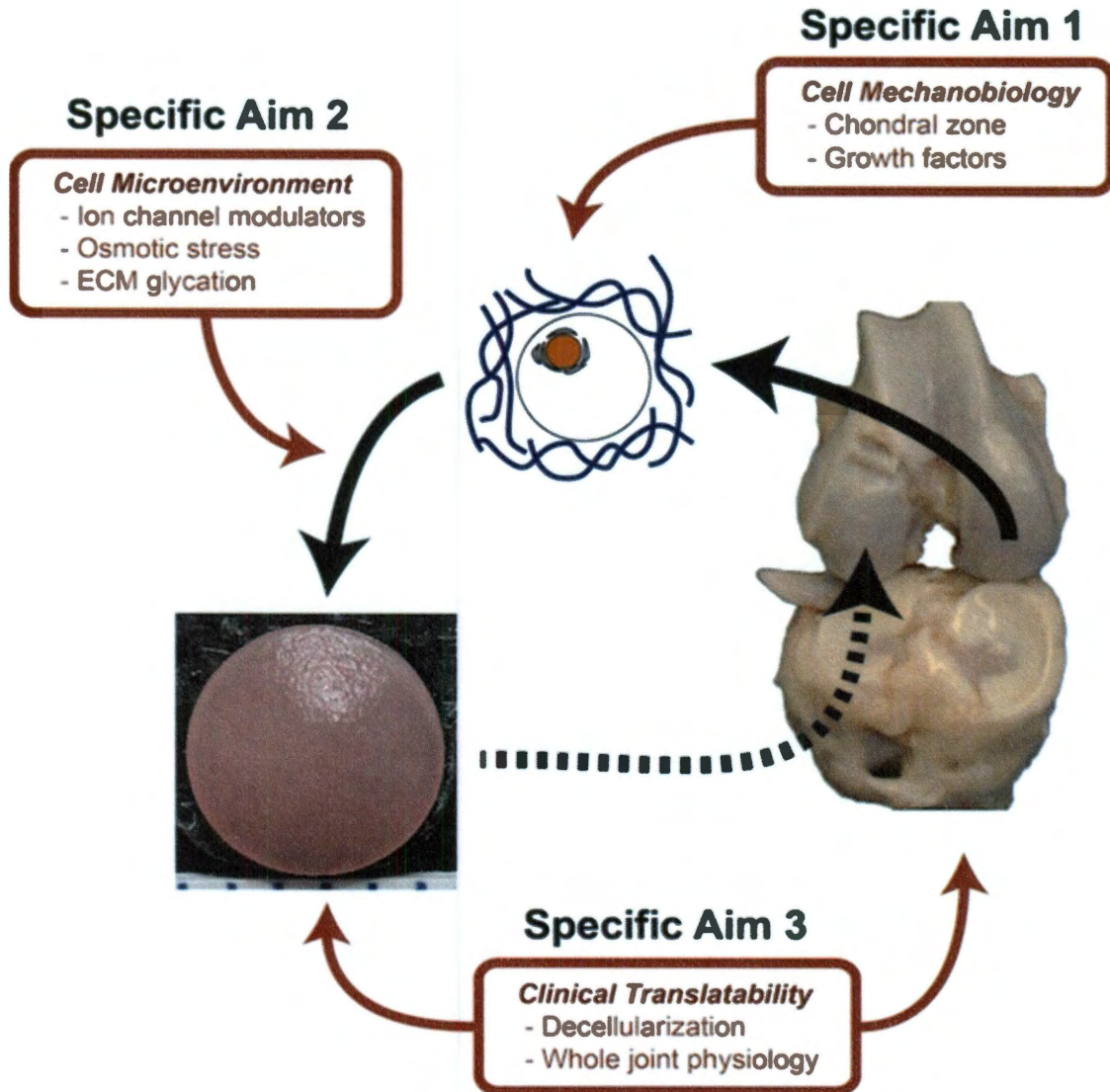


Figure 1-1. Multiscale strategies for cartilage repair

An illustration of the overall design of this thesis, which consists of three specific aims that employ intervention and assessment at the nuclear, cellular, matrix, tissue, and whole joint levels.

Overview of thesis chapters

The chapters that comprise this thesis are constructed to provide the reader with an understanding of current knowledge in the field, descriptions of study designs, comprehensive accounts of experimental methods, complete presentations of qualitative and quantitative results, and, finally, thorough discussions of the data and their implications for future investigations. An overview of the logical structure of this thesis follows below.

Chapter 1 briefly reviews articular cartilage anatomy, physiology, and pathophysiology, as well as the clinical and economic burden of degenerative joint disease. This chapter serves as a background and motivation for the rest of the thesis by describing both the structure-function relationships within articular cartilage and the devastating consequences of osteoarthritis. After Chapter 1, the remainder of this thesis presents specific details and results of experiments performed to address the following global objective: to use a multiscale approach to identify and manipulate physiologic and *in vitro* developmental milieus towards the functional repair of articular cartilage.

Chapters 2 and 3 describe studies that together comprise the first specific aim, which was to probe cartilage phenotype at the single cell level. Chapter 2 details the development of a real-time RT-PCR assay to quantify gene expression in single chondrocytes. This assay was used to quantify cell-to-cell variability in gene expression, and well as to examine the influence of seeding time, chondral zone, and growth factors on the gene expression of important anabolic and catabolic ECM proteins. Chapter 3 presents an in-depth

investigation of single cell structure-function relationships. Chondrocytes from different zones were exposed to growth factors, and assessments were performed on chondrocyte gene expression, cytoskeleton architecture, cell morphology, and material properties. Unconfined compression was used to determine the viscoelastic properties of single chondrocytes, and fluorescent staining was performed to assess changes in cytoskeleton organization. The real-time single cell RT-PCR assay developed as part of Chapter 2 was used in Chapter 3 to evaluate changes in the gene expression of an important chondrocyte structural protein. Taken together, these chapters exploring the phenotype of the single chondrocyte set the stage for further work on the role of the cellular microenvironment in cartilage homeostasis.

Chapters 4, 5, and 6 together constitute the second specific aim, which was to modulate the chondrocyte microenvironment for enhanced cartilage tissue engineering. For the studies described in these three chapters, tissue constructs were grown *in vitro* using the self-assembly process, in which articular chondrocytes are seeded at a high density into non-adherent, cylindrical molds. These chondrocytes condense into free-floating, disc-shaped constructs that then proceed to synthesize ECM that resembles articular cartilage found *in vivo*. Chapter 4 describes a study in which the Ca²⁺-permeable transient receptor potential vanilloid 4 (TRPV4) ion channel was activated *in situ* to examine whether modulating intracellular ion concentrations would result in tissue-level changes in the biochemical content and mechanical properties of self-assembled constructs. Chapter 5 presents a study in which self-assembled constructs were

exposed to hypo-osmotic and hyper-osmotic stress, either in static or dynamic conditions. This head-to-head comparison of static versus dynamic, hypo-osmotic versus hyper-osmotic loading demonstrated that an optimal osmotic regimen can be employed to enhance tissue engineered cartilage. Chapter 6 details a study in which ribose, an agent known for its propensity to initiate non-enzymatic glycation of collagen, was used to improve construct biochemical and biomechanical properties. An optimal treatment time window was determined for which construct functional properties experienced the greatest improvement, and the study showed that non-enzymatic glycation is an effective method for enhancing tissue engineering strategies that does not pose a risk for cytotoxicity *in vitro*. Altogether, the studies presented in Chapters 4, 5, and 6 establish powerful methods for producing tissue engineered cartilage with robust biochemical and biomechanical properties.

Chapters 7 and 8 constitute the third specific aim, which was to improve the potential clinical translatability of *in vitro* cartilage repair strategies. Chapter 7 describes a two-phased study for optimizing the decellularization of xenogenic self-assembled articular cartilage constructs. The first phase of the study was a head-to-head comparison of various decellularization regimens selected from the literature for other tissue types. Based on this comparison, one agent was selected that provided the optimal combination of histologic decellularization, biochemical decellularization, and maintenance of tissue functional properties. The second phase of the study examined various durations of treatment with the agent selected in the first phase. This study showed that there exists an ideal

intervention window during which tissue can be decellularized without loss of important extracellular matrix content. Finally, Chapter 8 presents a study in which all the major tissues of the immature bovine knee joint were assessed in terms of histology, collagen content, crosslink abundance, and tensile properties. The goal of this study was to establish biochemical and biomechanical benchmarks for future work on engineering cartilage and other tissues for eventual integration into the whole, intact joint. This study examined condylar cartilage, patellar cartilage, medial and lateral menisci, cranial and caudal cruciate ligaments (analogous to anterior and posterior cruciate ligaments in humans), medial and lateral collateral ligaments, and patellar ligament. Results from the study reinforced structure-function relationships within the joint and provided important data on immature tissue properties.

The cumulative knowledge established by this thesis is summarized in the Conclusions chapter. Results are evaluated in the context of the global objective of the thesis. Implications of the data and important recommendations for future work are discussed.

**Chapter 1. Articular cartilage structure, function,
and disease**

Abstract

Articular cartilage lines the surfaces of long bones and serves an important role in normal joint mechanics. The cells that give rise to cartilage are called chondrocytes. The majority of the tissue is made up of an extracellular matrix (ECM) comprised largely of collagen type II and proteoglycans, a specialized glycoprotein consisting of long chains of glycosaminoglycans (GAG) linked to a core protein. Together, the presence and organization of collagen and GAG give rise to the tensile and compressive properties of the tissue, respectively. Cartilage pathophysiology involves the destruction of ECM and, in some cases, phenotypic alteration of chondrocyte metabolism. The inflammatory changes that arise from this degradation comprise osteoarthritis, a disease of considerable economic and clinical burden. The field of tissue engineering aims to alleviate this burden by developing biologic materials *in vitro* to replace damaged cartilage *in vivo*. A self-assembly process has emerged as one strategy to engineer cartilage replacements *in vitro*.

Articular cartilage composition

Articular cartilage is a glistening tissue found at the articulating surfaces of diarthrodial joints. Its major functions are to provide lubrication and distribute loads during joint motion. Structurally, articular cartilage is an avascular, hypocellular tissue composed of a copious extracellular matrix (ECM) [7, 14, 28, 51]. The sole cell type found within healthy articular cartilage is the chondrocyte, which makes up approximately 1-5% of the tissue [9, 93]. Produced by and

surrounding these chondrocytes is an ECM rich in collagen type II and proteoglycans, the latter of which is made up of long, unbranched, highly charged chains of glycosaminoglycans (GAG) covalently linked to a core protein [93, 171, 188]. In terms of quantitative biochemical content, collagen comprises approximately 15-22% of the tissue's wet weight, and GAG comprises 4-7% [7]. The remaining wet weight of the tissue is made up of water, which is retained within the ECM by fixed negative charges along GAG chains. The strong attraction between GAG chains and water produces a cellular osmotic microenvironment that can be very different from other tissues in the body [25]; these mechanical and osmotic milieus within cartilage are profoundly important for chondrocyte homeostasis. Because the tissue lacks a vascular supply, chondrocytes are adapted to a low nutrient, hypoxic setting [9]; however, fluid flow is essential for nutrient transfer within the tissue. As described in the following sections, alterations in the mechanical or osmotic environment of the tissue can have deleterious effects on chondrocyte metabolism and ECM homeostasis, which can manifest as pathologic changes at the tissue level.

Tissue organization

In terms of tissue organization, articular cartilage is characterized by a zonal architecture. It can be divided into four distinct zones: superficial, middle, deep, and calcified [106]. Each zone has been shown to vary in terms of ECM composition, biosynthesis, gene expression, chondrocyte morphology, and mechanical properties [17, 54, 199, 239, 240]. Differences across zones have

also been observed in mechanical properties at the level of the single chondrocyte [130, 207, 209-211]. Additionally, one particularly important structural feature that varies between zones is the orientation of the network of collagen type II [24, 151, 243]. In the superficial zone, collagen is aligned parallel to the articulating surface of the tissue. In the middle zone, collagen is organized randomly. In the deep zone, collagen is largely oriented in struts perpendicular to the subchondral bone. This differential organization confers distinct zone-dependent mechanical properties that allow proper mechanical function *in vivo* [181]; for example, during joint motion, the superficial zone experiences considerable shear stress, whereas the deep zone resists significant compressive loads .

Material properties and mechanical function

As an orthopaedic tissue, articular cartilage plays a vital role in biomechanics. Proper joint function depends on normal cartilage anatomy and physiology. To this end, the tissue's physiologic behavior is often defined in terms of its material properties. In compressive deformation, articular cartilage is described under linear biphasic theory to have three material properties [155]: aggregate modulus (i.e., compressive stiffness), permeability (i.e., resistance to fluid flow), and Poisson's ratio (a ratio of lateral to axial deformation). The compressive properties of the tissue are understood to arise primarily from its GAG content. Due to a dense concentration of negative charges within sulfated GAG chains, the tissue exerts an attractive pull on cations, thereby creating a positive osmotic

pressure that causes swelling [124]. During compressive deformation, the interstitial water supports the majority of the initial load, and friction between the water and ECM helps to transmit and dissipate forces [108, 218]. Equilibrium is reached when the osmotic pressure equals the load, and removal of the load causes fluid to return into the tissue.

In tension, under principles of linear elasticity [118], articular cartilage is described by its Young's modulus (i.e., tensile stiffness), ultimate tensile strength (i.e., maximum stress before tissue failure), and Poisson's ratio. The tensile properties of cartilage are conferred by the dense network of collagen type II in its ECM [181]. This tensile integrity depends on collagen fibril diameter and on crosslinks between collagen molecules within the helical collagen fibril. During tissue maturation, crosslinks form between collagen molecules as a result of both enzymatic and non-enzymatic processes [74-76, 181]; these crosslinks serve to provide even greater tensile stiffness and strength by reinforce the collagen network.

Pathophysiology of osteoarthritis

In large part because articular cartilage is avascular and hypocellular, the tissue suffers from an intrinsic inability to repair itself after injury [116]. Damage wrought by trauma or arthritis is therefore irreversible and leads inexorably to pain and disability [28]. In cases where focal defects in the cartilage surface communicate with medullary bone, mesenchymal progenitors from the bone marrow can elicit a healing response [14, 83]; however, this process generally results in formation of

a mechanically inferior tissue that resembles fibrocartilage, which is high in collagen type I rather than type II and relatively poor in GAG [38]. Because this repair tissue is insufficient to endure the physiologic demands inherent to proper cartilage function, further biomechanical breakdown occurs, leading to a cycle of degenerative changes that precipitate the onset of osteoarthritis.

In osteoarthritis, chondrocyte metabolism and ECM biosynthesis cannot keep pace with tissue degradation [3]. A combination of biomechanical and biochemical processes contribute to this breakdown. As suggested above, biomechanical degradation of the tissue results from altered joint anatomy. Risk for cartilage degeneration rises considerably for patients who suffer a traumatic injury to another tissue within the joint – for example, a tear in the knee meniscus, or a rupture of the anterior cruciate ligament [139]. These injuries prevent normal joint mechanics. Even temporarily altered joint kinematics can have devastating consequences on cartilage survival [28, 29]. Osteoarthritis is characterized by changes at the cell, ECM, and gross macroscopic levels. At the cell level, chondrocyte metabolism transitions from anabolic to catabolic synthesis, prioritizing the secretion of pro-inflammatory cytokines and matrix metalloproteinases (MMP) [4, 107]. At the ECM level, the architecture of the collagen network begins to change [91, 144], and loss of GAG ensues, resulting in decreased tissue hydration from the reduction in fixed charge density [144, 145]. Grossly, cartilage ravaged by osteoarthritis is characterized by surface roughening and abrasions, fissures, and discoloration [32, 60].

Clinical and economic burden

Conditions afflicting the orthopaedic soft tissues, including osteoarthritis and traumatic injury, result in substantial healthcare costs and work-related disability. The prevalence and severity of orthopaedic conditions result in annual costs of \$510 billion [1], of which osteoarthritis alone contributes to \$60 billion [30], figures which are expected to increase as the population ages. For osteoarthritis alone, which can arise as a result of injury to any of these tissues [139], it is projected that 67 million individuals will be diagnosed by 2030 [101]. Osteoarthritis is also associated with a significant reduction in quality of life due to disabling pain and limited physical function [179, 180]. This immobility often leads to an indolent lifestyle that precipitates obesity, diabetes, and heart disease, and other co-morbidities.

Patients with signs and symptoms of osteoarthritis are typically treated conservatively at first, receiving physical therapy [5], medication for pain relief and, later, anti-inflammatory drugs or injections. However, these therapies cannot arrest or reverse the degenerative changes wrought by osteoarthritis. When pain becomes debilitating, a patient's only recourse is surgical intervention [45]. In general, surgery offers significant improvements in quality of life, but not all patients qualify for surgery; the decision to operate is often guided by patient age and co-morbidities [184, 219, 247]. Moreover, surgical treatments such as total joint replacement are highly invasive, require extensive recovery and rehabilitation times, and may often involve costly revision surgeries [164]. Biological treatments such as autografts and allografts present additional

challenges such as secondary surgeries, immunogenicity [20], and limited cell sources.

Tissue engineering of articular cartilage

There is tremendous clinical need for suitable replacements for damaged articular cartilage. Tissue engineering has emerged as an attractive strategy for growing cartilage within a laboratory for later implantation into patients. A chief obstacle to successful orthopaedic tissue engineering, however, is that the tissue must possess robust biochemical and biomechanical properties that will allow it to thrive in the demanding loading environment of the intact joint [35, 89]. Towards this end, strategies have focused on functional tissue engineering, wherein optimizing the biomechanical function of engineered constructs is an overriding priority. The canonical paradigm in functional tissue engineering is to seed cells onto three-dimensional biomaterial scaffolds, then treat these developing constructs with exogenous stimuli, such as bioactive agents or mechanical bioreactors [66].

Some strategies in cartilage tissue engineering depart from the classical paradigm by eliminating the use of a scaffold [105, 178, 203]. In particular, our laboratory has developed an approach termed the self-assembly process, wherein chondrocytes are seeded at a high density into non-adherent, shape-specific molds fabricated from 2% agarose. Within a few hours, the cells condense into a tightly-packed, three-dimensional mass. Over the course of the following days and weeks, the cells secrete a cartilage-specific ECM, high in

collagen type II and GAG. The self-assembly process is associated with high N-cadherin expression and recapitulates features of *in vivo* cartilage development, such as early pericellular localization of collagen type VI [163]. A key advantage of cartilage self-assembly is that, because it does not involve the use of a biomaterial scaffold, it circumvents the typical challenges associated with scaffold use, such as toxicity, biodegradability, stress shielding, and diminished juxtacrine and paracrine signaling [105]. Another salient benefit is that, since it is a strictly cell-mediated phenomenon, it can serve as a model system for examining the direct effects of biochemical [68, 158, 160] and biophysical [62, 64, 67] stimuli on cell physiology and *in vitro* ECM development.

Although progress has been made in identifying beneficial stimuli for self-assembly, the functional properties of self-assembled cartilage constructs still fall short of native tissue values. Therefore, it is imperative that additional treatment modalities be evaluated. Motivated both by clinical need and scientific challenge, the work described in this thesis examines cartilage physiology and *in vitro* development at multiple levels of complexity.

Chapter 2. Gene expression of single articular chondrocytes^{*}

^{*} Chapter published as **Eleswarapu SV**, Leipzig ND, and Athanasiou KA, "Gene expression of single articular chondrocytes," *Cell and Tissue Research* 2007.

Abstract

While previous studies in the field of tissue engineering provide important information about articular cartilage, their conclusions are based on population averages and do not account for variations in cell subpopulations. To obtain a precise understanding of chondrocytes, we investigated the effects of cartilage zone and seeding duration on single chondrocyte gene expression to select an optimal zone for tissue engineering (Phase I), followed by an evaluation of growth factor exposure on the zone selected in Phase I (Phase II). In Phase I, superficial and middle/deep bovine articular chondrocytes were seeded in monolayer for 3 or 18 h. In Phase II, middle/deep chondrocytes (selected in Phase I) received 100 ng/ml IGF-I for 3 h. Real-time RT-PCR was used to quantify GAPDH abundance and the relative abundances of aggrecan, collagens I and II, cartilage oligomeric matrix protein (COMP), matrix metalloproteinase-1 (MMP-1), and tissue inhibitor of metalloproteinase-1 (TIMP-1). GAPDH varied zonally, but neither time nor IGF-I had an effect, suggesting that GAPDH is a suitable housekeeping gene for comparisons within each zone, but not across zones. IGF-I increased expression of aggrecan ($p=0.0003$) and collagen II ($p<0.0001$) in middle/deep chondrocytes seeded for 18 h. TIMP-1 expression increased with time in control cells ($p<0.03$), suggesting that chondrocytes enter a matrix protective state after seeding. IGF-I diminished this effect ($p<0.03$), suggesting that treatment with IGF-I refocuses chondrocytes on matrix production rather than on protection from metalloproteinases. Concomitant to increasing TIMP-1, MMP-1 was detectable by 18 h in superficial cells, providing

further evidence of a trend toward matrix degradation with time. Collagen I was undetected in all cells, and no differences were observed for COMP, confirming that no dedifferentiation or osteoarthritic changes occurred. Taken together, these results establish a unique understanding of individual chondrocyte behavior.

Introduction

Articular cartilage is an avascular tissue with a zonal architecture that serves to reduce frictional loading conditions at joint surfaces. The low cellularity and absence of vasculature limits the capacity for damaged cartilage to regenerate [129]. Cartilage tissue engineering has shown exciting potential for solving the problem of regenerating articular cartilage for patients with focal cartilage lesions or osteoarthritis. Several strategies have been developed for engineering functional articular cartilage *in vitro*, but they fall short in achieving the characteristics of native cartilage. A better understanding of chondrocyte biology is needed to tailor more successful strategies for cartilage tissue engineering.

Structurally, articular cartilage can be divided into four distinct zones: superficial, middle, deep, and calcified. Zonal differences in extracellular matrix composition, biosynthesis, gene expression, cell morphology, and mechanical properties have been well documented [17, 54, 199, 239, 240]. Differences in mechanical properties across zones have also been observed at the level of the single chondrocyte [209]. However, the precise phenotypic differences between

zones must be studied more thoroughly at the cellular level to illuminate their consequences for cartilage tissue engineering strategies.

Despite an abundance of studies on the effects of growth factors on chondrocyte proliferation and biosynthesis, no study to date has examined the fundamental response of an individual chondrocyte to growth factor stimuli. Previous studies have examined responses of chondrocyte populations to different environmental conditions, but these studies do not take into account variations among subpopulations of cells, or among single cells. In particular, insulin-like growth factor-I (IGF-I) has shown remarkable promise in stimulating matrix synthesis, increased proliferation, and maintenance of phenotype [22, 23, 52, 55, 87, 147, 228], but further study of chondrocyte behavior is warranted to determine whether the documented effects of IGF-I can be resolved at the single cell level, or if those effects are simply representative of differences in subpopulations *in vitro*.

In response to the need for further investigation of chondrocyte behavior, a single cell approach has been proposed and implemented [206]. Briefly, chondrocytes are exposed to a variety of physical or biochemical stimuli, and then examined for changes in gene expression to ascertain the immediate downstream effects of the particular stimuli. While considerable progress has been made on the characterization of single chondrocyte biomechanics [121, 130-132, 209], this study is the first to examine the direct effects of environmental conditions on the fundamental biological response of single chondrocytes. Our experimental approach (Figure 2-1) was divided into two phases. In Phase I, we

sought to determine the effects of cartilage zone and seeding duration on the gene expression of single chondrocytes. Specifically, the objective of Phase I was to determine the cartilage zone from which chondrocytes are best suited for tissue engineering efforts by analyzing the expression of genes associated with anabolic, catabolic, and dedifferentiation processes in zonal chondrocytes. This objective is in line with our efforts to define a more successful strategy for the tissue engineering of articular cartilage, for which a principal aim is to utilize highly metabolically active chondrocytes to recapitulate the matrix-rich architecture found *in vivo*. Our initial expectation for Phase I was that chondrocytes from the middle/deep zone would be found to be best suited for tissue engineering applications, since it has been shown that progressively deeper layers of cartilage are more metabolically active and biosynthetic than superficial layers [17, 54, 239, 240]. In Phase II, we examined the influence of IGF-I exposure and seeding time on chondrocytes from the zone selected in Phase I. In particular, the objective of Phase II was to assess the optimal condition for which expression of matrix proteins increased and catabolic molecules decreased. Since monolayer culture is associated with dedifferentiation [197], we sought to determine phenotypic changes that may occur on a short time scale; such changes could have important consequences for tissue engineering modalities.

Real-time reverse transcription-polymerase chain reaction (RT-PCR) was used in Phase I to determine the effects of seeding time (3 or 18 h) on chondrocytes from both zones, and in Phase II to determine the combinatorial

effects of growth factor exposure (100 ng/ml IGF-I) and seeding time (3 or 18 h) on chondrocytes from the zone selected in Phase I. The overall hypothesis of this study was that chondrocytes would exhibit zone- and time-dependent differences in gene expression, as well as increased expression of matrix proteins and decreased expression of catabolic molecules in response to growth factor exposure. Moreover, we expected cells to retain major characteristics of primary chondrocytes and exhibit little dedifferentiation.

Materials and methods

Tissue harvest and cell seeding

Articular chondrocytes were harvested aseptically from distal metatarsal cartilage of one-year-old steers obtained from local abattoirs. The top 10-20% of the joint surface, identified as superficial zone tissue, was removed by drawing a scalpel blade firmly across the cartilage. The remaining uncalcified cartilage was removed and identified as middle/deep zone tissue. Previous work in our laboratory has demonstrated that this zonal abrasion technique successfully separates zonal tissue [54]. Harvested tissue was minced into small fragments and placed in a solution of 2 mg/ml collagenase type II (Worthington) in supplemented Dulbecco's modified Eagle medium (DMEM) containing 10% fetal bovine serum (FBS), 100 U/ml penicillin-streptomycin, 0.25 mg/ml fungizone and 0.1 mM non-essential amino acids (NEAA) (Invitrogen) for 6 h with continuous stirring at 37°C and 10% CO₂. After digestion, the resulting cell suspensions were pelleted, with the supernatants removed. Superficial zone chondrocytes and

middle/deep zone chondrocytes were resuspended and plated separately onto a tissue culture treated plastic dish. Seeding was confined to a 2 cm diameter circular area using silicone isolators (PGC Scientifics) to yield an approximate areal cell density of 3.3×10^4 cells/cm². The plates were incubated for either 3 or 18 h at 37°C and 10% CO₂.

Growth factor treatment

After determining which zonal population was more metabolically active and thus better suited for tissue engineering (Phase I), Phase II focused on testing the effects of IGF-I. For both cell seeding durations (3 and 18 h), a single zonal population of chondrocytes was exposed to either no growth factor (control) or 100 ng/ml IGF-I for the final 3 h of attachment, so that IGF-I exposure time was identical for both seeding durations. IGF-I was obtained from PeproTech Inc. This concentration of IGF-I represented a saturation concentration, as determined by values reported in the literature [52, 87, 244].

Single chondrocyte isolation

After cell attachment, the media was removed and the culture dish was filled with fresh supplemented DMEM containing 30 mM HEPES buffer (Fisher Scientific) warmed to 37°C to sustain the culture in ambient laboratory conditions. IGF-I was included in the fresh media for the IGF-I treated groups. Chondrocytes were captured using a glass micropipette pulled and microforged to an inner diameter of approximately 15 µm and a CellTram Vario hydraulic microaspirator

(Eppendorf). Firmly attached single cells were collected by gentle suction pressure. Captured cells were then ejected into lysis buffer (Stratagene) for RNA isolation.

RNA isolation and real-time RT-PCR

Total RNA was isolated from single chondrocytes using the Absolutely RNA Nanoprep protocol (Stratagene) with DNase I treatment. The purified total RNA for each chondrocyte was eluted into a volume of 8 µl for the RT reaction. Single cell RNA was incubated with 1 mM dNTPs, 0.5 µM oligo(dT)₂₀ primers, and 0.5 µM random hexamers for 5 min at 65°C to anneal primers to the template RNA, followed by addition of buffer, 2.5 mM MgCl₂, 1 mM dithiothreitol (DTT), SuperScript III RT enzyme (Invitrogen), and RNase inhibitor for 10 min at 25°C for further primer annealing, 50 min at 50°C for reverse transcription, and 5 min at 85°C to terminate the reaction. Gene expression was assayed using multiplex real-time PCR performed on a Rotor-Gene 3000 (Corbett Research) with HotStarTaq polymerase (Qiagen), 5 mM MgCl₂, and 2.5 mM dNTPs. The HotStarTaq polymerase was activated at 95°C for 15 min, followed by 55 cycles of 95°C for 15 s and 60°C for 30 s. Fluorescence measurements (on Cy5, FAM, and ROX) were taken every cycle at the end of the 60°C step to provide a quantitative, real-time analysis of the genes analyzed. Primers were synthesized by Sigma-Genosys (Woodlands), and gene-specific hydrolysis probes were synthesized by Biosearch Technologies (Novato). Primer and probe sequences and concentrations for aggrecan, collagen I, collagen II, and glyceraldehyde 3-

phosphate dehydrogenase (GAPDH) were used as reported previously [52]. The oligonucleotide sequences for cartilage oligomeric matrix protein (COMP), matrix metalloproteinase-1 (MMP-1), and tissue inhibitor of metalloproteinase-1 (TIMP-1) are provided in Table 2-1. These were designed from bovine mRNA sequences from the National Center for Biotechnology Information (NCBI). Three separate PCR reactions were performed on each single cell cDNA sample: (1) aggrecan / collagen II / GAPDH, (2) collagen I / COMP / GAPDH, and (3) MMP-1 / TIMP-1 / GAPDH.

Evaluation of GAPDH as a housekeeping gene

GAPDH abundance was determined quantitatively from real-time PCR. The threshold cycle (C_T) for GAPDH in each single cell cDNA sample was determined at 20% of the maximum of the second derivative of fluorescence with respect to cycle number, as determined by comparative quantitation analysis in the Rotor-Gene 6.0 program. Efficiency of the PCR was calculated by running a standard curve for serially diluted cDNA from large populations of bovine chondrocytes. Abundance values (A) were determined using a method adapted from Pfaffl [169]. Briefly, A is determined as follows, where E is primer efficiency:

$$A = \frac{1}{(1 + E)^{C_T}}$$

Higher abundance values indicate that the gene is expressed to a greater extent than genes with lower abundance values.

Relative abundance

Relative abundance for each gene of interest was normalized using GAPDH to account for variations in the overall transcriptional level in individual cells, as well as for minor errors in pipetting and RNA isolation. Genes of interest were aggrecan, collagen I, collagen II, COMP, MMP-1, and TIMP-1. The C_T for each gene of interest was calculated as described for GAPDH. Relative abundance (R) of each gene of interest (GOI) was calculated from E and C_T :

$$R_{GOI} = \frac{(1 + E_{GAPDH})^{C_{T,GAPDH}}}{(1 + E_{GOI})^{C_{T,GOI}}}$$

Relative abundance values greater than 1.0 indicate that the gene of interest is expressed to a greater extent than GAPDH.

Statistics

All results are reported as mean \pm standard deviation. Abundance and relative abundance data were checked for normal distribution with statistical measures in JMP IN 5.1 (SAS Institute) before linear statistics were performed with JMP. For Phase I, the effects of cartilage zone (superficial vs. middle/deep) and seeding time (3 h vs. 18 h) on the abundance of GAPDH and the relative abundances of genes of interest were tested with two-factor ANOVA. For Phase II, a single zonal population was selected to test the effects of seeding time (3 h vs. 18 h) and growth factor exposure (control vs. 100 ng/ml IGF-I) on the abundance of GAPDH and the relative abundances of genes of interest with two-factor ANOVA. If a significant difference ($p < 0.05$) was found, a *post-hoc* analysis using Tukey's

Honestly Significant Difference (HSD) was performed to test significance for all comparisons.

Results

Phase I: Influence of cartilage zone and seeding time

It was found that all abundance and relative abundance data exhibited a log-normal distribution; therefore all statistics were performed with log transformed data. Data on GAPDH abundance are presented in Figure 2-2. No significant difference in GAPDH expression was found from 3 h to 18 h, but cartilage zone emerged as a significant factor for GAPDH abundance ($p < 0.0001$). As a consequence of the zonal variation in GAPDH abundance results, relative abundance comparisons can be made within each zone, but not across zones. Superficial zone relative abundance results are presented in Figure 2-3. In superficial cells, TIMP-1 expression approximately tripled from 3 h to 18 h ($p < 0.03$) (Figure 2-3C). Concurrently, MMP-1 was undetectable at 3 h but was detected at 18 h (Figure 2-3D). No significant differences were found for superficial cells in the relative abundances of aggrecan, collagen II, or COMP over time. Middle/deep zone relative abundance results are presented in Figure 2-4. In middle/deep cells, collagen II significantly decreased from 3 h to 18 h by approximately 60% ($p < 0.05$) (Figure 2-4B). TIMP-1 expression approximately tripled from 3 h to 18 h (Figure 2-4C). However, no significant differences were found in aggrecan, COMP, or MMP-1 relative abundances from 3 h to 18 h. Collagen I expression was not detected in any middle/deep or superficial cells.

GAPDH abundance was three times greater in middle/deep chondrocytes compared to superficial chondrocytes. Due to this increased metabolic activity, middle/deep chondrocytes were selected for Phase II of this study.

Phase II: Effects of seeding time and IGF-I on middle/deep cells

Data in Phase II were collected separately from Phase I, and statistics were performed on log transformed data to provide a Gaussian distribution. GAPDH abundance was not found to be significantly different across treatment groups within the middle/deep zone. GAPDH abundance results were as follows for middle/deep chondrocytes: at 3 h, control cells were $3.8 \times 10^{-10} \pm 2.9 \times 10^{-10}$ and IGF-I treated cells were $3.4 \times 10^{-10} \pm 2.5 \times 10^{-10}$, while at 18 h, control cells were $5.0 \times 10^{-10} \pm 2.7 \times 10^{-10}$ and IGF-I treated cells were $4.5 \times 10^{-10} \pm 3.4 \times 10^{-10}$. Therefore, relative abundance comparisons can be made across treatments for all genes of interest. For aggrecan relative abundance, seeding time ($p=0.0002$) and IGF-I treatment ($p<0.002$) were significant factors. On post-hoc analysis, the interaction of seeding time and IGF-I treatment revealed that aggrecan relative abundance in middle/deep chondrocytes treated with IGF-I and seeded for 18 h was significantly different from all other groups ($p=0.0003$), with expression approximately six times the average of the other groups (Figure 2-5A). Seeding time alone was significant for collagen II relative abundance in middle/deep chondrocytes ($p<0.006$). Additionally, collagen II relative abundance in middle/deep chondrocytes treated with IGF-I and seeded for 18 h was significantly different from all other groups ($p<0.0001$), with expression

approximately three times the average of the other groups, as revealed by post-hoc analysis on the interaction of seeding time and IGF-I treatment (Figure 2-5B). Other significant differences among treatment groups for collagen II relative abundance are noted in Figure 2-5B. For TIMP-1 relative abundance, seeding time ($p < 0.0001$) and IGF-I treatment ($p < 0.01$) were significant factors. On post-hoc analysis, the interaction of seeding time and IGF-I treatment revealed that TIMP-1 relative abundance in control middle/deep chondrocytes seeded for 18 h was significantly different from all other groups ($p < 0.03$), with an expression approximately four times the average of the other groups (Figure 2-5C). No significant differences were found in MMP-1 (Figure 2-5D) or COMP relative abundances in middle/deep cells. Collagen I expression was once again not detected in any cells.

Discussion

This study succeeded in quantifying gene expression in single articular chondrocytes for the first time. Questions of cartilage maintenance and phenotype have been investigated at the tissue and cell population levels, but the single cell approach to study articular cartilage provides important insights into the fundamental physiology of chondrocytes. We have attempted to address several major aspects of cartilage tissue engineering: the role of cartilage zones in shaping chondrocyte behavior, how cell attachment time influences gene transcription, and the effect of growth factor stimulation on the regulation of

matrix genes. The full exploration of these issues at the single cell level allows a more accurate picture of chondrocyte behavior to emerge.

In Phase I of this study, we compared chondrocytes from the superficial and middle/deep zones to determine which zone was best suited as a source of cells for the purpose of cartilage tissue engineering. Our first step in Phase I was to evaluate differences in GAPDH expression across zones to determine its use as an internal reference, or housekeeping gene, in multiplex real-time PCR. Once thought to be an optimal endogenous control due to its ubiquitous expression and moderate abundance, GAPDH has been shown to vary in certain experimental conditions [34, 56, 111]. It is becoming increasingly clear that GAPDH may be an inappropriate internal standard for real-time PCR in the absence of proper, experiment-specific validation. In particular, GAPDH has been shown recently to be an unsuitable housekeeping gene in comparing injured cartilage to healthy tissue, even when total RNA is normalized to account for differences in the number of viable cells available for analysis [127]. Moreover, another candidate gene often used as an internal control, β -actin, was recently shown to vary across zones [131]. Thus, it is crucial to identify cases in which GAPDH can and cannot be used as an internal standard for cartilage studies. We sought to determine the suitability of GAPDH as an internal standard by examining its abundance. The findings of this study demonstrate a zone-dependent difference in GAPDH abundance (Figure 2-2). However, seeding time did not have an effect on GAPDH expression in cells from the same zone. These results indicate that GAPDH is an unsuitable housekeeping gene for

comparisons between the middle/deep and superficial zones of cartilage. On the other hand, GAPDH does serve as an appropriate housekeeping gene within a particular zone. It should be noted that while groups within a zone were not significantly different, the amount of variability from cell to cell was quite large (with a large range for sample size), as evidenced by each group's standard deviation. However, there is no means by which to normalize RNA otherwise, and the variability observed may result not only from cell-to-cell variation, but from potential loss of material in the multiple steps in RNA isolation and handling, which is precisely the sort of error accounted for though the use of a housekeeping gene. Hence, the use of GAPDH as a housekeeping gene in single cell work was warranted.

Furthermore, these results illustrate an important, fundamental metabolic difference between middle/deep and superficial chondrocytes. Manifold differences between cartilage zones have been demonstrated previously [17, 54, 131, 132, 199, 209, 239, 240]. By honing in on GAPDH, we have evaluated a gene constitutively expressed by all metabolically active cells in the body. That a zone-dependent difference is detectable provides further evidence that chondrocytes from different zones may be metabolically, and thus fundamentally, different. Additionally, the greater abundance of GAPDH in middle/deep chondrocytes compared to superficial chondrocytes agrees with past work showing that progressively deeper layers of cartilage are more metabolically active than superficial layers [17, 54, 239, 240]. These observations of GAPDH

abundance establish the need for further study on the constitutive metabolic behavior of zonal chondrocytes.

The greater metabolic activity in middle/deep chondrocytes led us to select that zone for further experimentation in Phase II, in which we examined the combinatorial effects of seeding duration and IGF-I exposure on middle/deep chondrocytes. Treatment with IGF-I did not result in a significant difference in GAPDH abundance in middle/deep chondrocytes, further establishing GAPDH as a suitable housekeeping gene for comparisons made within a particular zone. Seeding time alone was not a significant factor in the expression of aggrecan or collagen II in superficial chondrocytes (Phase I), but it was significant in the expression of aggrecan and collagen II in middle/deep chondrocytes (Phases I and II). IGF-I was found to significantly increase aggrecan and collagen II gene expression over time in middle/deep chondrocytes (Figures 2-5A and 2-5B). This effect was pronounced even though the exposure time to IGF-I was limited to 3 h, indicating that only a minimal duration of growth factor exposure is necessary to elicit positive signals for matrix production. Increased aggrecan and collagen II gene expression in the presence of IGF-I agrees with previous work on chondrocyte populations [52] and periosteal explants [150]. The latter study corroborates our observation that brief exposure to IGF-I is sufficient to enhance aggrecan and collagen II expression. Overall, translating the sum of our observations into applications for tissue engineering, the optimal environmental conditions for matrix production by middle/deep chondrocytes appears to be a combination of longer seeding combined with IGF-I treatment.

In addition to the effects of seeding time and growth factor exposure on the expression of important matrix molecules, we studied changes in MMP-1 and TIMP-1 expression in both Phase I and Phase II. MMP-1 is an important component in cartilage degradation and tissue remodeling, while TIMP-1 acts to keep the effects of MMP-1 in check [231]. Together, the balance of MMP-1 and TIMP-1 mediates matrix degradation in cartilage. With longer seeding, TIMP-1 increased significantly in superficial cells (Figure 2-3A) and middle/deep cells (Figure 2-5C). In superficial chondrocytes, MMP-1 was undetectable at 3 h but was expressed by 18 h (Figure 2-3B). These results suggest that as chondrocytes attach in monolayer, they have a tendency to initiate catabolic gene expression (MMP-1) and concomitantly enter a state of cell protection (TIMP-1). Even though MMP-1 was not shown to be significantly different with time in middle/deep chondrocytes, TIMP-1 upregulation suggests that the cells appear prepared to cope with catabolic trends. However, IGF-I diminishes the effect of seeding time on TIMP-1 expression in middle/deep chondrocytes. In doing so, IGF-I appears to refocus the cell on matrix production, as evidenced by the increased levels of aggrecan and collagen II (Figures 2-5A and 2-5B), rather than on protection of the cell from metalloproteinases (conferred by TIMP-1). It has been shown that a population of articular chondrocytes in culture react to interleukin-1 (IL-1), a known modulator of matrix degradation, by expressing TIMP-1 sooner than MMP-1 [2]. That study's observation that TIMP-1 expression precedes MMP-1 expression *in vitro* is in agreement with our finding that TIMP-1

was upregulated prior to any detectable change in MMP-1 expression in single chondrocytes.

No change in collagen I or COMP was observed in either zone for any condition. Collagen I served as a negative control for chondrocytic phenotype, since collagen I is found abundantly in fibroblast-like cells and is a marker for chondrocyte dedifferentiation [53]. Therefore, it is clear that all cells examined in this study were phenotypically chondrocytes and had not yet experienced dedifferentiation. Similarly, increases in COMP have been associated with osteoarthritic changes in articular cartilage [193, 205], and so it is expected that COMP expression may only increase dramatically in deleterious environmental conditions. COMP has also been shown to be a good marker of chondrocyte phenotype that is downregulated during dedifferentiation [248]. The absence of a change in COMP expression in either zone indicates that the chondrocytes examined in this study retained a fairly healthy, non-osteoarthritic phenotype.

Finally, the real-time single cell RT-PCR (scRT-PCR) assay developed in the course of this work serves as a powerful tool for amplifying the considerably small amount of starting mRNA in a single chondrocyte. The assay affords us the ability to quantify precise changes in gene expression from one cell to the next. While scRT-PCR has emerged as a robust technique in studying other cell types, such as neurons [97] and T cells [125], the technique has remained unused in the field of cartilage tissue engineering until now. Moreover, our scRT-PCR assay for chondrocytes will be useful in future studies focusing on mechanotransduction at the cellular level.

The work presented here establishes a unique understanding of chondrocyte biology at the level of the single cell. In total, single chondrocyte gene expression was shown to be influenced by a combination of seeding time and exposure to IGF-I, while a clear metabolic difference was demonstrated across cartilage zones. This study lays the groundwork for future investigations of the mechanobiology of single chondrocytes, especially in determining the combinatorial effects of direct compression and growth factor exposure on chondrocyte gene expression [131, 206, 208]. Already, IGF-I together with dynamic compression have been shown to synergistically enhance protein and proteoglycan content in chondrocyte-seeded agarose constructs [147]. Much work remains to be done at the single cell level to confirm or explain these phenomena observed at higher levels. An understanding of individual chondrocyte behavior would yield major insight into the development of novel strategies for articular cartilage regeneration.

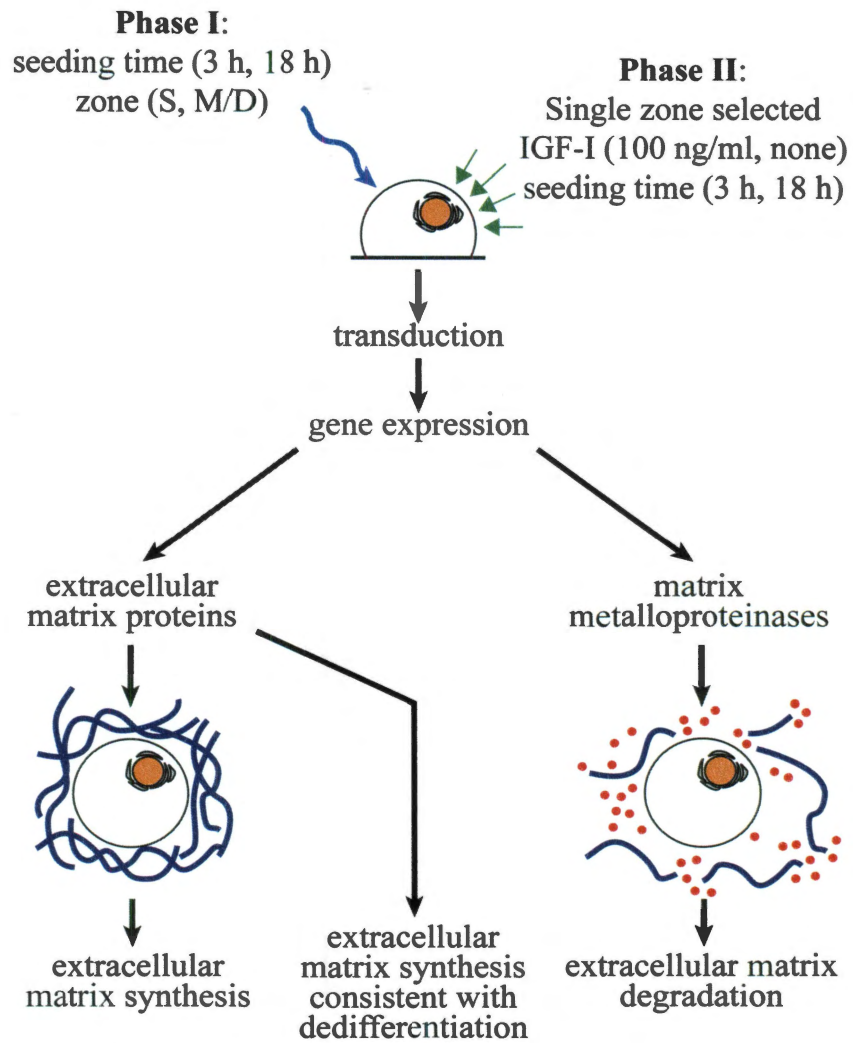


Figure 2-1. Single cell approach

Single cell approach to study the influences of growth factor exposure, seeding time, and cartilage zone on biosynthetic and catabolic gene expression.

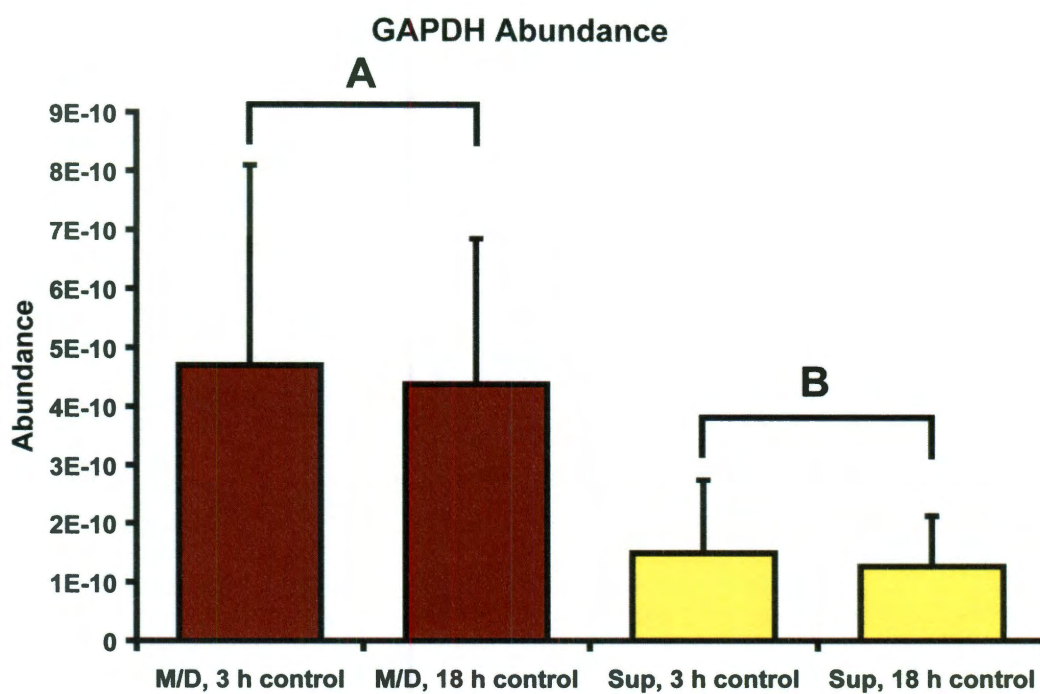


Figure 2-2. Phase I GAPDH mRNA abundance

GAPDH mRNA abundance in middle/deep (M/D) and superficial (Sup) chondrocytes. Results are presented as mean \pm standard deviation. Groups marked "A" are significantly different from groups marked "B" ($p < 0.0001$). Values for n ranged from 12 to 19.

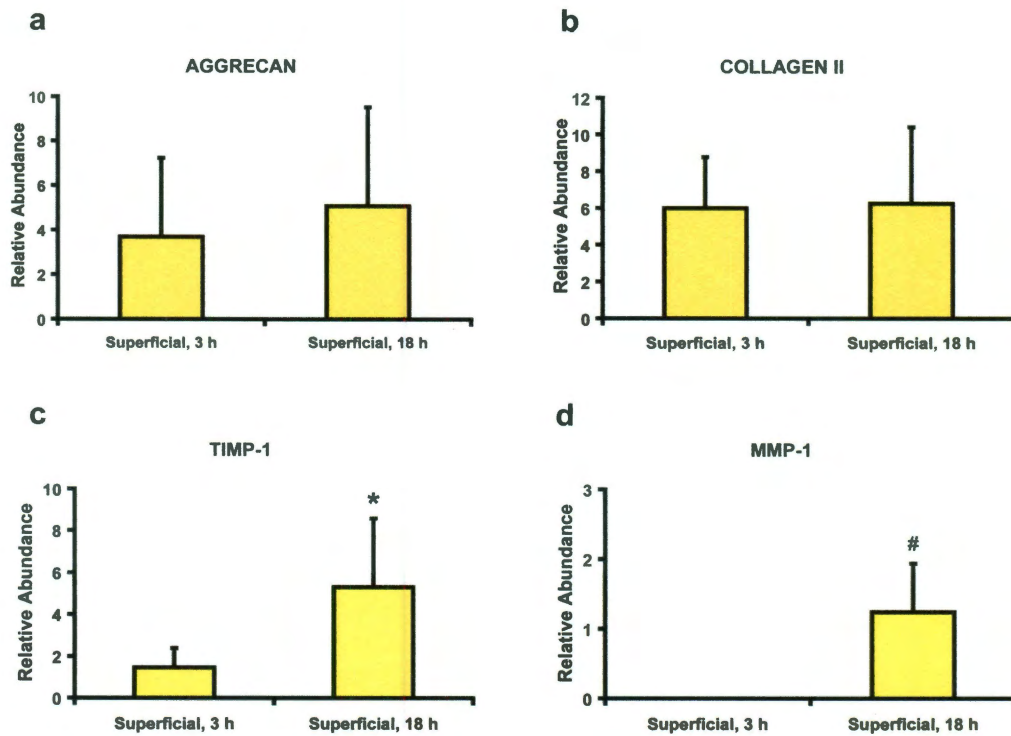


Figure 2-3. Phase I superficial zone gene expression results

Aggrecan (a), collagen II (b), TIMP-1 (c), and MMP-1 (d) mRNA relative abundance in superficial chondrocytes. TIMP-1 (c) increased from 3 to 18 hours (*, $p < 0.03$). MMP-1 was expressed (#) from 3 to 18 hours (D). Values for n were 5 at 3 hours and 6 at 18 hours for TIMP-1, and 4 at 18 hours for MMP-1.

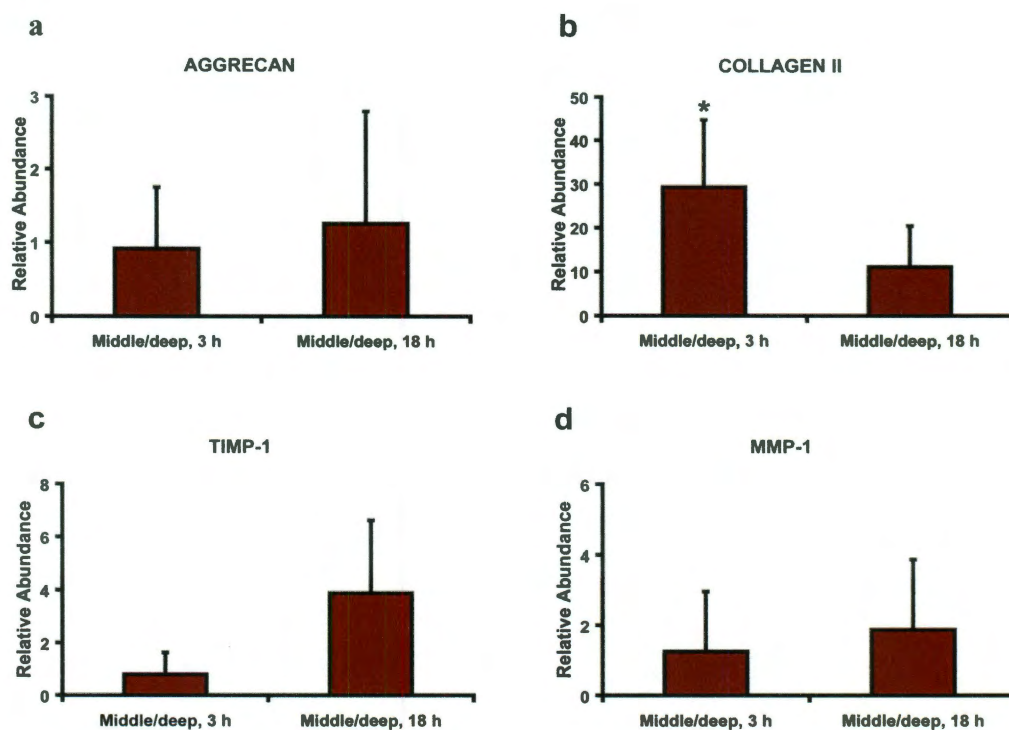


Figure 2-4. Phase I middle/deep zone gene expression results

Relative abundances of aggrecan (a), collagen II (b), TIMP-1 (c), and MMP-1 (d) in middle/deep chondrocytes. Collagen II (b) decreased from 3 to 18 hours (*, $p < 0.05$). Values for n ranged from 3 to 14.

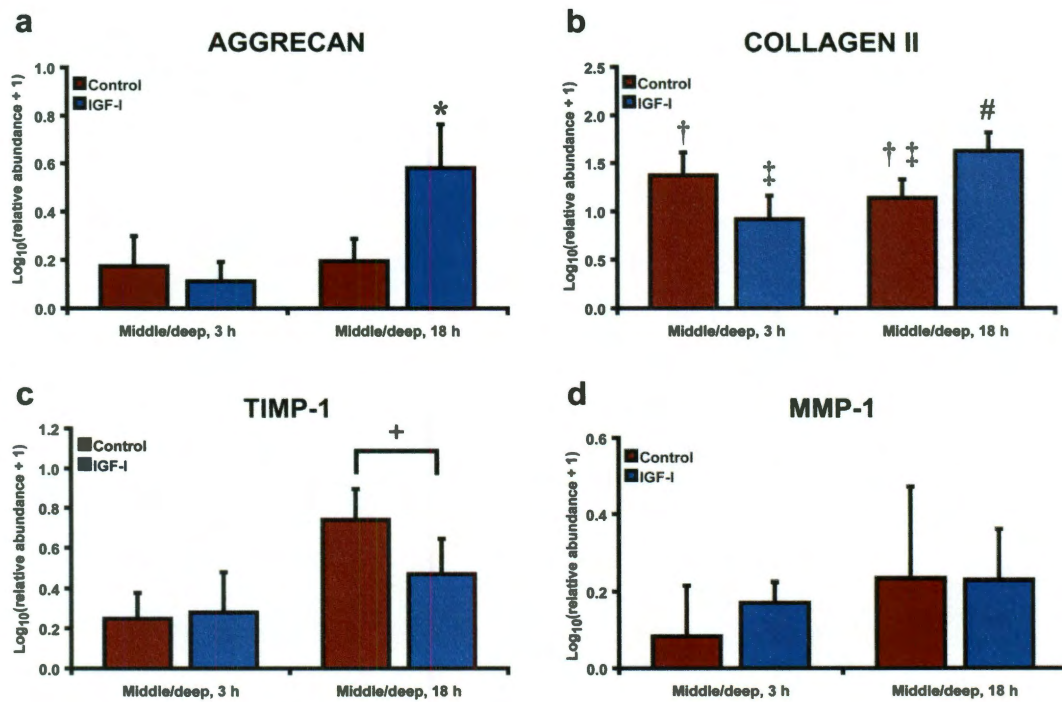


Figure 2-5. Phase II gene expression results

Effects of seeding time and IGF-I treatment on middle/deep chondrocytes. (a) IGF-I significantly increases aggrecan in middle/deep chondrocytes seeded for 18 hours (*, $p=0.0003$). (b) Collagen II relative abundance in IGF-I treated middle/deep chondrocytes seeded for 18 hours was significantly greater than all other treatment groups (#, $p<0.0001$), while control and IGF-I treated middle/deep chondrocytes seeded for 3 hours were significantly different ($p<0.05$). (c) TIMP-1 increases significantly from 3 to 18 hours in middle/deep control chondrocytes (+, $p<0.03$). (d) MMP-1 was unchanged in middle/deep chondrocytes. Values for n ranged from 7 to 14 for aggrecan, 6 to 13 for collagen II, 6 to 11 for TIMP-1, and 3 to 7 for MMP-1.

Table 2-1. Sequences for real-time RT-PCR target genes

Primer/probe sequences, dyes, and quenchers for real-time PCR target genes.

Gene name (accession number, product size)	Forward primer (5' to 3'), concentration Reverse primer (5' to 3'), concentration Probe (5' to 3'), concentration, dye/quencher
Cartilage oligomeric matrix protein (X74326, 72bp)	TCAGAAGAGCAACGCAGAC, 100 nM TCTTGGTCGCTGTCACAA, 100 nM CAGAGGGATGTGGACCACGACTTC, 100 nM, ROX/BHQ-2
Matrix Metalloproteinase-1 (X74326, 82bp)	CAAATGCTGGAGGTATGATGA, 50 nM AATTCGGGAAAGTCTTCTG, 50 nM TCCATGGATGCAGGTTATCCCAA, 125 nM, Cy5/BHQ-2
Tissue Inhibitor of Matrix Metalloproteinase-1 (NM174471, 75bp)	GAGATCAAGATGACTAAGATGTTCAA, 75 nM GGTGTAGATGAACCGGATG, 75 nM AGGGTTCAGTGCCTTGAGGGATG, 100 nM, ROX/BHQ-2

Chapter 3. Effects of growth factors on the biomechanics and cytoskeleton of single chondrocytes*

* Chapter published as Leipzig ND, **Eleswarapu SV**, and Athanasiou KA, "The effects of TGF-beta1 and IGF-I on the biomechanics and cytoskeleton of single chondrocytes," *Osteoarthritis and Cartilage* 2006.

Abstract

Ascertaining how mechanical forces and growth factors mediate normal and pathologic processes in single chondrocytes can aid in developing strategies for the repair and replacement of articular cartilage destroyed by injury or disease. This study examined effects of TGF- β 1 and IGF-I on the biomechanics and cytoskeleton of single zonal chondrocytes. Superficial and middle/deep bovine articular chondrocytes were seeded on tissue culture treated plastic for 3 and 18 h and treated with TGF- β 1 (5 ng/mL), IGF-I (100 ng/mL), or a combination of TGF- β 1 (5 ng/mL) + IGF-I (100 ng/mL). Single chondrocytes from all treatments were individually studied using viscoelastic creep testing and stained with rhodamine phalloidin for the F-actin cytoskeleton. Lastly, real-time RT-PCR was performed for β -actin. Creep testing demonstrated that all growth factor treatments stiffened cells. Image analysis of rhodamine phalloidin stained chondrocytes showed that cells from all growth factor groups had significantly higher fluorescence than controls, mirroring creep testing results. Growth factors altered cell morphology, since chondrocytes exposed to growth factors remained more rounded, exhibited greater cell heights, and were less spread. Finally, real-time RT-PCR revealed no significant effect of growth factor exposure on β -actin mRNA abundance. However, β -actin expression varied zonally, suggesting that this gene would be unsuitable as a PCR housekeeping gene. These results indicate that TGF- β 1 and IGF-I increase F-actin levels in single chondrocytes leading to stiffening of cells; however, there does not appear to be direct transcriptional regulation of unpolymerized β -actin. This suggests that the

observed response is most likely due to signaling cross-talk between growth factor receptors and integrin/focal adhesion complexes.

Introduction

Existing research has highlighted the need for the complete characterization of cellular milieus, especially toward understanding the processes of mechanotransduction in native and engineered tissues. Such knowledge would foster understanding of mechanical forces and their role in cell and tissue function. It would also be vital to elucidating disease etiologies, as well as the processes of formation and regeneration in tissues. In terms of tissue engineering, this knowledge would provide insight into the forces required for directing cells toward growing functional tissues *in vitro*.

Articular cartilage has been chosen as a leading target for tissue engineering for the simple fact that one in five adults experience significant morbidity due to cartilage injury and disease. Furthermore, articular cartilage engineering may appear to be an easy problem to tackle, considering that the tissue is avascular and contains very few cells. However, the tissue has a complex structure, exhibits a high degree of heterogeneity, and functions under an intensely strenuous environment. Articular cartilage is normally divided into four zones: superficial, middle, deep, and calcified. As reviewed [129], each zone has distinct differences in extracellular matrix (ECM) distribution, biosynthesis, gene expression, cell morphology, and physical properties.

Tissue engineering of cartilage thus far has proven unsuccessful in terms of replicating a fully functional tissue capable of withstanding the strenuous biomechanical environment within synovial joints. So far researchers have revealed that two stimuli, mechanical forces and chemical signals, seem to be important for influencing cartilage tissue formation, as well as its disease pathways. Studies with explants and chondrocytes have demonstrated that specific regimens of hydrostatic pressure, compression, and fluid forces can induce positive changes in gene expression and matrix synthesis [31, 94, 175, 191, 216, 229], while other regimens, namely static loads, can induce degenerative changes [31, 175]. However, the precise levels of mechanical stimulation necessary to elicit chondrocyte response to mechanical loading are not clearly understood. A variety of growth factors and cytokines have been studied for their potential use in stimulating articular cartilage regeneration. Two growth factors have shown the most promise as demonstrated by stimulation of matrix synthesis, increased proliferation, and maintenance of phenotype: transforming growth factor- β 1 (TGF- β 1) [81, 82, 143, 174, 186] and insulin-like growth factor-I (IGF-I) [22, 23, 87, 142, 162, 228]. It has also been shown that these growth factors can have synergistic effects when treating chondrocytes [244].

Previous research demonstrates the tremendous promise growth factors have shown for influencing cells toward tissue formation [22, 23, 81, 82, 87, 142, 143, 162, 174, 186, 228, 244]. Most cartilage or chondrocyte based studies have analyzed the response of explants or large populations of cells. These studies

are important for understanding physiological responses of cartilage, but they neglect to account for variations among either single cells or subpopulations of cells. Thus, it is necessary to take a reductionist approach by first studying single chondrocyte physiology to fully understand how cell responses translate to overall cartilage responses [206]. We are specifically interested in examining how growth factors influence single chondrocytes and how mechanical forces can modify these responses.

To date, several groups have attempted to describe cell signaling after TGF- β 1 and IGF-I treatment. These studies have focused on signaling between TGF- β 1 and IGF-I growth factor receptors and integrins [128, 198, 204]. The process of integrin activation in conjunction with IGF-I stimulation has been linked to the activation of signaling intermediates in several cell types. One such study demonstrated that chondrocytes plated on type I or type II collagen followed by IGF-I stimulation resulted in association of focal adhesion kinase (FAK) with α 1 integrins, vinculin, and paxillin, as well as induction of greater Shc (adaptor protein) expression [204]. It was postulated that IGF-I receptors cooperate with integrins to regulate focal adhesion proteins and are linked to the MAPK signaling pathway by a common Shc-growth factor bound protein 2 (GRB2) intermediate. TGF- β 1 stimulation has also been tied to integrin activation in chondrocytic cells. For example, one study has shown that TGF- β 1 stimulation and α 2 β 1 integrin activation (by type II collagen stimulation) led to synergistic increases in the phosphorylation of Smad2 and Smad3 [198]. The signaling between TGF- β 1 and integrins was demonstrated to occur before Smad

phosphorylation. It has also been demonstrated that inhibiting FAK decreases cell attachment and blocks integrin signaling [128].

Before one can hope to describe the mechanotransductive processes occurring *in vivo* and *in vitro* in native and engineered cartilage, a better understanding of individual chondrocyte behavior is necessary. We have previously described the development of devices able to mechanically test single adherent chondrocytes and osteoblasts [121, 130, 213] for determining their mechanical properties. The most recent setup of our device utilizes unconfined creep compression on single cells [130].

The overall objective of this study was to determine what effects TGF- β 1 and IGF-I would have on the mechanical properties of single articular chondrocytes, temporally and as a function of zone. The primary goal of this study was to quantify biomechanical alterations in single chondrocytes pertinent toward tissue regeneration or the etiology of disease states. Understanding a single chondrocyte's biomechanical response to static compression has implications towards understanding the forces responsible for initiating both anabolic and catabolic changes in cartilage. Based on the known actions of TGF- β 1 and IGF-I [22, 23, 81, 82, 87, 128, 142, 143, 162, 174, 186, 198, 204, 228, 244], our hypothesis was that these growth factors would lead to preservation of a more rounded chondrocytic phenotype. Based on previous work, we expected to observe differences between zones [209], growth factor treatments [22, 23, 81, 82, 87, 128, 142, 143, 162, 174, 186, 198, 204, 228, 244], and possible synergistic effects between TGF- β 1 and IGF-I [244]. For this study we used

single cell unconfined creep compression, fluorescence microscopy, and real-time RT-PCR to determine what effects the growth factors TGF- β 1 (5 ng/mL), IGF-I (100 ng/mL), and a combination of TGF- β 1 (5 ng/mL) and IGF-I (100 ng/mL), would have on zonal chondrocytes after 3 and 18 h of attachment.

Materials and methods

Cell culture

Articular cartilage was obtained from the distal metatarsal joint of approximately 18 month old steers obtained from local abattoirs. Chondrocyte harvest, isolation, and culture followed previously described protocols [130]. Briefly, the superficial and middle/deep zones were separated and digested overnight at 37°C and 10% CO₂ in a solution of 2 mg/mL collagenase type 2 (Worthington) in supplemented Dulbecco's modified Eagle medium (DMEM) containing 10% fetal bovine serum (FBS), 100 U/mL penicillin-streptomycin, 0.25 μ g/mL fungizone, and 0.1 mM non-essential amino acids (NEAA) (Invitrogen). After digestion, the cell mixture was centrifuged and resuspended in supplemented DMEM. The cell suspension was seeded onto a tissue culture treated plastic (TCP) 150 x 20 mm dish (plasma treated by Techno Plastic Products) and confined to a 2 cm diameter area using silicone isolators (PGC Scientifics) to yield an areal cell density of approximately 3.3×10^4 cells/cm². The plates were incubated for either 3 or 18 h at 37°C and 10% CO₂ prior to compression testing. These seeding times were selected such that we could characterize cellular events occurring immediately after attachment.

Three h is usually the approximate time that cells begin attaching. Cells are more firmly attached by the overnight, 18 h time point.

Growth factor treatment

The growth factors TGF- β 1 and IGF-I were selected for this study. These growth factors were used at a single concentration each, based on high or saturation values found in the literature [22, 23, 81, 82, 87, 142, 143, 162, 174, 186, 228, 244]. For TGF- β 1 and IGF-I, concentrations of 5 ng/mL and 100 ng/mL, respectively, were selected for experimentation. A third growth factor treatment was selected using a combination of TGF- β 1 and IGF-I at a concentration of 5 ng/mL and 100 ng/mL, respectively. Both growth factors were obtained from PeproTech Inc. For both cell seeding times (3 and 18 h), cells were exposed to the appropriate growth factor for the final 3 h of attachment. The design of this experiment is presented in Table 3-1.

Single cell creep testing

Unconfined creep compression tests were performed using a system developed in our laboratory, originally designed for displacement-controlled indentation testing of single cells [213]. Since its original design, this device has been modified first for indentation creep testing [121] and finally for the purpose of unconfined creep testing [130]. This device is designed to apply a constant stress on adherent cells while employing cantilever beam theory to track the resulting

cellular deformation. Single cell unconfined compression is achieved by the application of a 50.8 μm diameter tungsten probe (Advanced Probing).

After cell attachment, the media were removed from the culture dish and replaced with supplemented media containing 30 mM HEPES buffer (Fisher Scientific, Pittsburgh, PA) warmed to 37°C to buffer pH changes when moving to ambient conditions. TGF- β 1, IGF-I, or the combination of TGF- β 1 and IGF-I were included in the fresh media for the corresponding treatment group. The dish was then placed into the apparatus and maintained at ambient conditions for creep testing.

Creep testing was performed as described previously [130]. Briefly, single cells were creep tested using a test load of 50 nN. This test load was lower than what was previously used and resulted in cellular strains at or below 30% to conform to continuum model assumptions. The contact stress for each cell was determined via reticle measurement (Nikon USA) of the cell diameter before compression. Contact stress was calculated by dividing the test load by the area of the cell. Cell height was determined by comparing probe contact with the cell to the measured distance to the dish.

Determination of single chondrocyte material properties

The creep response of single chondrocytes to unconfined compression was modeled using a closed-form continuum mechanics model presented earlier [130]. Briefly, to model the creep response, a solid disc geometry was used to describe a chondrocyte attached to a substrate. Studies in our laboratory using

interferometry suggested this to be an appropriate approximation for the shape of a single chondrocyte [201]. With this geometry in mind, we considered the cell as a disc, under small deformation exposed to an instantaneous and constant load.

From the standard linear solid (Kelvin) model, and assuming the cell to be isotropic, incompressible, and homogeneous, the following solution was formulated to describe the viscoelastic creep response of a cell:

$$u_z(r,0,t) = \frac{2\sigma}{3E_\infty} z(r,0) \left[1 + \left(\frac{\tau_\epsilon}{\tau_\sigma} - 1 \right) e^{-\frac{t}{\tau_\sigma}} \right] H(t)$$

$$E_0 = E_\infty \left(\frac{\tau_\sigma}{\tau_\epsilon} \right)$$

$$\mu = E_\infty (\tau_\sigma - \tau_\epsilon)$$

where u_z is the deformation, σ is the contact stress, E_∞ is the relaxed modulus, z is the height of the cell, t_s is the creep time constant, t_e is the stress relaxation time constant, $H(t)$ is the unit step function, E_0 is the instantaneous modulus, and μ is the intrinsic viscosity.

Creep experimentation generated three sets of data for each cell: displacement versus time, force versus time, and force versus displacement. The force versus time data were used to confirm constant force during testing, while the force versus displacement data were used to determine contact with the cell. The resulting creep curves were fitted and material properties were generated for the viscoelastic model via the non-linear Levenburg-Marquardt method, using MATLAB 6.5 (MathWorks).

Fluorescence microscopy: F-actin staining

To compare the filamentous actin (F-actin) distribution and organization, all treatment groups (Table 3-1) were stained with rhodamine phalloidin. Fluorescent derivatives of phallotoxins have been demonstrated to specifically bind to filamentous, but not to globular actin (G-actin) [49]. A number of studies have used fluorescently modified phallotoxins to quantify the amount of F-actin through fluorescent measurements, including image analysis [104, 120, 133, 177]. Chondrocytes were seeded using the protocol above, except they were cultured on 24 x 30 mm tissue culture treated Thermanox plastic coverslips (Nalgene). Silicon isolators and the same cell density were used for seeding. After the culture period, cells were washed twice with PBS warmed to 37°C. The cells were then fixed with fresh 3.7% paraformaldehyde for 10 min at room temperature, washed three times with PBS, and then permeabilized in 0.1% Triton X-100 in PBS for 5 min. After three more PBS washes, the fixed cells were incubated in rhodamine phalloidin (2 U per coverslip; Molecular Probes) in 1% BSA in PBS for 20 min, followed by three final washes with PBS. Each Thermanox coverslip was mounted between a microscope slide and glass coverslip using ProLong Gold with DAPI (Molecular Probes). These samples were viewed with an Axioplan 2 microscope (Carl Zeiss) and a CoolSNAP_{HQ} CCD camera (Photometrics). Images were acquired and analyzed using Metamorph 4.15 (Universal Imaging Corporation). All images were acquired in gray scale and colorized for presentation using Metamorph. For comparison of staining intensity, light exposure was kept to a minimum, and exposure time for

digital photographs was kept at 30 ms. Overlaying and image processing were accomplished with Adobe Photoshop 7.0 (Adobe Systems).

The relative intensity of F-actin was determined for multiple cells in each treatment group using Metamorph to analyze the raw images. A region of interest was selected around a single cell and from this an average intensity (gray value) was obtained. The same size region was also selected over a nearby area without any cells to obtain a reading for the background fluorescence. The difference of these numbers was the cell's relative staining intensity. Average gray value (AGV) in a region of interest was determined with the following equation: $AGV = \text{total of all gray values} / \text{the total number of pixels}$. No threshold was set in the measurement of AGV for this analysis.

Gene expression of β -Actin

Generally speaking, in healthy non-muscle tissue two isoforms (β - and γ -) of actin exist within a cell. Although little is known about the exact functions of each isoform, β - and γ -actins have been associated with numerous microfilament structures and β -actin has been implicated in cell migration and cell motility.

Populations of 2×10^5 chondrocytes were seeded in 24 well TCP plates. Each treatment group is represented in triplicate, yielding 48 samples. After 3 and 18 h of attachment, samples were lysed and their RNA was isolated using the RNAqueous kit (Ambion). Total RNA concentration and purity were measured by a NanoDrop spectrophotometer (NanoDrop Technologies), which allows standardization by total RNA for the reverse transcription (RT) reaction. Before

the RT reaction, RNA was subjected to DNase treatment. For the RT reaction, 38 μL of RNA was incubated with oligo(dT) primer at 65°C for 5 min. After cooling to room temperature, a 50 μL reaction was incubated with the RNA-oligo(dT) mix, buffer, 4mM dNTPs (1mM each dNTP), 40 U RNase inhibitor, and 50 U Stratagene StrataScript RT enzyme for 60 min at 42°C. After cDNA synthesis, real-time PCR amplification for β -actin was performed using a RotorGene 3000 (Corbett Research). A forward primer, reverse primer, and gene-specific probe were used. The 5' to 3' sequences for the forward primer, reverse primer, and probe were designed from bovine and human mRNA sequences from the National Center for Biotechnology Information (NCBI). The probe chemistry used in PCR reactions is 5' FAM and 3' BHQ-1. For real-time PCR analysis of each sample, 1 μL of DNA sample, buffer, 3.5 mM MgCl, 0.2 mM DNTPs, 100 nM of each forward and reverse primer, 100 nM probe, and 0.625 U HotStarTaq (Qiagen, Valencia, CA) were prepared in a 25 μL reaction volume. The real-time analysis involves a 15 min activation step, followed by 50 cycles of 15 s at 95°C, 30 s at 60°C, and a fluorescence measurement.

The calculation of mRNA abundance of β -actin for all sample groups is facilitated by normalization with respect to total RNA concentration into the RT reaction. Abundance (A) was calculated from the takeoff cycle (C_t) of β -actin and the efficiency (E) of the reaction determined from a standard curve. The abundance equation used (adapted from Pfaffl) [169] was:

$$A = \frac{1}{(1 + E)^{C_t}}$$

The abundance was used to compare the expression of β -actin in all treatment groups.

Data/statistical analysis

All results are reported as mean \pm standard deviation. Statistical analysis of the data were performed using JMP IN 5.1 (SAS Institute). The effects of zone, attachment time, and growth factor treatment were tested with three-factor ANOVA. The significance of these factors was determined for gene abundance. Where ANOVA reveals differences, a Tukey's Honestly Significant Difference (HSD) *post hoc* test was performed to make pair-wise comparisons among means.

Results

Viscoelastic properties

An example of a typical creep curve from a single cell is presented in Figure 3-1. This viscoelastic response was demonstrated by all 240 cells that were tested. These creep data were separately curve fit using the equation presented such that the instantaneous modulus, relaxed modulus, and apparent viscosity were determined for each treatment. A summary of the mean material properties (E_{∞} , E_0 , μ) is presented in Figure 3-2. Compression with a test load of 50 nN did not appear to change cell area during testing or the calculation of contact stress. Experimentation required 15 animals and statistical analysis showed that animal

was not a significant factor for any cell property (E_{∞} , E_0 , μ , cell diameter, and cell height).

Three-factor ANOVA with *post hoc* analysis showed that each growth factor treatment (TGF- β 1, IGF-I, and TGF- β 1 + IGF-I) was a significant factor compared to no growth factor treatment for both the relaxed modulus (Figure 3-2A, $p < 0.0001$) and instantaneous modulus (Figure 3-2B, $p < 0.0001$). Individual growth factor treatments were not statistically different from each other, and synergism was not observed from the combination of TGF- β 1 + IGF-I. Growth factor treatment increased the relaxed modulus by 86% over controls and increased the instantaneous modulus by 136%. Furthermore, the combination of TGF- β 1 and IGF-I significantly increased the apparent viscosity (Figure 3-2C) by 45% over controls ($p = 0.01$). Attachment time did not have a significant effect on instantaneous modulus ($p = 0.57$), relaxed modulus ($p = 0.17$), or apparent viscosity ($p = 0.06$). ANOVA also showed that zone was a significant factor on the relaxed modulus ($p = 0.0025$), with superficial cells having a total mean relaxed modulus (0.91 ± 0.28 kPa) that was 11% larger than middle/deep cells (0.82 ± 0.25 kPa). The interaction of zone and growth factor treatment was significant for the relaxed modulus ($p < 0.0001$) and *post hoc* analysis showed that the interaction term superficial*(TGF- β 1 + IGF-I) resulted in a significantly higher relaxed modulus than middle/deep*(TGF- β 1 + IGF-I) and all other interactions (Figure 3-2A, $p < 0.05$). This zone*growth factor interaction may have leveraged the effect of zone in the statistical analysis of the relaxed modulus.

Cells appeared more spread at 18 h, as demonstrated by smaller heights and greater diameters than cells at 3 h. After 3 h of attachment, cells had an average height of $7.40 \pm 2.15 \mu\text{m}$ and an average diameter of $11.94 \pm 1.21 \mu\text{m}$. In comparison, after 18 h attachment cell height was $6.09 \pm 1.93 \mu\text{m}$ and cell diameter was $13.00 \pm 1.34 \mu\text{m}$. ANOVA showed significant effects of attachment time with cell height decreasing from 3 to 18 h ($p < 0.0001$) and cell diameter increasing from 3 to 18 h ($p < 0.0001$). Additionally, chondrocytes treated with growth factors (TGF- β 1, IGF-I, and TGF- β 1 + IGF-I) had significantly greater cell heights as compared to control cells ($p < 0.0001$) but were not significantly different from each other. At 3 h, growth factor treatment led to an average cell height of $7.86 \pm 2.07 \mu\text{m}$ compared to control cells at $6.00 \pm 1.76 \mu\text{m}$. For growth factor treatment at 18 h of attachment, cell height was $6.60 \pm 1.84 \mu\text{m}$, whereas that of controls was $4.42 \pm 1.11 \mu\text{m}$. Three-factor ANOVA showed that growth factor treatment was a significant factor on cell diameter ($p = 0.003$). Growth factor treatment led to smaller cell diameters ($12.22 \pm 1.24 \mu\text{m}$) compared to control cells ($12.50 \pm 1.54 \mu\text{m}$). Zone was not a significant factor for cell height or diameter.

Actin staining/fluorescent intensity

The results of cell staining with rhodamine phalloidin and DAPI for all treatment groups are presented in Figure 3-3. Cell spreading increased from 3 to 18 h of seeding time as did the degree of actin organization. A majority of chondrocytes from the growth factor treatment groups (Figure 3-3E-P) exhibited a brighter halo

at the periphery of the cell as compared to control cells (Figure 3-3A-D). Images taken after 18 h of seeding (Figure 3-3 left 8 panels) showed larger cells with discernable stress fibers, which were not visible at 3 h (Figure 3-3, right 8 panels).

Seven to ten fluorescent images of cells were taken from each treatment group at 100X magnification. Collectively, the images contained an average of 51 cells for each treatment group. Average relative intensity values were determined for each treatment. The average relative intensity values mirrored the creep compression results (Figure 3-4) and *post hoc* analysis showed an 86% increase for each growth factor treatment over controls ($p < 0.0001$). The TGF- β 1 group also exhibited a significant decrease in fluorescent intensity in comparison to IGF-I and in comparison to TGF- β 1 + IGF-I ($p < 0.0001$). Fluorescence intensity decreased by 24% at 18 h attachment as compared to 3 h ($p = 0.0004$).

β -actin gene expression

Real-time PCR analysis was completed in duplicate on 48 samples, a standard dilution curve (serial dilutions of stock DNA: 10X, 100X, 1,000X, 10,000X), and no-template controls (NTCs), requiring two runs on the RotorGene. NTC amplification was not observed and reaction efficiency for each run was 96% and 97%. The results of β -actin abundance (Figure 3-5) did not show a significant effect for any growth factor treatment ($p = 0.70$), attachment time ($p = 0.09$), or zone ($p = 0.54$). However, a significant interaction was seen for zone and attachment time ($p < 0.0001$). This is due to the fact that superficial zone chondrocytes had a

significantly lower ($p < 0.0001$) abundance ($2.80 \pm 0.76 \times 10^{-7}$) at 3 h as compared to 18 h ($4.63 \pm 1.80 \times 10^{-7}$).

Discussion

The unconfined creep compression results of this study demonstrate for the first time that the growth factors TGF- β 1 and IGF-I, alone and in combination, significantly increase the stiffness of single zonal chondrocytes without synergistic effects observed between the two growth factors. Measurements of cell dimensions also demonstrate that these growth factor treatments alter the morphology of chondrocytes. The creep testing results further confirm that a viscoelastic model, assuming simple disc geometry, is suitable for modeling the response of a single chondrocyte to unconfined creep compression. This model also serves as a valuable tool for distinguishing the effects of growth factors on the mechanical properties of single cells. These findings yield important information toward understanding the process of mechanotransduction, which is gaining prominence as a crucial actor in tissue homeostasis and disease, as well as in the formation and maintenance of cell phenotypes. Determination of single cell mechanical properties fosters understanding of a cell's local mechanical environment and that environment's role in shaping cellular physiology. Specifically for chondrocytes, it is important to understand the precise forces germane to tissue formation, and the etiopathogenesis of osteoarthritis, and how growth factors can modify these responses. Examination of single chondrocytes has already revealed important information in terms of relating mechanical

properties to disease states [6, 224], cytoskeletal composition [225], and the actions of growth factors [128, 198, 204]. This study adds to the current knowledge of growth factor effects on the cytoskeleton of single chondrocytes and provides insight to the study of basic cell functions.

The findings of this study demonstrate that separate techniques can be utilized to obtain similar information on the biomechanical nature of single chondrocytes. Creep compression of single chondrocytes showed mechanical stiffening induced by growth factors that corresponded with higher relative intensity measurements of chondrocytes stained with rhodamine phalloidin. These concomitant increases suggest that treatment with TGF- β 1 and/or IGF-I increases the levels of F-actin within chondrocytes. This further implies that treatment with TGF- β 1 and/or IGF-I leads to an increase in the number of actin filaments with concomitant or subsequent cellular stiffening. Previous work has shown that actin microfilaments and possibly intermediate filaments contribute significantly to the biomechanical properties of single chondrocytes as measured by micropipette aspiration [225]. Also, TGF- β 1 and IGF-I have previously been shown to increase the attachment of chondrocytes when compared to serum free controls [138, 204], suggesting increased focal adhesions and greater actin organization due to growth factor exposure. The growth factor treatments used in this study appear to affect cell stiffening in a similar manner, since analogous results were seen in all growth factor groups. Growth factor stimulation seems to be necessary for increases in F-actin as well as for cell stiffening to occur, since cells seeded for 3 and 18 h that were not exposed to growth factors did not show

increased levels of F-actin or any cell stiffening. Further, synergistic effects were not observed when chondrocytes were stimulated with both TGF- β 1 and IGF-I. These observations suggest the possibility of a common, yet currently unknown, mechanism.

The cell stiffening and increased F-actin that chondrocytes exhibited after TGF- β 1 and IGF-I exposure most likely involves a gene and/or protein response within single cells. These growth factors have a well documented effect on gene expression [81; 82, 244]; therefore, the stiffening mechanism may involve transcriptional changes of cytoskeletal and cytoskeletal related proteins. However, this does not appear to be the case since the expression of β -actin, as measured by real-time RT-PCR, demonstrates that TGF- β 1 and IGF-I do not significantly increase mRNA levels for β -actin. We speculate that this may indicate that the pool of monomeric actin (G-actin) available for polymerization may not be increasing from direct transcription of the actin gene. Even though β -actin gene expression does not increase with growth factor treatment, translational regulation of G-actin levels may be occurring. A likely candidate could include eukaryotic initiation factor 2A (eIF2A) which has been demonstrated to regulate protein translation and is important in actin cytoskeletal organization in yeast [122]. These findings suggest that the observed response of chondrocytes to TGF- β 1 and IGF-I is most likely occurring somewhere at the protein level. Previous research concerning chondrocytes, integrin activation, and stimulation by TGF- β 1 or IGF-I has shown that signaling between focal adhesion complexes and growth factor receptors may occur [128, 198, 204]. For IGF-I it is

clear that a Shc and Shc-GRB2 complex are important intermediates for linking to the MAPK pathway [204]. Current research has not yet revealed intermediate proteins connecting TGF- β 1 and integrins to cell signaling or specifically Smad signaling. The increases in F-actin and cell stiffening seen in this study most likely involve intracellular signaling proteins that localize at focal adhesions as well as adaptor proteins.

Zonal differences in articular cartilage and isolated chondrocytes have been well characterized, not only in gene expression and synthesis [17, 18, 54], but also in mechanical properties [209]. Several findings in this study further confirm that superficial chondrocytes differ physiologically from middle/deep chondrocytes. These data are in agreement with results from a recent study in our laboratory [209] that showed biomechanical differences between superficial and middle/deep chondrocytes. The real-time PCR results for expression of β -actin also illustrate differential responses of superficial and middle/deep cells during cell attachment. These results suggest that β -actin does not serve as a desirable housekeeping gene for chondrocytes, since expression is not constant across all treatments. As Figure 3-5 shows, middle/deep chondrocytes maintain a relatively constant level of β -actin expression from 3 to 18 h of attachment time, while superficial chondrocytes have a lower level of β -actin expression at 3 h. By 18 h β -actin expression increases to a level equal to that of middle/deep chondrocytes at both 3 and 18 h attachment. This may be due to a differential response of superficial cells as compared to middle/deep cells when cells are digested from tissue and plated. The lower abundance of β -actin mRNA at 3 h

does not seem sufficient to affect either the mechanical properties or the amount of F-actin in superficial chondrocytes. Some explanation can be garnered from previous work that has demonstrated that differences exist in the organization and the quantities of both actin and vimentin in zonal chondrocytes. Zonal differences have been observed in actin microfilament organization *in vivo* and in cells grown in monolayer [57, 117, 126] as well as in vimentin filament assembly and disassembly during organ culture [57]. It is interesting to note that zonal differences in cell morphology were not observed in this study. If chondrocytes exhibited similar morphologies to what is seen *in situ*, one would expect superficial cells to exhibit smaller cell heights and larger cell diameters than middle/deep zone cells. It appears that collagenase digestion followed by seeding in monolayer may alter the cytoskeleton such that morphology differences between zones no longer exist.

In contrast to studies with other cell types, attachment time did not play a factor in increasing chondrocyte stiffness as measured by single cell creep compression. The mechanical testing results of this study confirm a previous study from our group that demonstrated no significant effect of attachment time on any of the material properties of single chondrocytes as determined with the same creep testing device [209]. In contrast, fluorescence intensity of F-actin decreased from 3 to 18 h (Figure 3-4). Decreased intensity measurements most likely are due to a diminished actin polymerization front, since less of a bright halo was seen in fluorescent staining of single cells at 18 h of attachment (Figure 3-3). This may suggest that chondrocytes at 3 h have a denser network of actin

microfilaments at the cell periphery where the cell is actively attaching and spreading. Previous research has correlated increases in cell stiffness with increased cell spreading and ECM contacts in bovine endothelial cells tested by twisting attached magnetic beads on the cell surface [232, 233]. These differing behaviors can be attributed to cell type. Bovine articular chondrocytes do not adhere as easily as endothelial cells; at 3 h of attachment, chondrocytes remain round and are not firmly attached. Many of these cells can be detached by prodding with the compression probe or by a harsh PBS wash. At 18 h, chondrocytes are just starting to spread; however, a large percentage of rounded cells remain. There may be a threshold number of focal adhesions required to significantly stiffen a cell; therefore, attachment times greater than 18 h could show increased chondrocyte spreading and possibly increased cell stiffening.

We propose that the combination of integrin activation from cellular attachment and stimulation with TGF- β 1 and IGF-I leads to increased actin polymerization as characterized by increases in F-actin and stiffening of the cytoskeleton. The increased polymerization is most likely due to signaling between integrins and growth factor receptors. These findings offer important information for cartilage physiology, tissue engineering of articular cartilage, and osteoarthritis. The activation of integrins through ECM binding and cross-talk with growth factor receptors might be a crucial process *in vivo*, especially for cartilage regeneration. The results of this study demonstrate that 3 h of TGF- β 1 and IGF-I exposure cause significant changes to the actin cytoskeleton of single chondrocytes. This response may be short term or may continue with prolonged

growth factor exposure. It is possible that cytoskeletal stiffening is part of a chondrocyte's preparation for the increased synthetic or proliferative activities that have been observed previously in populations of these cells. Our group is particularly interested in understanding how mechanical forces and growth factors affect processes in single chondrocytes (Figure 3-6). This study establishes that by administering a characterized mechanical testing environment to single chondrocytes, their biomechanical response to external stimuli, such as growth factors, can be determined. The next step is to use this knowledge to correlate changes in gene expression and signaling with the direct compression of single chondrocytes. Growth factor stimulation surely plays a role in this response and may offer synergistic effects with certain modalities of mechanical stimulation. For cartilage, such synergism may influence tissue regeneration or inhibit damage/disease states caused by injurious mechanical loading. Connecting the application of force to changes in cell gene expression and signaling has broad implications; not only for the study of mechanotransduction, but for understanding disease etiologies and the formation or regeneration of tissues.

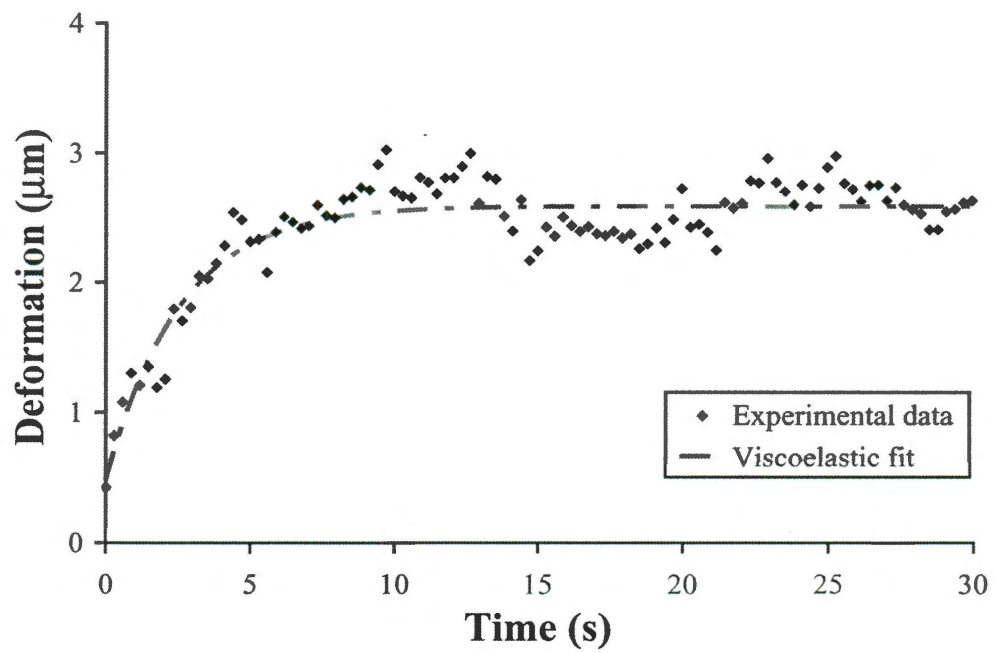


Figure 3-1. Viscoelastic creep response of a single chondrocyte

Creep curve from a single chondrocyte, representing a typical viscoelastic response. The viscoelastic curve fit is included (dashed gray line).

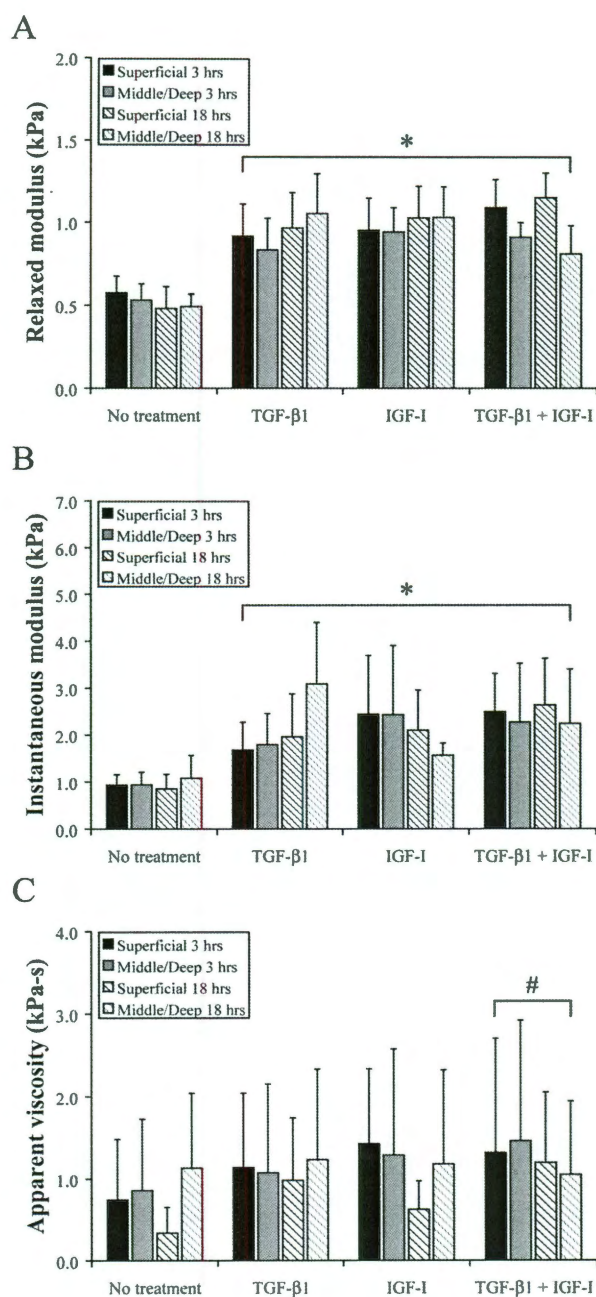


Figure 3-2. Viscoelastic properties of single articular chondrocytes

Viscoelastic properties as a function of growth factor treatment, zone, and seeding time. The relaxed modulus (A) and instantaneous modulus (B) were significantly greater for growth factor treated chondrocytes as compared to controls (*, $p < 0.0001$). The combination of TGF- β 1 + IGF-I significantly increased the apparent viscosity (C) over controls (#, $p = 0.01$) but not compared to other growth factor treatments. Values of n ranged from 13 to 20.

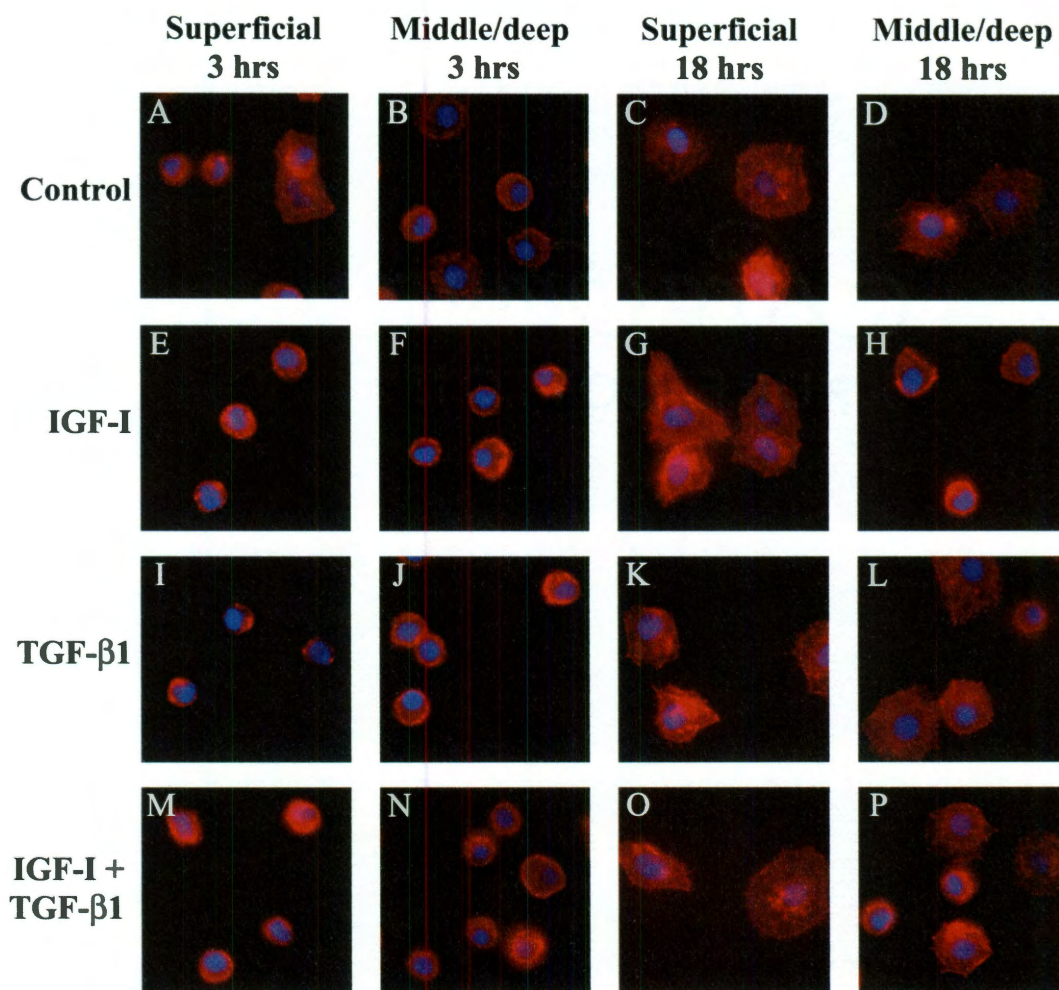
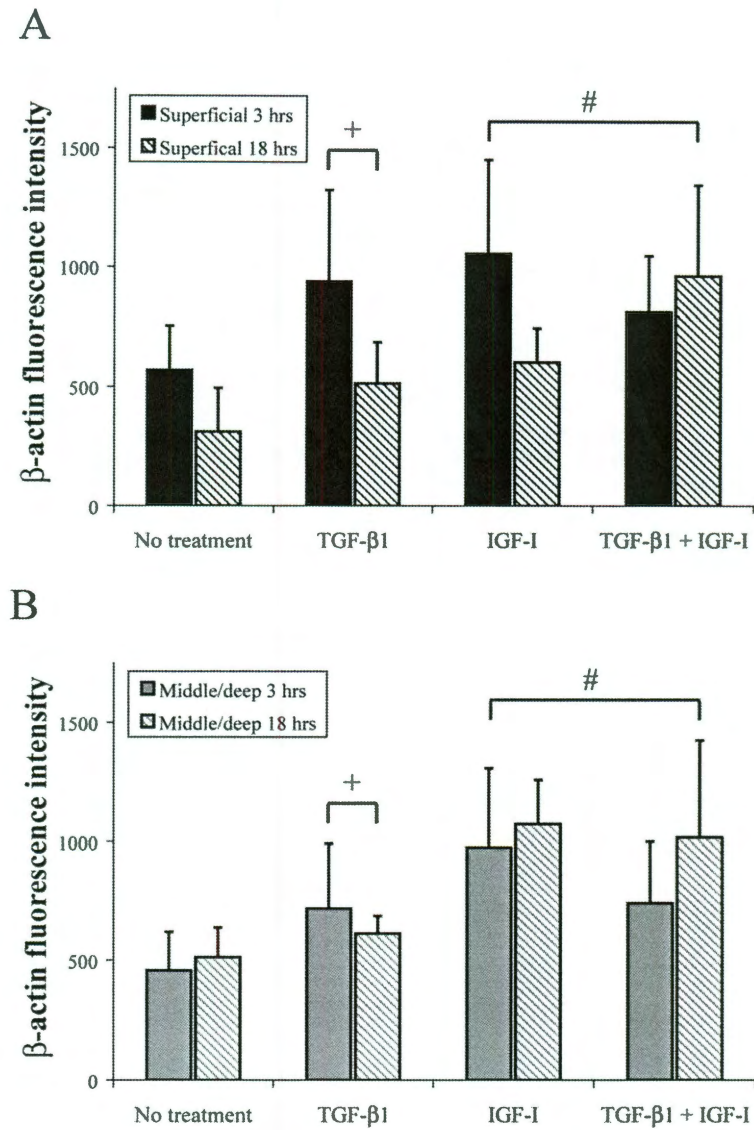


Figure 3-3. Fluorescence images of each treatment group (100X)

F-actin is stained with rhodamine phalloidin (red) and the nucleus is stained with DAPI (blue). Cells have more intense F-actin staining in growth factor groups and are less spread than control cells. Also, all groups show increased cell spreading from 3 to 18 h.



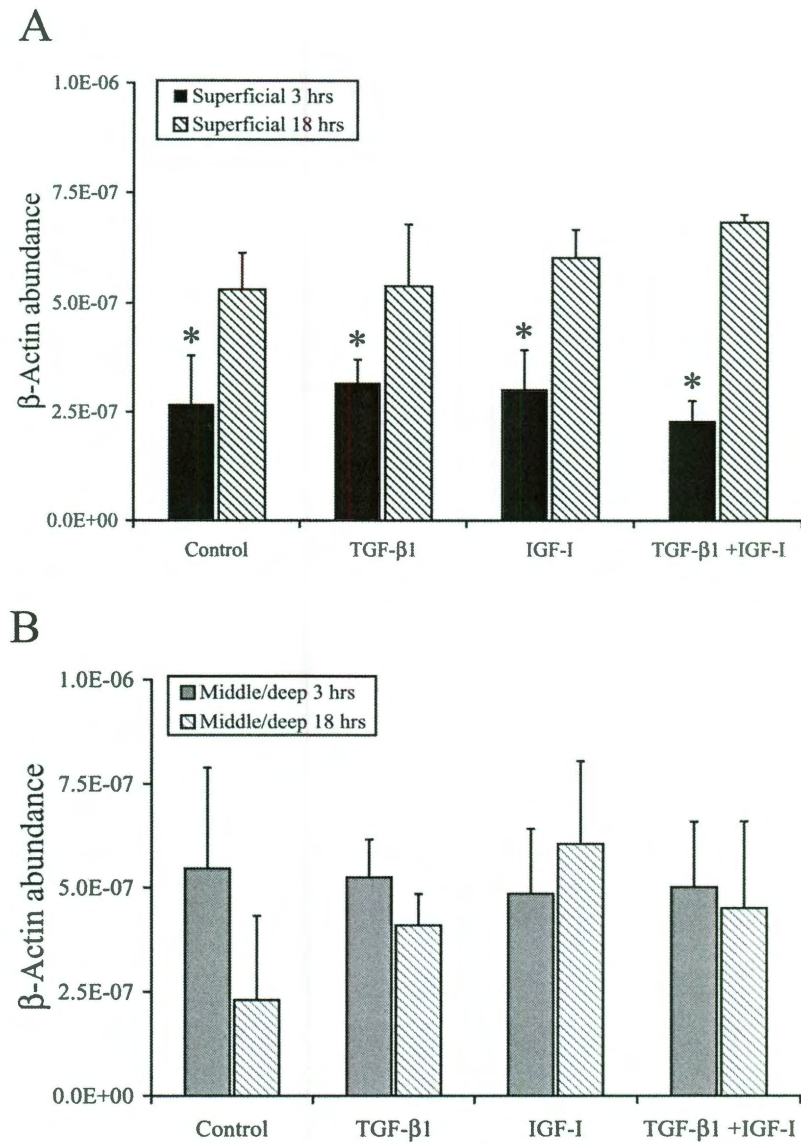


Figure 3-5. β -actin mRNA abundance

Superficial (A) and middle/deep (B) chondrocytes mRNA abundance. Results are presented as average \pm standard deviation. Asterisk (*) indicates significance of 3 h as compared to 18 h for superficial zone ($p < 0.0001$).

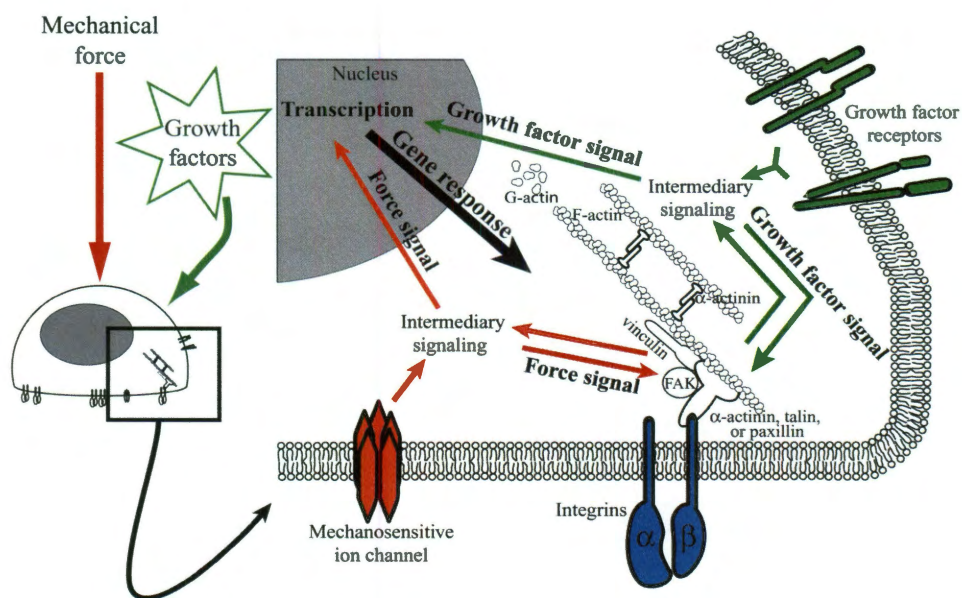


Figure 3-6. Mechanical and growth factor stimulation in single cells

Growth factors have been shown to affect nuclear and integrin/focal adhesion signaling (right side of figure). Mechanical forces can be sensed by a variety of cellular proteins, such as mechanosensitive ion channels and integrins. These forces have also been shown to affect nuclear and integrin/focal adhesion signaling (left side of figure). Our group hopes to determine the interplay that may exist when cells are exposed to both stimuli.

Table 3-1. Experimental design

Attachment time	Zone	Growth factor treatment
3 hrs	Superficial	Control
		TGF- β 1
		IGF-I
		TGF- β 1 + IGF-I
	Middle/Deep	Control
		TGF- β 1
		IGF-I
		TGF- β 1 + IGF-I
		8 treatment groups

Growth factor exposure for entire 3 hrs of seeding
(except for control)

Attachment time	Zone	Growth factor treatment
18 hrs	Superficial	Control
		TGF- β 1
		IGF-I
		TGF- β 1 + IGF-I
	Middle/Deep	Control
		TGF- β 1
		IGF-I
		TGF- β 1 + IGF-I
		8 treatment groups

15 hrs seeding followed by 3 hrs of growth factor
exposure (except for control)

Chapter 4. TRPV4 channel activation improves the tensile properties of self-assembled cartilage*

* Chapter submitted for publication as **Eleswarapu SV** and Athanasiou KA, "TRPV4 channel activation improves the tensile properties of tissue engineered articular cartilage."

Abstract

A persistent hurdle in cartilage tissue engineering is to produce tissues with biochemical and biomechanical properties robust enough to meet the aggressive physiological demands of the native joint. In an effort to improve these properties, tissues grown *in vitro* are often subjected to mechanical stimuli that aim to recapitulate *in vivo* loading conditions. These mechanical stimuli are thought to produce downstream alterations in intracellular ion concentrations, which ultimately give rise to increased biosynthesis. There is mounting evidence that these perturbations in the cellular microenvironment are regulated by the Ca^{2+} -permeable transient receptor potential vanilloid 4 (TRPV4) channel. In this study, we examined the effects of targeted TRPV4 activation on self-assembled articular cartilage constructs. The objectives of this study were 1) to determine whether TRPV4 activation would enhance self-assembled constructs, 2) to identify an optimal treatment time window for TRPV4 activation, and 3) to compare TRPV4 activation to Na^+/K^+ pump inhibition, which has been shown previously to improve construct tensile properties. This study employed a two-phased approach. In Phase I, self-assembled constructs were grown for 4 weeks and subjected to treatment with the TRPV4 agonist 4 α -phorbol-12,13-didecanoate (4 α -PDD) during three treatment time windows: $t=6-10$ days, $t=10-14$ days, and $t=14-18$ days. Treatment during $t=10-14$ days produced an 88% increase in collagen and a 153% increase in tensile stiffness. This treatment window was carried forward to Phase II. In Phase II, we performed a head-to-head comparison between TRPV4 activation using 4 α -PDD and Na^+/K^+

pump inhibition using ouabain. Treatment with 4 α -PDD produced improvements on par with ouabain (91% to 107% increases in tensile stiffness). The results of this study demonstrate the effectiveness of ion channel modulation as a strategy for improving engineered tissues. To our knowledge, this is the first study to examine TRPV4 channel activation in tissue engineering.

Introduction

Injury to the cartilage found at the articulating surfaces of diarthrodial joints is irreversible and leads inescapably to pain and disability [28]. Tissue engineering aims to replace damaged articular cartilage by producing biologic replacements *in vitro* for eventual *in vivo* implantation. A persistent hurdle in cartilage tissue engineering is to produce tissues with biochemical and biomechanical properties robust enough to meet the aggressive physiological demands of the native joint [51]. To address this challenge, our laboratory has developed a self-assembly process for engineering cartilage constructs [105]. Self-assembly involves seeding chondrocytes at high density into pre-fabricated, non-adherent, cylindrical molds. Cells condense into free-floating, disc-shaped constructs and, over time, synthesize an extracellular matrix (ECM) rich in collagen and sulfated glycosaminoglycans (GAG), components that give the tissue its tensile and compressive integrity [163]. To date, however, native tissue functional properties remain elusive.

In pursuit of strategies to improve the properties of engineered cartilage constructs, researchers in the field have developed a variety of mechanical

stimulation techniques that purport to reproduce the dynamic physiologic loading conditions experienced by native cartilage in the intact joint. Some of these strategies include dynamic compression [46, 114, 134, 136, 147, 154], fluid shear [58, 59, 246], hydrostatic pressure [65, 71, 92, 215, 226, 234], and osmotic stress [72, 73, 194, 195]. Unifying these strategies is the idea that changes in the macroscopic environment of the tissue can give rise to beneficial perturbations in the *in situ* cellular microenvironment. Dynamic changes at the cellular level manifest physiologically as transient alterations in intracellular ion concentrations. For example, hydrostatic pressure inhibits the action of the Na⁺/K⁺ pump [92], an ATPase that pumps ions against a concentration gradient to maintain a higher intracellular concentration of K⁺ than Na⁺. Thus, by inhibiting the Na⁺/K⁺ pump, hydrostatic pressure produces increased levels of intracellular Na⁺. A recent study from our group [160] showed that the selective inhibition of the Na⁺/K⁺ pump using 20 μM ouabain in self-assembled cartilage constructs was able to produce significant increases in collagen content and tensile properties, a result that recapitulated our group's previous success with hydrostatic pressure [63].

Another example of a dynamic tissue-level stimulus giving rise to changes at the cellular level is cyclic deformational loading. During joint motion, compressive loading of cartilage causes fluid expulsion, which creates a temporary hyper-osmotic microenvironment for chondrocytes within the tissue. This hyper-osmotic stress has been shown to produce transient increases in intracellular Ca²⁺ [72, 73, 245], which can drive gene expression toward ECM biosynthesis [167, 222]. The precise mechanism underlying this osmoregulation

in cartilage remains unclear. However, there is mounting evidence that the chondrocyte response to osmotic stress may be regulated by the transient receptor vanilloid 4 (TRPV4) channel [90, 170], a Ca^{2+} -permeable membrane protein found across many tissue types [112]. Although a handful of recent papers have examined the molecular and cellular physiology of the TRPV4 channel in chondrocytes, no study to date has selectively targeted the TRPV4 channel for use in a tissue engineering strategy.

Encouraged by results from the literature that suggest that the TRPV4 channel plays a vital role in chondrocyte physiology, we decided to examine the effects of TRPV4 activation on self-assembled articular cartilage constructs. The objectives of this study were 1) to determine whether TRPV4 activation would enhance the biochemical and biomechanical properties of self-assembled constructs, 2) to identify an optimal treatment time window for TRPV4 activation, and 3) to compare TRPV4 activation to Na^+/K^+ pump inhibition. This study employed a two-phased approach. In Phase I, constructs were self-assembled from bovine chondrocytes and subjected to treatment with the TRPV4 agonist 4 α -phorbol-12,13-didecanoate (4 α -PDD) during three treatment time windows: $t=6-10$ days, $t=10-14$ days, and $t=14-18$ days. Constructs were grown until $t=28$ days, at which time they were evaluated morphologically, biochemically, and biomechanically. The optimal 4 α -PDD treatment time window was then carried forward to Phase II. In Phase II, we performed a head-to-head comparison between TRPV4 activation using 4 α -PDD and Na^+/K^+ pump inhibition using ouabain; we also examined the combination of 4 α -PDD and ouabain. It was

hypothesized that 1) TRPV4 activation would improve construct properties, 2) an optimal treatment time window exists for which constructs undergo greatest improvement, and 3) activation of TRPV4 would produce results comparable to those observed with inhibition of the Na^+/K^+ pump. Assessments included gross morphology, biochemical analysis for GAG and collagen, and biomechanical testing.

Materials and methods

Chondrogenic medium

This study employed a chemically defined medium termed “chondrogenic medium,” which has been used previously by our group [62, 160, 163] and contains the following components: DMEM with 4.5 mg/mL of glucose and L-glutamine (Invitrogen); 100 nM dexamethasone (Sigma); 0.1 mM non-essential amino acids (Invitrogen); 1% ITS+ (insulin, human transferrin, and selenous acid; BD Biosciences); 1% penicillin-streptomycin-fungizone (BioWhittaker); 50 $\mu\text{g}/\text{mL}$ ascorbate-2-phosphate; 40 $\mu\text{g}/\text{mL}$ L-proline; and 100 $\mu\text{g}/\text{mL}$ sodium pyruvate (Fisher Scientific). Importantly, chondrogenic medium contains 151 mM Na^+ , 5.2 mM K^+ , and 1.7 mM Ca^{2+} , which are near physiologic serum concentrations [93]. Medium osmolarity was assessed using a VAPRO 5520 vapor pressure osmometer (Wescor) and was determined to be ~ 347 mOsm.

Chondrocyte isolation

Cartilage was harvested from the distal femurs and patellofemoral grooves of week-old male calves (Research 87, Inc.) shortly after slaughter, then digested in 0.2% collagenase type II (Worthington) for 24 h. To normalize variability among animals, each leg came from a different animal, and cells from 8 legs were pooled to create a mixture of chondrocytes. Separate harvests were conducted for each phase of this study. Cells were counted using a hemocytometer and then frozen at -80°C in DMEM containing 20% FBS and 10% DMSO.

Preparation of agarose wells for construct self-assembly

Cylindrical, non-adherent wells were prepared using a technique adapted from previous work [105, 163]. Briefly, a stainless steel mold consisting of 5 mm diameter cylindrical prongs was placed into sterile, molten 2% agarose in a 48-well plate. The agarose solidified at room temperature for 1 h, and the stainless steel mold was carefully removed. Two changes of chondrogenic medium were used to completely saturate the agarose well by the time of cell seeding.

Self-assembly of cartilage constructs

Chondrocytes were thawed and counted within 5 days of being isolated and frozen. After thawing, cell viability was >90%. To create each construct, 5.5 million cells in 100 μ L of chondrogenic media were seeded into each cylindrical agarose well, followed by addition of 400 μ L chondrogenic media after 4 h. Cells settled and condensed into free-floating cylindrical disc-shaped constructs; $t=1$

day was defined as 24 h after seeding. All constructs were cultured in the agarose wells until $t=10$ days, at which point they were gently unconfined and transferred to 48-well plates unrestricted by circumferential confinement. Constructs received 500 μL medium change every 24 h and remained in culture until $t=28$ days. All culture was performed at 37°C and 10% CO_2 .

Phase I: Evaluation of time windows for TRPV4 activation

In Phase I, we tested the hypothesis that TRPV4 channel activation can improve the biochemical and biomechanical properties of tissue engineered cartilage. We further sought to determine the optimal time window for performing this stimulation. Self-assembled constructs were treated with a TRPV4 channel agonist, 4 α -PDD (Enzo Life Sciences), during three treatment windows: $t=6-10$ days, $t=10-14$ days, and $t=14-18$ days. During treatment, constructs were cultured in petri dishes for 1 h with ~ 4 mL chondrogenic medium containing 10 μM 4 α -PDD. Control constructs were also moved to petri dishes containing chondrogenic medium during this time. Treatment was followed by a 30 min wash step in chondrogenic medium without 4 α -PDD before the constructs were returned to their wells. Treatment occurred at the same time every day over the course of 5 days.

Phase II: TRPV4 activation versus Na^+/K^+ pump inhibition

A previous study from our group showed that inhibition of the Na^+/K^+ pump improved the tensile properties of tissue engineered cartilage [160]. In Phase II,

we performed a head-to-head comparison between TRPV4 activation and Na^+/K^+ pump inhibition. We further sought to determine the effects of the combination of these two stimuli. The regimen for TRPV4 activation was chosen from the most effective treatment time window determined in Phase I: 10 μM 4 α -PDD during $t=10-14$ days (see Results section for details). The regimen for Na^+/K^+ pump inhibition was selected from previous work done by our group [160]: 20 μM ouabain during $t=10-14$ days. During $t=10-14$ days, constructs were cultured in petri dishes for 1 h with ~ 4 mL chondrogenic medium containing either 10 μM 4 α -PDD, 20 μM ouabain (Sigma), or both agents. Control constructs were also moved to petri dishes containing chondrogenic medium during this time. Treatment was followed by a 30 min wash step in chondrogenic medium before the constructs were returned to their wells. Treatment occurred at the same time every day over the course of 5 days.

Gross morphology and specimen portioning

At $t=28$ days, constructs were removed from culture. Photographs were taken, and dimensions were measured from photographs using ImageJ software (National Institutes of Health). Wet weights (WW) were recorded, and constructs were portioned for analysis. A 3 mm diameter punch was taken from the construct's center for indentation testing. The remaining outer ring was split into portions for biochemical analysis and tensile testing.

Biochemical analysis

Biochemical samples were weighed wet, frozen, and lyophilized. Samples were digested with 125 µg/mL papain (Sigma) for 18 h at 65°C. Total DNA content was assessed with the Quant-iT PicoGreen dsDNA Assay Kit (Invitrogen), and cell number was estimated assuming 7.8 pg DNA per cell. Sulfated GAG content was quantified using the Blyscan Glycosaminoglycan Assay (Biocolor). Following hydrolysis with 4 N sodium hydroxide for 20 min at 110°C, total collagen content was quantified with a modified chloramine-T hydroxyproline assay [105, 238]. Sircol collagen standard (Biocolor) was used such that the standard curve reflected collagen amount, eliminating the need to convert hydroxyproline to collagen. Total collagen and sulfated GAG were normalized to WW and cell number for making comparisons.

Tensile testing

Tensile specimens were cut into dog-bone shapes with 1 mm gauge lengths. Specimen thickness and width were measured from photographs using ImageJ software. Specimens were then affixed with glue to paper tabs outside the gauge length, and these tabs were gripped during testing. A uniaxial materials testing system (Instron Model 5565) was employed to determine tensile properties. Tensile tests were performed until failure at a strain rate of 1% of the gauge length per second. Force-displacement curves were generated, and stress-strain curves were calculated by normalizing to specimen dimensions. Young's modulus, a measure of tensile stiffness, was determined by least squares fitting

of the linear region of the stress-strain curve. The ultimate tensile strength (UTS) was determined as the maximum stress reached during a test.

Creep indentation testing

A creep indentation apparatus was used to determine the compressive behavior of each construct [12]. Each 3 mm sample was affixed to a stainless steel surface and equilibrated for 20 min in PBS. A 0.7 g (0.007 N) mass was applied with a 0.8 mm diameter flat, porous indenter tip, and specimens crept until equilibrium. Specimen thickness was measured from photographs using ImageJ software. Aggregate modulus, a measure of compressive stiffness, was calculated using a semi-analytical, semi-numeric, linear biphasic model [12].

Statistical analysis

All quantitative biochemical and biomechanical assessments were made using $n=6-8$. Data are presented as means \pm standard deviations. Single factor ANOVA was employed in each phase of the study to assess for differences among experimental groups. Statistical significance was defined as $p<0.05$. If significant differences were observed, a Tukey's HSD *post hoc* test was performed to determine specific differences among groups. All statistical analyses were performed using JMP 9.0.2 (SAS Institute).

Results

Phase I: Evaluation of time windows for TRPV4 activation

In Phase I, we studied the effects of treating self-assembled articular cartilage constructs with 4 α -PDD, an agonist of the TRPV4 channel. We examined the use of 10 μ M 4 α -PDD during three different treatment time windows: $t=6-10$ days, $t=10-14$ days, and $t=14-18$ days. Gross morphological measurements of all constructs at $t=28$ days are presented in Table 4-1. No differences were found in construct diameter, thickness, or wet weight (WW) among groups.

Biochemical analyses were conducted to quantify construct cellularity, collagen content, and GAG content. Construct biochemical data are provided in Table 4-2. No differences were found in cell numbers across treatment times. Collagen/WW was highest in constructs treated with 4 α -PDD during days 10-14 (88% increase over control), followed by constructs treated during days 14-18 (40% increase over control). When normalized to cell number, these differences in collagen content were maintained, with approximately the same magnitude increases. There were no differences observed in GAG content across treatment time windows.

Uniaxial tensile and creep indentation tests were performed to determine construct tensile and compressive properties. Tensile stiffness and strength data for Phase I are shown in Figure 4-1. Young's moduli for control, treatment on days 6-10, treatment on days 10-14, and treatment on days 14-18 were 269 ± 73 , 328 ± 80 , 681 ± 224 , and 464 ± 69 kPa, respectively. Constructs treated with 4 α -PDD during days 10-14 had the highest Young's moduli (153% increase over

control). UTS values for control, treatment on days 6-10, treatment on days 10-14, and treatment on days 14-18 were 112 ± 43 , 138 ± 27 , 261 ± 94 , and 182 ± 46 kPa, respectively. Constructs treated with 4 α -PDD during days 10-14 had the highest UTS (133% increase over control). With respect to compressive stiffness, the aggregate moduli for control, treatment on days 6-10, treatment on days 10-14, and treatment on days 14-18 were 75 ± 19 , 72 ± 21 , 82 ± 20 , and 76 ± 25 kPa, respectively; no differences were found in aggregate moduli across groups.

Altogether, treatment with 4 α -PDD during days 10-14 provided the greatest increases in collagen content and tensile properties. Based on these results, this treatment regimen was carried forward into Phase II.

Phase II: TRPV4 activation versus Na⁺/K⁺ pump inhibition

In Phase II, we compared the effects of TRPV4 activation to the effects of Na⁺/K⁺ pump inhibition, and we further studied whether the combination of these two stimuli would outperform their individual use. Self-assembled articular cartilage constructs were treated with either 10 μ M 4 α -PDD, 20 μ M ouabain, or a combination of the two during $t=10-14$ days. Constructs were grown in culture to $t=28$ days. At the end of culture, constructs treated with ouabain or with the combination of 4 α -PDD and ouabain were visibly smaller than control constructs or constructs treated with 4 α -PDD alone (Figure 4-2). Diameter, thickness, and WW values are provided in Table 4-1. Constructs treated with ouabain or with both agents had significantly smaller diameters (17% and 14% decreases from

control, respectively), thicknesses (49% and 33% decreases), and wet weights (60% and 57% decreases).

Construct biochemical data for Phase II are provided in Table 4-2. Treatment with 4 α -PDD, ouabain, or their combination resulted in significant increases in collagen/WW compared to control (increases of 80%, 118%, and 93%, respectively), but no differences between each other. Collagen production per cell was greatest in constructs treated with 4 α -PDD (85% increase over control), with no differences among control, ouabain, or the combination 4 α -PDD and ouabain. GAG/WW was not different across groups, but GAG production per cell was significantly decreased in constructs treated with ouabain (60% decrease from control) and the combination of 4 α -PDD and ouabain (57% decrease from control). No differences were observed in cell number across groups.

Biomechanical properties were again assessed with uniaxial tensile and creep indentation testing. Tensile stiffness and strength data for Phase II are shown in Figure 4-3. Young's moduli for control, treatment with 4 α -PDD, treatment with ouabain, and combined treatment were 282 ± 105 , 538 ± 133 , 572 ± 136 , and 583 ± 121 kPa, respectively. Treatment with 4 α -PDD, ouabain, and their combination resulted in significant increases in Young's moduli compared to control (91%, 103%, and 107% increases, respectively), but no differences between each other. UTS values for control, treatment with 4 α -PDD, treatment with ouabain, and combined treatment were 106 ± 29 , 203 ± 64 , 256 ± 89 , and 251 ± 61 kPa, respectively. Treatment with ouabain or with the combination of

4 α -PDD and ouabain produced the greatest improvements in construct UTS (141% and 136% increases over control, respectively), followed by treatment with 4 α -PDD (91% increase over control, but not statistically significant). In terms of compressive properties, aggregate moduli for control, treatment with 4 α -PDD, treatment with ouabain, and combined treatment were 67 ± 14 , 73 ± 18 , 67 ± 19 , and 74 ± 23 kPa, respectively; no differences were found in aggregate moduli across groups.

Discussion

This study employed a two-phased approach to evaluate the effects of TRPV4 channel activation on tissue engineered articular cartilage. Experimental results supported the hypotheses motivating this study: 1) TRPV4 activation resulted in significant improvements in construct biochemical and biomechanical properties; 2) culture days 10-14 were identified as the optimal treatment time window to produce the greatest improvements in constructs; and 3) activation of TRPV4, a Ca²⁺-permeable channel, produced results comparable to Na⁺/K⁺ pump inhibition. To our knowledge, this is the first study to examine TRPV4 channel activation in tissue engineering. The results of this investigation demonstrate that direct chemical modulation of intracellular ion concentrations can be a powerful tool in tissue engineering.

In Phase I, it was found that the optimal time window for TRPV4 activation in self-assembled articular cartilage constructs is during culture days 10-14. Compared to control, treatment with the TRPV4 channel agonist 4 α -PDD during

days 10-14 led to significant improvements in collagen content (88% increase), tensile stiffness (153% increase), and tensile strength (130% increase). However, constructs were not improved by treatment during days 6-10 or 14-18, thereby highlighting the importance of timing during *in vitro* tissue development. The beneficial effects of treatment during days 10-14 are corroborated by previous work showing that other stimuli also produce their maximal effects during this time window [63, 68, 160]. To understand why this time period is so crucial, it is important to consider the developmental milestones of constructs during self-assembly, a process that has been shown to resemble *in vivo* cartilage development [163]. During self-assembly, collagen production peaks between days 10-14 of culture, while GAG production continues indiscriminately. This rapid synthesis of GAG with no new collagen secretion contributes to pre-stress within the nascent ECM, thereby compromising the engineered tissue's tensile properties [158, 200]. Directly modulating this imbalance between GAG and collagen has been shown to improve the tensile properties of self-assembled constructs [158, 159]. Thus, during days 10-14, before collagen production tapers and GAG production ramps up, cells within the developing construct may be more susceptible to interventions that induce new collagen biosynthesis. Based on the results from Phase I, the optimal treatment time window of $t=10-14$ days was carried forward to Phase II.

In Phase II, TRPV4 activation using 4 α -PDD was compared to Na⁺/K⁺ pump inhibition using ouabain. A previous study from our group showed that inhibition of the Na⁺/K⁺ pump using 20 μ M ouabain during days 10-14 of culture

improved the collagen content and tensile properties of self-assembled articular cartilage constructs [160], results that were corroborated by the present study. It was found that 10 μ M 4 α -PDD produced improvements in construct tensile properties that were comparable to 20 μ M ouabain, with no added benefit when the two stimuli were combined. Specifically, application of either 4 α -PDD or ouabain led to an approximately 2-fold increase in tensile stiffness. Though each agent produced an identical net enhancement in tensile stiffness, it is clear from the differences in construct sizes and biochemical content that the precise physiological responses to these agents, and therefore the mechanisms underlying tensile improvements, vary considerably.

Notably, treatment with ouabain significantly reduced GAG production on a per-cell basis. Lower GAG levels are associated with decreased size and wet weight in cartilage [10], and the subsequent reduction in size in ouabain-treated constructs led to an increase in the percentage of collagen per wet weight, even though the per-cell production of collagen did not change. These phenomena suggest that ouabain treatment promotes a maturational growth phenotype, in which the tissue maintains a uniform size during ECM synthesis and remodeling, rather than an expansive growth phenotype, in which the tissue experiences a volumetric increase in size during ECM deposition [10, 110, 158]. Maturational growth in cartilage is associated with greater tensile integrity compared to expansive growth.

Unlike ouabain, treatment of constructs with 4 α -PDD resulted in increased collagen production per cell, with no change in GAG production per cell. This net

increase in collagen deposition at a steady level of GAG production is likely responsible for the improved tensile stiffness of constructs treated with 4 α -PDD. It should be noted, however, that 4 α -PDD did not increase tensile strength (UTS) to the same magnitude achieved with ouabain. Therefore, it is possible that the benefits of maturational growth seen with ouabain treatment outweigh the biosynthesis triggered by 4 α -PDD. Moreover, combined treatment with 4 α -PDD and ouabain resulted in the same changes in size and biochemical content observed for treatment with ouabain alone, implying that Na⁺/K⁺ pump inhibition predominates over TRPV4 activation in producing effects at the cell and tissue levels. This observation is similar to a result from a previous study in which constructs were treated with a combination of ouabain and ionomycin, a Ca²⁺ ionophore; the combo did not outperform individual ouabain or ionomycin [160].

Further work is necessary to determine how alterations in intracellular ion concentrations elicited by direct or indirect stimuli lead to changes in chondrocyte ECM synthesis. Ion channels are thought to be involved in the cellular response to dynamic compression [46, 114, 154], fluid shear [58, 59, 246], hydrostatic pressure [65, 92, 226, 234], and osmotic stress [72, 73, 194, 195]. In particular, the TRPV4 channel has been shown to play a central role in regulating the chondrocyte response to osmotic stress [90, 170], as well as in promoting chondrogenic differentiation [156]. TRPV4 may also be implicated in osmotic stress-related pathogenesis of osteoarthritis [48]. The present study demonstrates that TRPV4 activation in engineered cartilage constructs can produce observable, tissue-level changes. Because of the osmosensitivity of

TRPV4, it will be important in the future to examine the combined effects of osmotic stress and TRPV4 modulation on tissue engineered cartilage. Future studies that involve confocal imaging of intact self-assembled constructs may provide a better understanding of the importance of TRPV4 during *in vitro* tissue development.

In summary, this study investigated whether activation of the Ca^{2+} -permeable TRPV4 channel would alter the biochemical and biomechanical properties of tissue engineered articular cartilage. It was shown that TRPV4 activation improved construct tensile properties, that the effects of TRPV4 activation were time-dependent, and that net improvements were on par with those produced by inhibiting the Na^+/K^+ pump. To our knowledge, this is the first study to examine TRPV4 channel activation in tissue engineering. The results of this study demonstrate the effectiveness of ion channel modulation as a strategy for improving the functional properties of engineered tissues. Further investigation of the role of TRPV4 in self-assembled constructs should be undertaken at both a mechanistic level (e.g., examine cell volume regulation and calcium transients *in situ*) and at a functional engineering level (e.g., assessment of different durations of TRPV4 activation, or combining TRPV4 activation or inhibition with hyper-osmotic or hypo-osmotic stimulation).

Table 4-1. Growth metrics of tissue engineered constructs.

In Phase I, no differences were found in construct diameter, thickness, or wet weight (WW) among groups. In Phase II, constructs treated with ouabain or with both 4 α -PDD and ouabain had significantly reduced diameters (0.83x and 0.86x control, respectively), thicknesses (0.51x and 0.67x control), and WW (0.40 and 0.43x control). Data are presented as means \pm standard deviations. Lowercase letters denote significant differences within a column; groups not connected by the same letter are considered significantly different ($p < 0.05$).

Group	Diameter (mm)	Thickness (mm)	WW (mg)
<i>Phase I (10 μM 4α-PDD)</i>			
Control	6.29 \pm 0.17	0.62 \pm 0.05	36.7 \pm 3.1
Treatment on days 6-10	6.27 \pm 0.16	0.63 \pm 0.05	37.2 \pm 2.8
Treatment on days 10-14	6.31 \pm 0.18	0.63 \pm 0.05	36.2 \pm 2.4
Treatment on days 14-18	6.26 \pm 0.16	0.62 \pm 0.06	37.2 \pm 2.8
<i>Phase II</i>			
Control	6.35 \pm 0.06 ^a	0.68 \pm 0.10 ^a	38.3 \pm 1.5 ^a
10 μ M 4 α -PDD	6.30 \pm 0.13 ^a	0.63 \pm 0.10 ^a	39.6 \pm 2.3 ^a
20 μ M ouabain	5.29 \pm 0.04 ^b	0.35 \pm 0.08 ^b	15.2 \pm 0.6 ^b
Combo	5.45 \pm 0.18 ^b	0.45 \pm 0.08 ^b	16.3 \pm 1.3 ^b

Table 4-2. Biochemical content of tissue engineered constructs.

In Phase I, collagen/WW was highest in constructs treated with 4 α -PDD during days 10-14 (1.88x control), followed by constructs treated during days 14-18 (1.40x control). These differences in collagen content were upheld when normalized to cell number. There were no differences observed in GAG content in Phase I. In Phase II, treatment with 4 α -PDD, ouabain, or their combination resulted in significant increases in collagen/WW compared to control (1.80x, 2.18x, and 1.93x control, respectively), but no differences between each other. Collagen production per cell was greatest in constructs treated with 4 α -PDD (1.85x control). GAG production per cell was significantly decreased in constructs treated with ouabain (0.40x control) and the combination of 4 α -PDD and ouabain (0.43x control). No differences in cell number were observed in Phase I or Phase II. Data are presented as means \pm standard deviations. Lowercase letters denote significant differences within a column; groups not connected by the same letter are considered significantly different ($p < 0.05$).

Group	Total cells (x 10 ⁶)	Collagen (% WW)	GAG (% WW)	Collagen (μ g/10 ⁶ cells)	GAG (μ g/10 ⁶ cells)
<i>Phase I</i>					
Control	5.64 \pm 0.33	5.9 \pm 0.7 ^c	3.6 \pm 0.5	383 \pm 60 ^c	232 \pm 44
Days 6-10	5.73 \pm 0.37	6.2 \pm 1.1 ^{bc}	3.7 \pm 0.4	401 \pm 82 ^{bc}	245 \pm 39
Days 10-14	5.71 \pm 0.43	11.1 \pm 2.3 ^a	3.4 \pm 0.9	694 \pm 97 ^a	212 \pm 46
Days 14-18	5.67 \pm 0.46	8.3 \pm 1.1 ^b	3.7 \pm 0.7	548 \pm 123 ^{ab}	242 \pm 62
<i>Phase II</i>					
Control	5.73 \pm 0.24	5.5 \pm 0.7 ^b	4.0 \pm 0.8	363 \pm 37 ^b	268 \pm 50 ^a
10 μ M 4 α -PDD	5.79 \pm 0.29	9.8 \pm 1.8 ^a	4.5 \pm 1.1	669 \pm 127 ^a	305 \pm 74 ^a
20 μ M ouabain	5.55 \pm 0.20	11.9 \pm 2.5 ^a	4.0 \pm 1.1	325 \pm 67 ^b	108 \pm 28 ^b
Combo	5.71 \pm 0.26	10.5 \pm 2.7 ^a	4.1 \pm 1.3	296 \pm 63 ^b	116 \pm 39 ^b

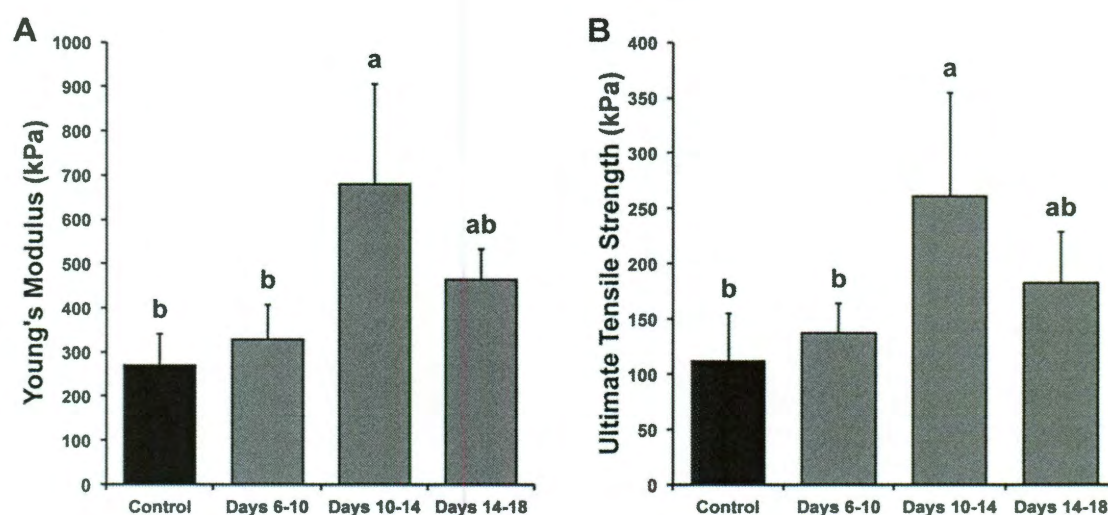


Figure 4-1. Phase I tensile properties of cartilage constructs

(A) Tensile stiffness for all groups. Constructs treated with 4 α -PDD during days 10-14 had the highest Young's moduli (153% greater than control). (B) Tensile strength for all groups. Constructs treated with 4 α -PDD during days 10-14 had the highest ultimate tensile strength (UTS) (133% greater than control). Data are presented as means + standard deviations. Lowercase letters denote significant differences; groups not connected by the same letter are considered significantly different ($p < 0.05$).

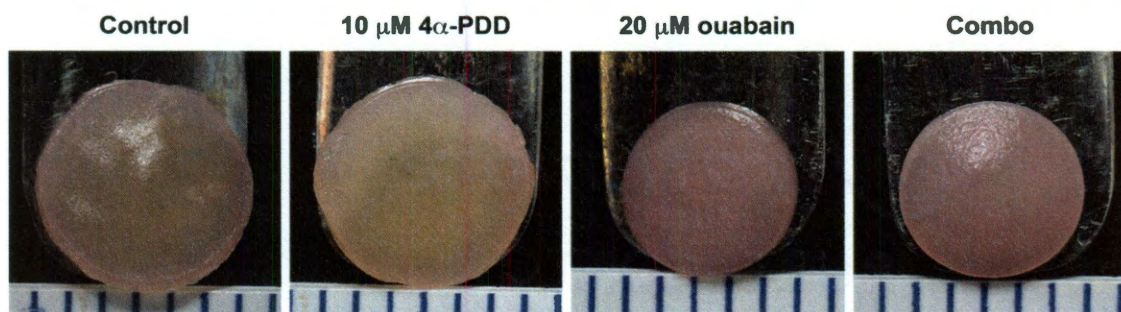


Figure 4-2. Phase II gross morphology of tissue engineered constructs

Photographs taken at 4 weeks. From left to right: representative photographs of constructs from the control group, treated with 10 μM 4α-PDD, treated with 20 μM ouabain, and treated with both with 10 μM 4α-PDD and 20 μM ouabain. Constructs treated with ouabain or with both 4α-PDD and ouabain were visibly smaller than control constructs or constructs treated with 4α-PDD alone. Scale markings are spaced 1 mm apart.

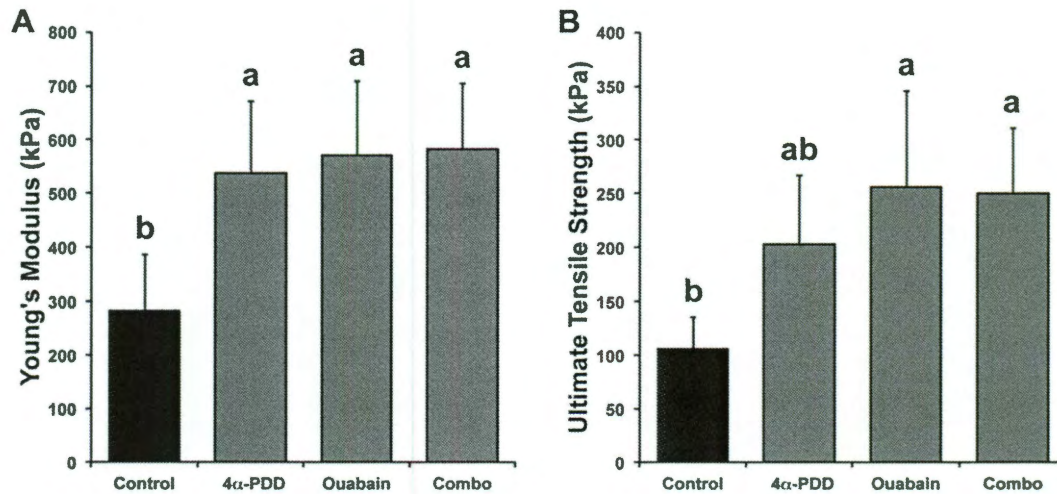


Figure 4-3. Phase II tensile properties of cartilage constructs

(A) Tensile stiffness for all groups. Treatment with 4α-PDD, ouabain, and their combination resulted in significant increases in Young's moduli compared to control (91%, 103%, and 107% increases, respectively), but no differences between each other. (B) Tensile strength for all groups. Treatment with ouabain or with the combination of 4α-PDD and ouabain improved construct UTS (141% and 136% increases over control, respectively), followed by treatment with 4α-PDD (91% increase over control, but not statistically significant). Data are presented as means + standard deviations. Lowercase letters denote significant differences; groups not connected by the same letter are considered significantly different ($p < 0.05$).

Chapter 5. Osmotic loading of self-assembled articular cartilage^{*}

^{*} Chapter submitted for publication as **Eleswarapu SV** and Athanasiou KA, "Osmotic loading of self-assembled articular cartilage."

Abstract

Articular cartilage lacks an intrinsic capacity to heal in response to trauma or arthritis. As such, there is a need for suitable biomaterial replacements for damaged cartilage. Tissue engineering aims to fulfill this need by fabricating cell-based replacements *in vitro*. A central objective of cartilage tissue engineering is to develop a biomaterial with robust biochemical and biomechanical properties. Osmotic loading has been shown to enhance biosynthesis in single cells, but there is a lack of literature on the effects of osmotic loading on engineered cartilage constructs. The objectives of this study were 1) to determine whether osmotic loading would enhance the biochemical and biomechanical properties of self-assembled articular cartilage constructs, and 2) to identify an optimal osmotic loading regimen for greatest construct improvement. Self-assembled constructs were grown for 4 weeks and were subjected to static (0 Hz) or dynamic (0.00083 Hz) application of hypo-osmotic (250 mOsm) or hyper-osmotic (450 mOsm) loading for 1 h per day during days 10-14 of culture. Iso-osmotic control constructs (350 mOsm) were grown in parallel, and construct morphology, histology, collagen and sulfated glycosaminoglycan (GAG) content, and tensile and compressive properties were evaluated. It was found that the optimal osmotic loading regimen was static application of hyper-osmotic medium. Compared to iso-osmotic controls, static hyper-osmotic constructs exhibited significant increases in GAG/WW (64% increase), collagen/WW (65% increase), compressive stiffness (94% increase), tensile stiffness (70% increase), and tensile strength (94% increase). Dynamic osmotic loading did not improve self-

assembled construct properties, though future work should examine different dynamic loading regimens. We conclude that osmotic loading is a powerful method for improving cellular biomaterials and that specific regimens exist to achieve optimal functional properties.

Introduction

Articular cartilage lines the surfaces of diarthrodial joints and serves to provide lubrication and load distribution during motion. Proper mechanical function is conferred by a copious extracellular matrix (ECM) composed primarily of collagen type II and glycosaminoglycans (GAGs). Due to the tissue's avascularity and hypocellularity, it lacks an intrinsic capacity to heal. Damage wrought by trauma or arthritis is therefore irreversible and leads inexorably to pain and disability [28]. Thus, there is considerable need for a suitable biomaterial replacement for damaged cartilage. Tissue engineering strives to address this need by fabricating cell-based replacements *in vitro*. A central goal of cartilage tissue engineering is to develop a biomaterial with robust biochemical and biomechanical properties [51].

Toward this end, our laboratory has developed a self-assembly process for engineering cartilage constructs [105]. In this technique, chondrocytes are seeded at a high density into pre-fabricated, non-adherent, cylindrical molds. In a process that resembles *in vivo* cartilage development, cells first condense into free-floating, disc-shaped constructs and then proceed to synthesize ECM [163]. Since this method does not employ a scaffold, it sidesteps concerns often

associated with traditional tissue engineering strategies, such as toxicity, biodegradability, and impaired cell signaling [105]. Additionally, because the self-assembly process is a purely cell-mediated phenomenon, it can serve as a model system for evaluating the direct effects of exogenous stimuli on cell behavior and ECM production [64, 67, 68, 159, 160].

Osmotic stress has been shown previously to affect cellular behavior and enhance biosynthesis in single chondrocytes [41, 42, 72, 73, 194-196, 222], and it is known to play a role in native cartilage function [21, 44, 77, 96, 134]. Despite the abundance of information on the behavior of suspended cells and native tissue in response to osmotic stress, there is a dearth of such evidence for engineered tissues, except for a recent study in which mature chondrocytes were encapsulated in agarose hydrogels and exposed to continuous hyper-osmotic stress [165]. It is widely understood that osmotic loading is an indirect consequence of deformational loading of articular cartilage *in vivo*. During joint motion, compressive loads force fluid out of the tissue, thereby creating a temporary effective hyper-osmotic microenvironment for chondrocytes within the tissue. This hyper-osmotic stress has been shown to result in shrinkage of cells [72], calcium fluxes across cell membranes and reorganization of actin stress fibers [72, 73, 245], alteration in nuclear geometry [79], greater nucleocytoplasmic transport [80], and increased intracellular signaling that drives gene expression [222], and, ultimately, ECM biosynthesis [102, 113, 167, 223].

Encouraged by these results from the literature, we decided to examine the effects of static and dynamic osmotic loading on self-assembled articular

cartilage constructs. The objectives of this study were 1) to determine whether osmotic loading would enhance the biochemical and biomechanical properties of self-assembled constructs, and 2) to identify an optimal osmotic loading regimen for greatest construct improvement. Constructs were self-assembled from bovine chondrocytes and subjected to 1 h of static or dynamic application of hypo-osmotic or hyper-osmotic loading during days 10-14 of culture. Control constructs were grown in parallel, and construct morphology, histology, biochemical content, and biomechanical properties were assessed at the end of 4 weeks. It was hypothesized that 1) osmotic loading would improve construct properties and 2) an optimal osmotic loading regimen exists for which constructs undergo greatest improvement.

Materials and methods

Medium formulations

This study employed three medium formulations: control medium, hypo-osmotic medium, and hyper-osmotic medium. Osmolarity was monitored using a VAPRO 5520 vapor pressure osmometer (Wescor). Iso-osmotic control medium (approximately 350 mOsm) is a chondrogenic medium described extensively by our group [64, 159, 163]: Dulbecco's modified Eagle's medium (DMEM) with 4.5 mg/mL of glucose and L-glutamine (Invitrogen); 100 nM dexamethasone (Sigma); 0.1 mM non-essential amino acids (Invitrogen); 1% ITS+ (insulin, human transferrin, and selenous acid; BD Scientific); 1% penicillin-streptomycin-fungizone (BioWhittaker); 50 µg/mL ascorbate-2-phosphate; 40 µg/mL L-proline;

and 100 µg/mL sodium pyruvate (Fisher Scientific). Hypo-osmotic medium (250 mOsm) was prepared by titrating distilled water into control medium. Hyper-osmotic medium (450 mOsm) was prepared by adding sucrose to control medium.

Chondrocyte isolation

Cartilage harvested from the distal femur and patellofemoral grooves of 1-week-old male calves (Research 87) was digested in 0.2% collagenase type II (Worthington) for 24 h. To normalize variability among animals, each leg came from a different animal, and cells from 8 legs were pooled to create a mixture of chondrocytes. Cells were counted using a hemocytometer and then frozen at -80°C in DMEM containing 20% FBS and 10% DMSO.

Preparation of agarose wells for construct self-assembly

Cylindrical, non-adherent wells were prepared using a technique adapted from previous work [105, 163]. Briefly, a stainless steel mold consisting of 5 mm diameter cylindrical prongs was placed into sterile, molten 2% agarose in a 48-well plate. The agarose solidified at room temperature for 60 min, and the stainless steel mold was carefully removed. Two changes of control medium were used to completely saturate the agarose well by the time of cell seeding.

Self-assembly and osmotic loading of cartilage constructs

Chondrocytes were thawed and counted within 5 days of being isolated and frozen. After thawing, cell viability was >90%. To create each construct, 5.5 million cells in 100 μ L of control medium were seeded into each cylindrical agarose well, followed by addition of 400 μ L control medium after 4 h. Cells settled and coalesced into free-floating cylindrical disc-shaped constructs; $t=1$ day was defined as 24 h after seeding. All constructs were cultured in the agarose wells until $t=10$ days, at which point they were gently unconfined and transferred to 48-well plates unrestricted by circumferential confinement. Constructs received 500 μ L medium change every 24 h and remained in culture until $t=28$ days. All culture was performed at 37°C and 10% CO₂.

This study examined the following five groups: control, Low Static, Low Dynamic, High Static, and High Dynamic. Control constructs received iso-osmotic control medium during $t=1-28$ days. Low Static constructs received hypo-osmotic medium for 1 h during $t=10-14$ days. Low Dynamic constructs were exposed to a 2-hour-long alternating regimen of 10 min of hypo-osmotic medium followed by 10 min of control medium during $t=10-14$ days. High Static constructs received hyper-osmotic medium for 1 h during $t=10-14$ days. High Dynamic constructs were exposed to a 2-hour-long alternating regimen of 10 min of hyper-osmotic medium followed by 10 min of control medium during $t=10-14$ days. All constructs received control medium when not undergoing treatment. During the Low Dynamic and High Dynamic treatment regimens, medium was added and

removed with care to minimize flow-induced shear effects on constructs. Constructs were assigned randomly to experimental groups.

Gross morphology and histology

At $t=28$ days, constructs were removed from culture. Photographs were taken, and dimensions were measured from photographs using ImageJ software (National Institutes of Health). Wet weights (WW) were recorded, and constructs were portioned for analysis. A 3 mm diameter punch was taken from the construct's center for indentation testing. The remaining outer ring was split into portions for histology, quantitative biochemistry, and tensile testing. For histology, constructs were cryoembedded and sectioned at 14 μm . Samples were fixed in 10% formalin and stained with Safranin-O/fast green (GAG).

Quantitative biochemistry

Biochemistry samples were weighed wet, frozen, and lyophilized. Dry weights (DW) were measured, after which samples were digested with 125 $\mu\text{g}/\text{mL}$ papain (Sigma) for 18 h at 65°C. Total DNA content was assessed with a PicoGreen Assay (Invitrogen), and cell number was estimated assuming 7.7 pg DNA per cell. Sulfated GAG content was quantified using the Blyscan Glycosaminoglycan Assay (Biocolor). Following hydrolysis with 4 N sodium hydroxide for 20 min at 110°C, total collagen content was quantified with a modified chloramine-T hydroxyproline assay [105, 238]. Sircol collagen standard (Biocolor) was used such that the standard curve reflected collagen amount, eliminating the need to

convert hydroxyproline to collagen. Total collagen and sulfated GAG were normalized to WW and DW for making comparisons.

Creep indentation testing

A creep indentation apparatus was used to determine compressive behavior of each construct [12]. Each sample was affixed to a stainless steel surface and equilibrated for 20 min in PBS. A 0.7 g (0.007 N) mass was applied with a 0.8 mm diameter flat, porous indenter tip, and specimens crept until equilibrium. Specimen thickness was measured from photographs using ImageJ software. Aggregate modulus, a measure of compressive stiffness, was calculated using a semi-analytical, semi-numeric, linear biphasic model [12].

Tensile testing

Tensile specimens were cut into dog-bone shapes with 1-mm gauge length. Specimen thickness and width were measured from photographs using ImageJ software. Specimens were then affixed with glue to paper tabs outside the gauge length, and these tabs were gripped during testing. A uniaxial materials testing system (Instron Model 5565) was employed to determine tensile properties. Tensile tests were performed until failure at a strain rate of 1% of the gauge length per second. Force-displacement curves were generated, and stress-strain curves were calculated by normalizing to specimen dimensions. Young's modulus, a measure of tensile stiffness, was determined by least squares fitting

of the linear region of the stress-strain curve. The ultimate tensile strength (UTS) was determined as the maximum stress reached during a test.

Statistical analysis

All quantitative biochemical and biomechanical assessments were made using $n=5-9$. Data are represented as means \pm standard deviations. To compare among treatment groups, single-factor ANOVA was employed, and statistical significance was defined as $P<0.05$. If significant differences were observed, a Fisher LSD *post hoc* test was performed to determine specific differences among groups.

To determine whether biochemical data correlated with biomechanical data, pairwise correlation analyses were performed using at least 20 data points. Probability distributions were inspected for each variable (collagen/WW, collagen/DW, GAG/WW, GAG/DW, Young's modulus, UTS, and aggregate modulus). Spearman's rank correlation coefficients (ρ) were then calculated to assess non-parametric statistical dependence between biochemical and biomechanical variables. Statistical significance for each Spearman's ρ was defined as $P<0.05$. All statistical analyses were performed using JMP 9.0.2 (SAS Institute).

Results

Gross appearance and histology

At $t=28$ days, constructs from every group had similar flat surfaces with no surface abnormalities (Figure 5-1). Diameter, thickness, and WW values are provided in Table 5-1. High Static and High Dynamic had significantly greater diameter (both 1.10x control) compared to all other groups. Low Dynamic and High Dynamic had the greatest thicknesses (1.15x and 1.12x control, respectively), followed by High Static (1.07x control). Low Dynamic and High Dynamic had significantly greater WW (1.07x and 1.06x control, respectively) compared to all other groups. On histology, all constructs stained positively for GAG (Figure 5-1).

Quantitative biochemistry

Cell numbers are shown in Table 5-2. High Static had a significantly higher cell number (1.16x control) compared to all other groups.

GAG/WW is shown in Figure 5-2A. GAG/WW values for control, Low Static, Low Dynamic, High Static, and High Dynamic were $3.9\pm 0.4\%$, $4.4\pm 0.6\%$, $3.5\pm 0.7\%$, $6.5\pm 1.1\%$, and $4.2\pm 0.7\%$, respectively. High Static had the greatest GAG/WW (1.64x control). GAG/DW, provided in Table 5-2, showed a similar trend to that observed for GAG/WW.

Collagen/WW is shown in Figure 5-3A. Collagen/WW values for control, Low Static, Low Dynamic, High Static, and High Dynamic were $3.3\pm 0.7\%$, $4.5\pm 0.8\%$, $3.2\pm 0.6\%$, $5.4\pm 0.9\%$, and $3.7\pm 0.6\%$, respectively. High Static had the

highest collagen/WW (1.65x control), followed by Low Static (1.38x control). Low Dynamic and High Dynamic were not different from control. Collagen/DW, provided in Table 5-2, showed a similar trend to that observed for collagen/WW.

Biomechanical evaluation

Compressive stiffness, represented by aggregate modulus, is shown in Figure 5-2B. Aggregate moduli for control, Low Static, Low Dynamic, High Static, and High Dynamic were 54 ± 12 , 61 ± 16 , 51 ± 14 , 104 ± 33 , and 60 ± 19 kPa, respectively. Trends for aggregate moduli followed those of GAG/WW. The highest aggregate modulus was found in the High Static group (1.94x control).

Tensile stiffness and strength are shown in Figure 5-3. Young's moduli for control, Low Static, Low Dynamic, High Static, and High Dynamic were 374 ± 93 , 430 ± 146 , 241 ± 74 , 635 ± 122 , and 411 ± 196 kPa, respectively. High Static had the highest Young's moduli (1.70x control). Low Dynamic had the lowest Young's moduli (0.64x control). UTS values for control, Low Static, Low Dynamic, High Static, and High Dynamic were 99 ± 55 , 189 ± 67 , 130 ± 30 , 192 ± 50 , and 125 ± 57 kPa, respectively. High Static and Low Static had the highest UTS (1.94x and 1.92x control, respectively), followed by High Dynamic (1.32x control).

Correlation analysis

Probability distributions were inspected in the raw data for each biochemical and biomechanical variable. Biochemical assessments (collagen/WW, collagen/DW, GAG/WW, and GAG/DW) conformed to normal distributions, but biomechanical

properties (tensile stiffness, tensile strength, and compressive stiffness) were found to have negative skews. Pairwise correlation analyses were performed between biomechanical properties and biochemical assessments. Based on the skewness of the biomechanical data, correlations were evaluated by calculating Spearman's ρ and associated P -values (Table 5-3). Strong, statistically significant correlations were found between collagen and all three biomechanical properties. Statistically significant correlations were found between GAG/WW and all three biomechanical properties, but GAG/DW appeared to correlate only with aggregate modulus.

Discussion

This study examined the effects of static and dynamic osmotic loading during self-assembly of articular cartilage constructs. Experimental results supported the hypotheses motivating this study: 1) osmotic loading of self-assembled constructs produced significant increases in biochemical and biomechanical properties, and 2) static exposure to hyper-osmotic medium was identified as the optimal osmotic loading regimen to produce the greatest improvements in constructs. Although the literature is replete with studies examining the effects of osmotic stress on individual cells [41, 42, 72, 73, 194-196, 222] and native tissue explants [21, 44, 77, 96, 134], this is the first study to undertake a systematic, head-to-head comparison of static and dynamic osmotic loading regimens on tissue engineered cartilage. Moreover, this is the first study to examine the direct effects of osmotic loading in a scaffoldless, cell-based biomaterial platform. The

results of this investigation demonstrate the power of osmotic loading as a stimulus to improve cellular biomaterials.

It was found that the optimal regimen for osmotic loading of self-assembled constructs is static application of hyper-osmotic medium for 1 h during $t=10-14$ days (the High Static group). Compared to control constructs, High Static constructs exhibited significant increases in GAG/WW (64% increase), collagen/WW (65% increase), compressive stiffness (94% increase), tensile stiffness (70% increase), and tensile strength (94% increase). The beneficial effects observed with treatment during $t=10-14$ days are corroborated by previous studies showing that other stimuli also produce their maximal effects when applied to constructs during the same time window [68, 160].

The improvements observed at the construct level are likely the consequences of changes occurring at the cellular level in response to osmotic stress. A number of potential cellular mechanisms have been proposed to explain the chondrocyte response to changes in osmolarity. For example, chondrocytes cope with osmotic stress through volume regulation. Cells undergo shrinkage in a hyper-osmotic environment; this cellular strain is associated with calcium transients and actin cytoskeleton reorganization [72, 73, 245], both of which are known to affect downstream signaling and, ultimately, gene expression. Furthermore, it has been shown previously that hyper-osmotic loading increases GAG synthesis at the cellular level, an effect shown to require p38 mitogen-activated protein kinase (MAPK) signaling [102]. Signaling via p38 MAPK also plays a role in hyper-osmotic stress-induced expression of SOX9, a transcription

factor important in regulating cartilage ECM genes [222]. Additionally, recent evidence suggests that hyper-osmotic stress induces a change in nuclear geometry, resulting in altered chromatin condensation, increased nuclear lacunarity, and greater nucleocytoplasmic transport [79, 80]. It is possible that volume regulation, signaling, and nuclear alteration operate in concert to produce tissue-level changes in the ECM over time; to test this hypothesis, a thorough examination of chondrocytes *in situ* during self-assembly must be undertaken.

It was found that, compared to controls, static application of hypo-osmotic medium for 1 h during $t=10-14$ days (the Low Static group) produced significant increases in collagen/WW (38% increase) and tensile strength (92% increase), but not in tensile stiffness. This absence of an effect in tensile stiffness is unexpected, given the relatively strong Spearman's ρ and P -values in pairwise correlations between collagen/WW and all three biomechanical properties (Table 5-3). One possible explanation is that collagen abundance may preferentially determine the tissue's failure point (and thus strength), whereas other components within the network, such as crosslinks, may determine the network's response to strain (and thus stiffness) [181]. As in High Static constructs, the effects observed in Low Static constructs may be explained by cellular changes in response to alterations in construct microenvironment. In particular, hypo-osmotic stimulation has been shown previously to induce actin reorganization and calcium signaling [73, 173]. Future work involving confocal imaging of intact self-assembled constructs may provide a better understanding of these and other responses to hypo-osmotic and hyper-osmotic stimulation.

Dynamic osmotic loading did not improve self-assembled constructs. The motivation to study dynamic osmotic loading comes from evidence in the literature that cyclic compressive deformation improves the properties of engineered cartilage [146, 161]. It is thought that fluid fluxes contribute to transitory alterations in tissue osmolarity that are sensed and responded to by chondrocytes. Previous studies have shown that replicating these compression-induced changes in osmolarity using dynamic osmotic loading may induce cellular biosynthesis [41, 42]. Guided by evidence in the literature that the time constant for regulatory volume decrease following hyper-osmotic stress is on the order of 5-8 min [33, 78, 173], we chose to examine a cyclic regimen of 10 min of osmotic load followed by 10 min of control medium (frequency of 0.00083 Hz) for 2 h during $t=10-14$ days. Because no effect was observed with a regimen of 0.00083 Hz, future work should evaluate a faster regimen, such as 0.0125 Hz [41], to determine if dynamic osmotic loading can produce detectable changes in self-assembled constructs. It is important to note, however, that just as differences were observed between static and dynamic stimulation in this study, static application of hydrostatic pressure on self-assembled constructs has been shown previously to outperform dynamic application (0.1 Hz and 1 Hz) [67]. It is possible that self-assembled constructs may not exhibit the same response to stimuli as scaffold-based biomaterials. Now that the present study demonstrates that self-assembled constructs respond successfully to static hyper-osmotic stimulation, future studies are merited to examine different frequencies of dynamic osmotic loading, as well as longer time courses of static application.

Pairwise correlation analyses revealed that collagen correlated strongly with all three biomechanical properties (tensile stiffness, tensile strength, and compressive stiffness), but GAG/DW correlated only with compressive stiffness, and not the tensile data (Table 5-3). The conventional understanding of cartilage structure-function relationships is that collagen confers the tissue's tensile properties and GAG gives rise to its compressive properties. The pairwise correlations suggest, however, that collagen fibers and GAG molecules may work in concert to provide compressive stiffness. Follow-up studies should examine the precise distribution of GAG within the collagen network of the self-assembled construct to shed light on the complex interplay between these ECM components.

Based on the results of this study, static application of hyper-osmotic medium appears to be the most promising osmotic loading regimen for improving the biochemical and biomechanical properties of self-assembled articular cartilage constructs. Further investigation of the role of medium osmolarity on self-assembled constructs should be undertaken at both a mechanistic level (e.g., examine cell volume regulation and calcium transients *in situ*) and at a functional engineering level (e.g., assessment of faster dynamic loading regimens, or increasing the duration of exposure to osmotic stress during static loading).

To our knowledge, this is the first study to perform a head-to-head comparison of static and dynamic osmotic loading regimens on tissue engineered cartilage. It is also the first study to examine the direct effects of osmotic loading in a scaffoldless, cell-based biomaterial. Static hyper-osmotic

stimulation of self-assembled constructs produced the greatest improvement in biochemical and biomechanical properties, including a near doubling of tensile stiffness and strength. Dynamic osmotic loading did not improve construct properties. The results of this study demonstrate the effectiveness of osmotic loading as a strategy for improving the functional properties of cellular biomaterials.

Table 5-1. Growth metrics of self-assembled constructs

Both static and dynamic exposure to hyper-osmotic medium (High Static and High Dynamic, respectively) resulted in 10% increases in construct diameter compared to control. Dynamic exposure to both hypo-osmotic and hyper-osmotic medium (Low Dynamic and High Dynamic, respectively) resulted in 15% and 12% increases in construct thickness compared to control, as well as in 7% and 6% increases in construct wet weight. Data are presented as means \pm standard deviations. Lowercase letters denote significant differences within a column; groups not connected by the same letter are significantly different ($P < 0.05$).

	Diameter (mm)	Thickness (mm)	Wet Weight (mg)
Control	5.81 \pm 0.15 ^c	0.52 \pm 0.04 ^b	38.4 \pm 1.7 ^b
Low Static	6.04 \pm 0.19 ^b	0.51 \pm 0.05 ^b	38.7 \pm 1.3 ^b
Low Dynamic	6.04 \pm 0.12 ^b	0.60 \pm 0.04 ^a	41.0 \pm 1.5 ^a
High Static	6.39 \pm 0.12 ^a	0.56 \pm 0.03 ^{ab}	38.2 \pm 1.4 ^b
High Dynamic	6.45 \pm 0.07 ^a	0.59 \pm 0.04 ^a	40.7 \pm 0.7 ^a

Table 5-2. Biochemical analysis of self-assembled constructs

Cell number, collagen/dry weight, and GAG/dry weight of self-assembled constructs. Static exposure to hyper-osmotic medium (High Static) resulted in a 16% increase in cell number compared to control, with no other significant differences in cell number among the other groups. High Static also had the highest collagen/DW (50% greater than control) and GAG/DW (42% greater than control). Data are presented as means \pm standard deviations. Lowercase letters denote significant differences within a column; groups not connected by the same letter are significantly different ($P < 0.05$).

	Cells ($\times 10^6$)	Collagen/DW (mg/mg)	GAG/DW (mg/mg)
Control	5.44 \pm 0.32	0.28 \pm 0.08 ^{bc}	0.33 \pm 0.08 ^b
Low Static	5.63 \pm 0.45	0.31 \pm 0.06 ^{bc}	0.32 \pm 0.10 ^b
Low Dynamic	5.35 \pm 0.73	0.24 \pm 0.07 ^c	0.42 \pm 0.08 ^{ab}
High Static	6.28 \pm 0.45 ^a	0.42 \pm 0.07 ^a	0.47 \pm 0.06 ^a
High Dynamic	5.41 \pm 0.49	0.34 \pm 0.06 ^{ab}	0.38 \pm 0.07 ^{ab}

Table 5-3. Pairwise correlations between biomechanics and biochemistry

Correlations are reported as Spearman's rank correlation coefficients (Spearman's ρ). Associated p -values are included. At least 20 data points were evaluated in each pairwise analysis. Statistically significant correlations were found between collagen and all three biomechanical properties. Statistically significant correlations were also found between GAG/WW and all three biomechanical properties, but GAG/DW appeared to correlate only with compressive stiffness.

	Tensile stiffness		Tensile strength		Compressive stiffness	
	Spearman's ρ	P	Spearman's ρ	P	Spearman's ρ	P
Collagen/WW	0.6426	0.0009	0.7209	0.0002	0.6055	0.0013
Collagen/DW	0.8656	<0.0001	0.6944	0.0005	0.5078	0.011
GAG/WW	0.4479	0.032	0.6128	0.0031	0.7037	<0.0001
GAG/DW	0.0899	0.68	-0.1767	0.44	0.4577	0.021

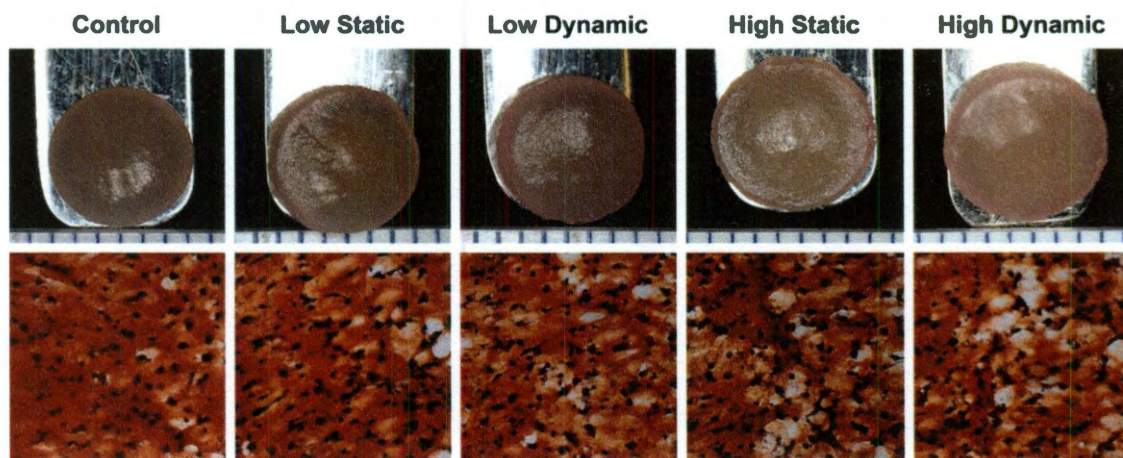


Figure 5-1. Gross morphology and histology of self-assembled constructs
Photographs at 4 weeks. From left to right: representative images of constructs from control, Low Static, Low Dynamic, High Static, and High Dynamic treatment groups. Constructs had a similar flat circular appearance with no surface abnormalities (top row). All constructs stained positively for GAG (bottom row).

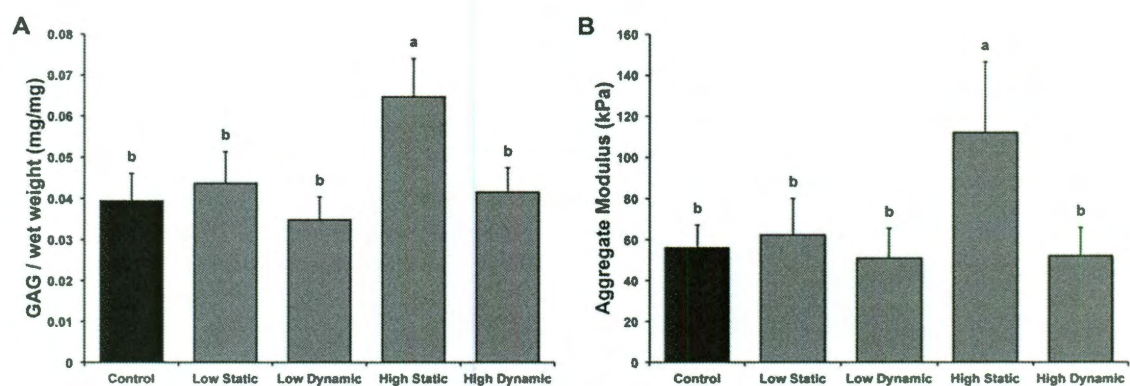


Figure 5-2. GAG content and compressive stiffness of constructs

(A) GAG/WW for all groups. Static exposure to hyper-osmotic medium (High Static) resulted in a 64% increase in construct GAG/WW compared to control. (B) Compressive stiffness for all groups. High Static constructs had the highest aggregate moduli (94% greater than control). As expected, trends for aggregate moduli followed GAG/WW trends. Data are presented as means \pm standard deviations. Lowercase letters denote significant differences; groups not connected by the same letter are significantly different ($P < 0.05$).

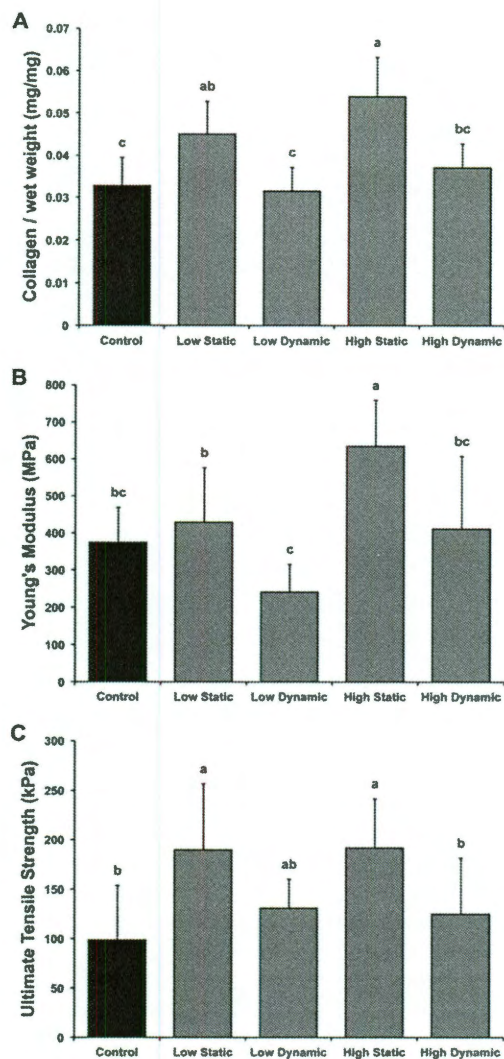


Figure 5-3. Collagen and tensile properties of self-assembled constructs

(A) Collagen/WW for all groups. Static exposure to hyper-osmotic medium (High Static) resulted in the greatest increase in construct collagen/WW (65% greater than control), followed by static exposure to hypo-osmotic medium (Low Static, 38% greater than control). (B) Tensile stiffness for all groups. High Static constructs had the highest Young's moduli (70% greater than control). Low Dynamic constructs had the lowest Young's moduli (36% less than control). (C) Tensile strength for all groups. High Static constructs and Low Static constructs had the highest UTS (94% and 92% greater than control, respectively), followed by High Dynamic constructs (32% greater than control). As expected, trends for tensile properties followed collagen/WW trends. Data are presented as means \pm standard deviations. Lowercase letters denote significant differences; groups not connected by the same letter are significantly different ($P < 0.05$).

Chapter 6. Temporal assessment of ribose treatment on self-assembled cartilage*

* Chapter published as **Eleswarapu SV**, Chen JA, and Athanasiou KA, "Temporal assessment of ribose treatment on self-assembled articular cartilage constructs," *Biochemical and Biophysical Research Communications* 2011.

Abstract

Articular cartilage lacks an ability to repair itself in response to degradation from traumatic injury or osteoarthritis. As such, there is a substantial clinical need for suitable replacements of damaged cartilage. Tissue engineering aims to fulfill this need by developing biologic replacement tissues *in vitro*. A major goal of cartilage tissue engineering is to produce tissues with robust biochemical and biomechanical properties. One technique that has been proposed to improve these properties in engineered tissue is the use of non-enzymatic glycation to induce collagen crosslinking, a particularly attractive solution because it avoids the risks of cytotoxicity posed by conventional crosslinking agents such as glutaraldehyde. The objectives of this study were 1) to determine whether continuous application of ribose would enhance the biochemical and biomechanical properties of self-assembled articular cartilage constructs, and 2) to identify an optimal time window for continuous ribose treatment. Self-assembled constructs were grown for 4 weeks using a previously established method and were subjected to continuous 7-day treatment with 30 mM ribose during the first, second, third, or fourth week of culture, or for the entire 4-week duration of culture. Control constructs were grown in parallel, and all groups were evaluated for gross morphology, histology, cellularity, collagen and sulfated glycosaminoglycan (GAG) content, and compressive and tensile mechanical properties. Compared to control constructs, it was found that treatment with ribose during week 2 and for the entire duration of culture resulted in significant 62% and 40% increases in compressive stiffness, respectively; significant 66%

and 44% increases in tensile stiffness; and significant 50% and 126% increases in tensile strength. Similar statistically significant trends were observed for collagen and GAG. In contrast, constructs treated with ribose during week 1 had poorer biochemical and biomechanical properties, although they were significantly larger and more cellular than all other groups. Based on these results, we conclude that non-enzymatic glycation with ribose is an effective method for improving tissue engineered cartilage and that specific temporal intervention windows exist to achieve optimal functional properties.

Introduction

Articular cartilage covers the surfaces of diarthrodial joints and serves to reduce friction and distribute loads during joint motion. Structurally, articular cartilage is an avascular, hypocellular tissue with an abundant extracellular matrix (ECM) rich in collagen type II and glycosaminoglycans (GAGs), which give rise to the tissue's tensile and compressive properties, respectively. Due to its avascularity and hypocellularity, cartilage lacks an intrinsic capacity to repair itself after painful destruction brought on by traumatic injury or osteoarthritis [28]. In the United States, osteoarthritis and related conditions contribute to direct expenditures of \$281.5 billion annually, a figure expected to increase as the population ages [1]. It is projected that 67 million people in the United States will be diagnosed with osteoarthritis by 2030 [101]. Thus, there is a substantial clinical need for suitable replacements of damaged or diseased cartilage. The field of tissue engineering aims to fulfill this need by developing biologic replacement tissues *in vitro* for

eventual *in vivo* implantation. A fundamental objective of cartilage tissue engineering is to produce tissues with robust biochemical and biomechanical properties [35].

To address this objective, our laboratory has developed a self-assembly process for engineering cartilage constructs [105]. The self-assembly process involves seeding chondrocytes at a high density into pre-formed, non-adherent, cylindrical wells. Cells coalesce into disc-shaped constructs and, over time, undergo biochemical and biophysical changes that approximate *in vivo* cartilage development [163]. Unlike traditional tissue engineering strategies, the self-assembly process does not employ a biomaterial scaffold, thereby circumventing the typical challenges associated with scaffold use, such as toxicity, biodegradability, stress shielding, and diminished juxtacrine and paracrine signaling [105]. An important advantage of the self-assembly process is that, since it is a strictly cell-mediated phenomenon, it can serve as a model system for examining the direct effects of biochemical [68, 158, 160] and biophysical [62, 64, 67] stimuli on cell physiology and *in vitro* ECM development. Although progress has been made in identifying beneficial stimuli for self-assembly, the functional properties of self-assembled cartilage constructs still fall short of native tissue values. Therefore, it is imperative that additional treatment modalities be evaluated.

One technique that has been proposed to improve the biomechanical properties of engineered tissue is the use of non-enzymatic glycation to induce collagen crosslinking [70, 86, 137, 190]. Collagen crosslinking through non-

enzymatic glycation involves three steps [26]. First, the aldehyde group of a reducing sugar, such as ribose, reacts with the nucleophilic ϵ -amino residue of lysine in the collagen polypeptide to form an unstable, reversible Schiff base (double-bond between carbon and nitrogen). One advantage of using ribose is that formation of the Schiff base occurs more rapidly with ribose compared to other sugars (e.g., 17x faster than glucose), largely due to its preferentially open-chain configuration [26]. In the second step of non-enzymatic glycation, the Schiff base undergoes Amadori rearrangement (movement of the double-bond from carbon-nitrogen to carbon-oxygen), producing a stable, less reversible ketone. Finally, over time, the Amadori products are degraded to form a variety of advanced glycation end-products (AGEs) [157], which accumulate in the ECM. Traditionally, the accumulation of AGEs has been understood to be an unwanted biochemical manifestation of aging and diabetes [26, 119, 152]. However, researchers have begun to recognize the potential benefits of non-enzymatic glycation as a tool to improve engineered tissue properties, especially without the risk of cytotoxicity posed by conventional crosslinking methods like glutaraldehyde fixation [70, 86, 103, 137, 189, 190].

In a recent experiment from our laboratory, self-assembled cartilage constructs were subjected to a 3.5 h treatment with one of four exogenous crosslinking agents on the final day of construct culture ($t=28$ days) [70]. A head-to-head comparison across treatment groups revealed that ribose produced the greatest improvements in tensile stiffness and ultimate tensile strength, beating glutaraldehyde, genipin, and methylglyoxal, as well as the control group.

Encouraged by these results and other studies in the literature, we decided to examine the effects of continuous ribose treatment on self-assembled cartilage constructs at different time windows throughout 4 weeks of culture.

The objectives of this study were 1) to determine whether continuous application of ribose would enhance the biochemical and biomechanical properties of self-assembled articular cartilage constructs, and 2) to identify an optimal time window for continuous ribose treatment. Constructs were self-assembled from bovine chondrocytes and subjected to continuous 7-day treatment with ribose during culture weeks 1, 2, 3, or 4, or for the entire 4-week duration of culture. Control constructs were grown in parallel. It was hypothesized that 1) ribose would improve construct biochemical and biomechanical properties, 2) an optimal treatment time window exists for which constructs undergo greatest improvement, and 3) ribose treatment for the entire duration of culture would produce the greatest effect on constructs. Assessments included gross morphology, histology, quantitative biochemistry, and biomechanical testing.

Materials and methods

Media formulations

This study employed two medium formulations: “control medium” and “ribose medium.” Control medium is a chondrogenic medium described extensively by our group [64, 158, 160]: Dulbecco’s modified Eagle’s medium (DMEM) with 4.5 mg/mL of glucose and L-glutamine (Invitrogen); 100 nM dexamethasone (Sigma); 0.1 mM non-essential amino acids (Invitrogen); 1% ITS+ (insulin,

human transferrin, and selenous acid; BD Scientific); 1% penicillin-streptomycin-fungizone (BioWhittaker); 50 µg/mL ascorbate-2-phosphate; 40 µg/mL L-proline; and 100 µg/mL sodium pyruvate (Fisher Scientific). Ribose medium is control medium plus 30 mM D-ribose (Sigma). This concentration of ribose was selected from literature that demonstrated beneficial effects of 30 mM ribose on specimen mechanical properties, with no deleterious effects on cell viability [70, 86]. Our chosen concentration of 30 mM ribose is far below the 250 mM ribose shown to be tolerated well by chondrocytes *in vitro* [190].

Chondrocyte isolation

Bovine chondrocytes were isolated as previously described [68]. Cartilage harvested from the distal femur and patellofemoral groove of 1-week-old male calves (Research 87) was digested in 0.2% collagenase type II (Worthington) for 24 h. Each leg came from a different animal, and cells from 8 legs were pooled to create a mixture of chondrocytes. Cells were counted using a hemocytometer and then frozen at -80°C in DMEM containing 20% fetal bovine serum (FBS) and 10% dimethyl sulfoxide (DMSO).

Preparation of agarose wells for construct self-assembly

Cylindrical, non-adherent wells were prepared in a 48-well plate using a technique adapted from previous work [105, 163]. A stainless steel mold consisting of 5 mm diameter cylindrical prongs was placed into sterile, molten 2% agarose in a 48-well plate. The agarose solidified at room temperature for 60 min,

and the stainless steel mold was carefully removed. Two changes of control medium were used to completely saturate the agarose well by the time of cell seeding.

Self-assembly and culture of cartilage constructs

Cells were thawed and counted within 5 days of being isolated and frozen. After thawing, chondrocyte viability was >90%. To create each construct, 5.5 million cells in 100 μ L of control medium were seeded into each cylindrical agarose well, followed by addition of 400 μ L control medium after 4 h. Cells settled and coalesced into free-floating cylindrical disc-shaped constructs; $t=1$ day was defined as 24 h after seeding. All constructs were cultured in the agarose wells until $t=10$ days, at which point they were gently and aseptically unconfined and transferred to 48-well plates unrestricted by circumferential confinement. Constructs received 500 μ L medium change every 24 h and remained in culture until $t=28$ days. All culture was at 37°C and 10% CO₂.

This study examined six groups, named as follows: Control, Week 1, Week 2, Week 3, Week 4, and All Weeks. Controls received control medium during $t=1-28$ days. Ribose-treated constructs received ribose medium during $t=1-7$ days (Week 1), $t=8-14$ days (Week 2), $t=15-21$ days (Week 3), $t=22-28$ days (Week 4), or $t=1-28$ days (All Weeks). All ribose-treated constructs received control medium when not undergoing ribose treatment. Constructs were assigned randomly to experimental groups.

Gross morphology and histology

At $t=28$ days, all constructs were removed from culture for assessment. Photographs were taken, and construct diameters were measured from digital photographs using ImageJ software (National Institutes of Health). Total construct wet weights (WW) were recorded, and constructs were portioned for analysis. A 3 mm diameter punch was taken from the construct's center for indentation testing. The remaining outer ring was split into portions for histology, quantitative biochemistry, and tensile testing. For histology, constructs were cryoembedded and sectioned at 14 μm . Samples were fixed in 10% formalin and stained with Safranin-O/fast green to examine GAG distribution and picosirius red to examine collagen content.

Quantitative biochemistry

Biochemistry samples were weighed wet, frozen overnight, and lyophilized. Dry weights (DW) were measured, after which samples were digested with 125 $\mu\text{g}/\text{mL}$ papain (Sigma) in 50 mM phosphate buffer, pH=6.5, containing 2 mM N-acetyl cysteine for 18 h at 65°C. Total DNA content was assessed with the Quanti-iT PicoGreen dsDNA Assay (Invitrogen), and cell number was calculated based on an estimation of 7.7 pg DNA material per cell. Sulfated GAG was quantified using the Blyscan Glycosaminoglycan Assay kit (Biocolor), based on 1,9-dimethylmethylene blue binding. Following hydrolysis with 4 N sodium hydroxide for 20 min at 110°C, total collagen content was quantified with a chloramine-T hydroxyproline assay [238]. Sircol collagen assay standard

(Biocolor) was used such that the standard curve reflected collagen amount, eliminating the need to convert hydroxyproline to collagen. Total collagen and sulfated GAG were normalized to WW and DW for making comparisons among treatment groups.

Creep indentation testing

A creep indentation apparatus was used to determine the compressive creep and recovery behavior of each construct [12]. Each sample was affixed to a stainless steel surface with cyanoacrylate glue and equilibrated for 20 min in PBS. A 0.7 g (0.007 N) mass was applied with a 0.8 mm diameter flat, porous indenter tip, and specimens crept until equilibrium. Specimen thickness was measured from digital photographs using ImageJ software. Aggregate modulus, a measure of compressive stiffness, was calculated using a semi-analytical, semi-numeric, linear biphasic model [12].

Tensile testing

Each tensile specimen was cut into a dog-bone shape with a 1-mm gauge length. Specimen thickness and width were measured from digital photographs using ImageJ software. Specimens were then affixed with cyanoacrylate glue to paper tabs outside the gauge length, and these tabs were gripped during testing. A uniaxial electromechanical materials testing system (Instron Model 5565) was employed to determine tensile properties. Tensile tests were performed until failure at a strain rate of 1% of the gauge length per second. Force-displacement

curves were generated, and stress-strain curves were calculated by normalizing data to specimen dimensions. The apparent Young's modulus, a measure of tensile stiffness, was determined by least squares fitting of the linear region of the stress-strain curve. The ultimate tensile strength (UTS) was determined as the maximum stress reached during a test.

Statistical analysis

All quantitative assessments were made using $n=5-9$. Numerical data are represented as means \pm standard deviations. To compare among treatment groups, single-factor ANOVA was employed, with Fisher LSD post hoc testing when warranted. Significance was defined as $p<0.05$.

Results

Gross appearance and histology

At the end of culture ($t=28$ days), all constructs were circular discs with enough structural integrity to be easily manipulated during all construct assessments. Constructs from every group had a similar flat surface appearance with no obvious surface abnormalities (Figure 6-1). Construct diameters and wet weights (WW) are provided in Table 6-1. Week 1 constructs had significantly greater diameters (1.06x control) and wet weights (1.34x control) compared to all other groups. On histology, all constructs stained positively for collagen and GAG throughout their thicknesses (Figure 6-1).

Quantitative biochemistry

Cell number, shown in Table 6-1, was estimated from DNA content using a conversion factor of 7.7 pg DNA per cell. Week 1 constructs were found to have a higher cell number (1.63x control) than every other group, with no other differences between groups.

Construct GAG/WW for each group is compared in Figure 6-2A. GAG/WW values for control, Week 1, Week 2, Week 3, Week 4, and All Weeks constructs were $4.6 \pm 0.6\%$, $3.8 \pm 0.7\%$, $6.2 \pm 1.5\%$, $4.4 \pm 1.3\%$, $5.0 \pm 0.6\%$, and $6.2 \pm 0.7\%$, respectively. Week 2 and All Weeks constructs had the greatest GAG/WW (1.34x and 1.35x control, respectively). Week 1 constructs had the least GAG/WW (0.82x control). GAG per dry weight (DW), provided in Table 6-1, showed a similar trend to that observed for GAG/WW.

Construct collagen/WW for each group is compared in Figure 6-3A. Collagen/WW values for control, Week 1, Week 2, Week 3, Week 4, and All Weeks constructs were $5.0 \pm 0.6\%$, $4.6 \pm 0.9\%$, $7.6 \pm 1.3\%$, $5.9 \pm 1.9\%$, $5.2 \pm 0.6\%$, and $10.1 \pm 3.4\%$, respectively. All Weeks constructs had the highest collagen/WW (2.04x control), followed by Week 2 constructs (1.53x control). Week 1, Week 3, and Week 4 constructs were no different from control. Similar trends were observed for collagen/DW (Table 6-1); however, Week 2 and All Weeks constructs did not differ from each other in collagen/DW.

Biomechanics

Creep indentation was employed to determine the aggregate modulus, a measure of compressive stiffness, of each self-assembled construct. Aggregate moduli for all constructs are compared in Figure 6-2B. Aggregate moduli for control, Week 1, Week 2, Week 3, Week 4, and All Weeks constructs were 138 ± 34 , 64 ± 22 , 193 ± 38 , 131 ± 27 , 152 ± 41 , and 224 ± 45 kPa, respectively. Trends for aggregate moduli followed those observed for GAG/WW. The highest aggregate moduli were found in All Weeks constructs (1.62x control), followed by Week 2 constructs (1.40x control). Week 1 constructs had the lowest aggregate moduli (0.46x control).

Tensile axial strain-to-failure testing was employed to determine the Young's modulus and UTS of each self-assembled construct. Young's moduli and UTS for all constructs are compared in Figure 6-3. Young's moduli and UTS for control, Week 1, Week 2, Week 3, Week 4, and All Weeks constructs were 717 ± 160 , 457 ± 106 , 1034 ± 141 , 888 ± 181 , 669 ± 130 , and 1192 ± 340 kPa, respectively. All Weeks constructs had the highest Young's moduli (1.66x control), followed by Week 2 constructs (1.44x control). Week 1 constructs had the lowest Young's moduli (0.64x control). UTS values for control, Week 1, Week 2, Week 3, Week 4, and All Weeks constructs were 366 ± 61 , 411 ± 147 , 551 ± 147 , 465 ± 101 , 376 ± 110 , and 830 ± 188 kPa, respectively. Trends for UTS appeared to reflect trends in collagen/WW. All Weeks constructs had the highest UTS (2.26x control), followed by Week 2 constructs (1.50x control).

Discussion

This study examined the effects of continuous ribose treatment over various time windows during self-assembly of articular cartilage constructs. Experimental results supported the hypotheses motivating the study: 1) treatment of self-assembled constructs with ribose produced significant increases in biochemical and biomechanical properties; 2) week 2 was identified as the optimal treatment time window to produce the greatest improvements in constructs; and 3) continuous ribose treatment for the entire duration of culture had the greatest effect on construct properties, notably producing a 62% increase in compressive stiffness, a 66% increase in tensile stiffness, and a 126% increase in tensile strength compared to control. To the best of our knowledge, this is the first study not only to systematically compare ribose treatment over various time windows during *in vitro* tissue development, but also to examine the direct effects of ribose treatment on both cells and their surrounding ECM during tissue engineering. This study demonstrates the effectiveness of ribose as an agent to improve tissue engineered materials.

It was found that the optimal time window for ribose treatment is during week 2 ($t=8-14$ days). Compared to controls, week 2 constructs exhibited significant improvements in GAG/WW (34% increase), collagen/WW (53% increase), compressive stiffness (40% increase), tensile stiffness (44% increase), and tensile strength (50% increase). To understand why intervening during week 2 can lead to such dramatic improvements in construct properties, it is important to consider the developmental milestones of self-assembling constructs. A

previous study from our laboratory characterized matrix development during self-assembly [163]. A principal finding of that work was that collagen production reaches a plateau between days 10-14 of culture, after which GAG production predominates. It is thought that the rapid increase in GAG production with no new collagen formation contributes to pre-stress within the fledgling collagen network, thereby compromising the engineered tissue's tensile mechanical properties [158, 200]. Altering this imbalance between GAG and collagen has been shown to improve the tensile properties of self-assembled constructs [158, 159] and native articular cartilage explants [10]. During week 2, before collagen production halts and GAG production ramps up, the developing ECM may be more susceptible to interventions like ribose that either reinforce existing matrix or induce new matrix biosynthesis. The beneficial effects of ribose treatment during week 2 are corroborated by previous work showing that other biochemical and biophysical stimuli also produce their maximal effects when applied to constructs during week 2 [62-64, 67, 68, 110, 160].

One interesting finding is that the results for collagen content reflected trends seen for tensile strength but do not track as closely with differences observed for tensile stiffness. It is widely understood that the tensile properties of cartilage are conferred by the tissue's collagen network. Collagen networks have complex, multi-scale structure-function relationships governed by peptide abundance, fibril organization, and crosslink presence [181]. A possible explanation for the fidelity between tensile strength and collagen content is that collagen abundance may preferentially determine the tissue's failure point (and

thus strength), whereas individual crosslinks within the network may determine the fiber bundle response to strain (and thus stiffness). Future studies on native cartilage should be undertaken to tease out structure-function relationships between collagen abundance, crosslinks, tensile stiffness, and tensile strength.

Increased GAG content and compressive stiffness in ribose-treated constructs may be explained by the effects of crosslinking, as well. Glycation-mediated crosslinking may be trapping GAGs within the stiffer, crosslinked network, thereby preventing GAG loss over the duration of culture. Higher compressive stiffness may be explained by tighter packing of GAG within the crosslinked collagen network. One way to test this hypothesis in the future may be to examine the ratio of GAG to pentosidine, a molecule derived from ribose that is responsible for crosslinks between lysine and arginine residues in collagen [181]. By studying correlations between GAG and pentosidine, inferences can be made about the effect of collagen crosslinking on GAG retention or loss.

Although the guiding principle underlying this study is that ribose induces crosslinking of the ECM through non-enzymatic glycation, the observed changes in biochemical content and biomechanical properties may be further explained by cellular metabolism or osmotic stress. Ribose is known to play a role in cellular metabolism [26], particularly as part of the pentose phosphate pathway [202], and therefore may influence chondrocyte biosynthesis during self-assembly. Additionally, the presence of ribose increases the effective osmolarity of ribose medium compared to control medium. Cells undergo shrinkage in a hyperosmotic environment; the resulting cellular strain is thought to alter chromatin

condensation and nucleocytoplasmic transport [79, 80]. The downstream effect of these nuclear changes may be increased biosynthesis of GAG or collagen, especially in response to continuous hyperosmotic stress. To test this concept in the future, one could examine the use of a non-reducing sugar such as sucrose to modulate osmolarity while preventing glycation; alternatively, the osmolarity of ribose-supplemented medium could be titrated using distilled water.

Of note is that constructs treated with ribose during the first week of culture exhibited significant decreases in biochemical and biomechanical properties but increases in size and cell number compared to all other groups. During the first week of culture, in a process resembling chondrogenesis *in vivo* [95], it has been shown previously by our laboratory that the nascent construct's efforts are focused primarily on cell clustering and condensation through upregulation of N-cadherin and other adhesion molecules, rather than on ECM synthesis [163]. As such, there is very little ECM available as a substrate for glycation by ribose. Thus, the prevailing effect of early ribose treatment may be metabolic or osmotic, rather than crosslink forming. Metabolically, it is possible that ribose had the effect of shunting cellular biosynthesis towards cell proliferation [26], which may explain the 63% increase in cell number in constructs treated with ribose during week 1. Thus it is not surprising that, given the greater cell number, constructs treated during week 1 have a larger size compared to constructs from other groups. It is important to note that despite the greater cell number and size, these constructs were unable to keep up with ECM synthesis observed in other groups. These effects are similar to results obtained

in a previous study from our group that investigated initial cell seeding initial cell seeding density in self-assembly and revealed an upper limit for effective tissue engineering [183].

Constructs treated with ribose throughout the entire duration of 4-week culture exhibited the greatest improvements in biochemical and biomechanical properties. It is possible that the beneficial effects seen with week 2 treatment were able to mitigate the negative effects seen with week 1 treatment in this group of constructs. Most importantly, however, the success of these constructs demonstrates that treatment with 30 mM ribose can be used safely in tissue engineering strategies with no risk of *in vitro* cytotoxicity. Future work is warranted, however, to assess biocompatibility *in vivo*, since previous work in the literature has suggested that AGEs may mark ECM proteins for targeted proteolysis [26].

This work provides evidence that continuous treatment with ribose can significantly enhance the biochemical and biomechanical properties of self-assembled cartilage constructs. We have identified an optimal time window for ribose application. Additionally, we provide evidence that 30 mM ribose can be used safely *in vitro* without risk of cell death or other deleterious effects. Finally, a major innovation of this study is that it evaluated ribose application during self-assembly, a purely cell-mediated phenomenon, from which direct effects on both cells and ECM were ascertained for the first time.

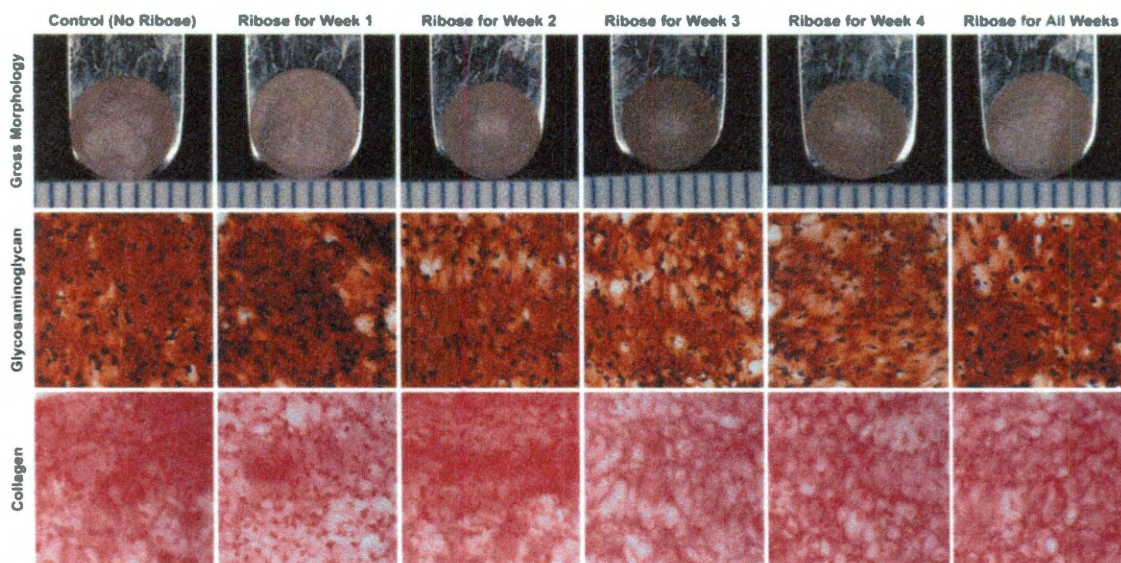


Figure 6-1. Gross morphology and histology of self-assembled constructs
Photographs at 4 weeks. From left to right: representative images of constructs from Control, Week 1, Week 2, Week 3, Week 4, and All Weeks ribose treatment groups. Constructs had a similar flat circular appearance with no surface abnormalities (top row). All constructs stained positively for collagen (middle row) and GAG (bottom row).

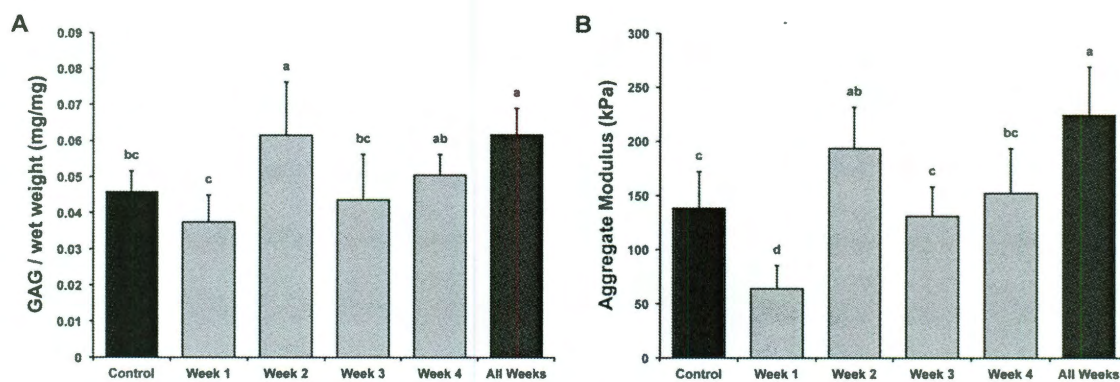


Figure 6-2. GAG content and compressive stiffness of constructs

(A) GAG/WW for all groups. Ribose treatment during Week 2 and All Weeks had the greatest GAG/WW (34% and 35% > control, respectively). Week 1 had the least GAG/WW (18% < control). (B) Compressive stiffness for all groups. The highest aggregate moduli were found in All Weeks (62% > control), followed by Week 2 (40% > control). Week 1 had the lowest aggregate moduli (54% < control). As expected, trends for aggregate moduli followed GAG trends. Data are presented as means + standard deviations. Groups not connected by the same letter are significantly different ($p < 0.05$).

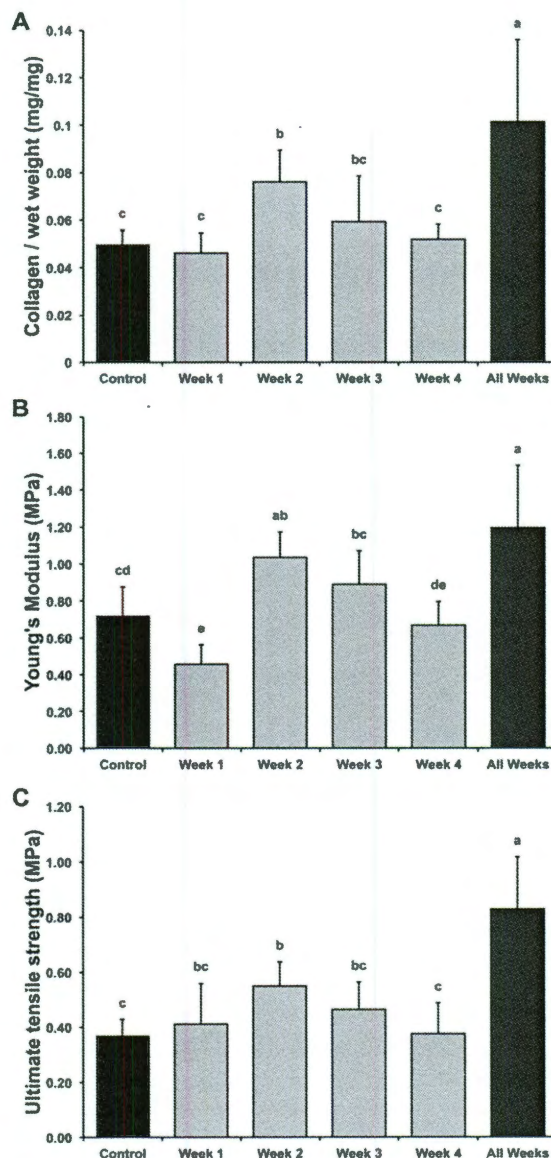


Figure 6-3. Collagen and tensile properties of self-assembled constructs

(A) Collagen/WW for all groups. Ribose treatment during All Weeks had the highest collagen/WW (104% > control), followed by Week 2 (53% > control). (B) Tensile stiffness for all groups. The highest Young's moduli were found in All Weeks (66% > control), followed by Week 2 (44% > control). Week 1 had the lowest Young's moduli (36% < control). (C) Tensile strength for all groups. All Weeks had the highest UTS (126% > control), followed by Week 2 (50% > control). UTS trends appeared to reflect collagen/WW trends. Data are presented as means + standard deviations. Groups not connected by the same letter are significantly different ($p < 0.05$).

Table 6-1. Growth metrics and biochemical content of constructs

Diameter, wet weight, cell number, collagen/dry weight, and GAG/dry weight of self-assembled constructs. Ribose treatment during Week 1 had the largest diameter (6% > control), wet weight (34% > control), and cell number (63% > control), with no other significant differences among the other groups. Week 2 and All Weeks had the highest collagen/DW (50% and 53% > control, respectively), and All Weeks had the highest GAG/DW (23% > control). Data are presented as means \pm standard deviations. Asterisks and lowercase letters denote significant differences within a column; groups not connected by the same letter are significantly different ($p < 0.05$).

	Dia. (mm)	WW (mg)	Cells ($\times 10^6$)	Collagen/DW (mg/mg)	GAG/DW (mg/mg)
Control	5.92 \pm 0.22	22.0 \pm 1.3	5.39 \pm 1.20	0.34 \pm 0.08 b	0.30 \pm 0.03 b
Week 1	6.28 \pm 0.2*	29.4 \pm 1.8*	8.78 \pm 2.51*	0.25 \pm 0.06 c	0.24 \pm 0.02 c
Week 2	5.78 \pm 0.10	20.4 \pm 1.3	4.89 \pm 0.68	0.51 \pm 0.08 a	0.33 \pm 0.05 ab
Week 3	5.80 \pm 0.17	20.6 \pm 1.7	4.68 \pm 1.66	0.44 \pm 0.11 ab	0.32 \pm 0.04 ab
Week 4	5.93 \pm 0.13	21.9 \pm 1.5	5.39 \pm 1.00	0.31 \pm 0.07 c	0.29 \pm 0.04 b
All Weeks	5.92 \pm 0.23	20.5 \pm 0.2	6.01 \pm 1.33	0.52 \pm 0.07 a	0.37 \pm 0.06 a

Chapter 7. Decellularization of tissue engineered cartilage^{*}

^{*} Chapter published as Elder BD⁺, **Eleswarapu SV⁺**, and Athanasiou KA, "Extraction techniques for the decellularization of tissue engineered articular cartilage constructs," *Biomaterials* 2009. ⁺ = Equal contribution.

Abstract

Several prior studies have been performed to determine the feasibility of tissue decellularization to create a non-immunogenic xenogenic tissue replacement for bladder, vasculature, heart valves, knee meniscus, temporomandibular joint disc, ligament, and tendon. However, limited work has been performed with articular cartilage, and no studies have examined the decellularization of tissue engineered constructs. The objective of this study was to assess the effects of different decellularization treatments on articular cartilage constructs, engineered using a scaffoldless approach, after 4 wks of culture, using a two-phased approach. In the first phase, five different treatments were examined: 1) 1% SDS, 2) 2% SDS, 3) 2% Tributyl phosphate, 4) 2% Triton X-100, and 5) Hypotonic followed by hypertonic solution. These treatments were applied for either 1 h or 8 h, followed by a 2 h wash in PBS. Following this wash, the constructs were assessed histologically, biochemically for cellularity, GAG, and collagen content, and biomechanically for compressive and tensile properties. In phase II, the best treatment from phase I was applied for 1, 2, 4, 6, or 8 h in order to optimize the application time. Treatment with 2% SDS for 1 h or 2 h significantly reduced the DNA content of the tissue, while maintaining the biochemical and biomechanical properties. On the other hand, 2% SDS for 6 h or 8 h resulted in complete histological decellularization, although GAG content and compressive properties were significantly decreased. Overall, 2% SDS, for 1 or 2 h, appeared to be the most effective agent for cartilage decellularization, as it resulted in decellularization while maintaining the functional properties. The results of this

study are exciting as they indicate the feasibility of creating engineered cartilage that may be non-immunogenic as a replacement tissue.

Introduction

Injuries to articular cartilage, whether traumatic or from degeneration, generally result in the formation of mechanically inferior fibrocartilage, due to the tissue's poor intrinsic healing response [27]. As such, tissue engineering strategies have focused on developing replacement tissue *in vitro* for eventual *in vivo* implantation. One such strategy employs a "self-assembly process" [105] in which chondrocytes can be used to form robust tissue engineered constructs without the use of a scaffold.

Although engineered articular cartilage tissue has recently been created with biochemical and biomechanical properties in the range of native tissue values [67], there are currently two significant limitations to cartilage tissue engineering. First, human cells are scarce in number and difficult to procure, and passage of these cells leads to dedifferentiation [53]. These issues make the use of autologous cells for cartilage repair difficult. Additionally, the majority of cartilage tissue engineering approaches have employed bovine or other animal cells, and tissues grown from these cells are xenogenic. Thus, their use may result in a severe immune response following implantation, though this has not been fully elucidated.

It is believed that a decellularized xenogenic tissue may be a viable option as a replacement tissue, as the antigenic cellular material will be removed while

preserving the relatively non-immunogenic extracellular matrix (ECM), as described in an earlier review [85]. Ideally, this will also preserve the biomechanical properties of the tissue. For instance, an acellular dermal matrix [43] has seen successful use clinically as the FDA approved Alloderm product. Additionally, acellular xenogenic tissues have been created for many musculoskeletal applications, including replacements for the knee meniscus [220], temporomandibular joint disc [141], tendon [39], and ACL [242], as well as in other tissues including heart valves, bladder [185], artery [50], and small intestinal submucosa. However, studies demonstrating the effects of tissue decellularization on cartilage are limited, and there are no studies demonstrating the effects of decellularization on musculoskeletal tissue engineered constructs.

Therefore, the objective of this study was to determine the effects of multiple decellularization treatments on construct cellularity, biochemical, and biomechanical properties. A two-phased approach was used in which an appropriate agent for decellularization was selected in phase I, and an appropriate treatment time was selected in phase II. It was hypothesized that cells could be removed from self-assembled constructs while preserving the biochemical and biomechanical properties. To test this hypothesis, self-assembled articular cartilage constructs were cultured for 4 wks, and then treated with 1% sodium dodecyl sulfate (SDS), 2% SDS, 2% Tributyl Phosphate (TnBP), 2% Triton X-100, or a hypotonic/hypertonic solution, for either 1 or 8 h. These treatments were selected from prior literature. Next, the treatment selected in phase I was applied for a period of 1, 2, 4, 6, or 8 h in phase II. The effects of the

decellularization treatments were assessed on construct cellularity and functional properties.

Materials and methods

Chondrocyte isolation and seeding

Cartilage was harvested from the distal femur of week-old male calves (Research 87) shortly after slaughter, and chondrocytes were isolated following digestion with collagenase type 2 (Worthington). To normalize variability among animals, each leg came from a different animal, and cells from all legs were combined together to create a mixture of chondrocytes; a mixture of cells from five legs was used in the study. Cell number was determined on a hemocytometer, and a trypan blue exclusion test indicated that viability remained >90%. Chondrocytes were frozen in culture medium supplemented with 20% FBS (Biowhittaker) and 10% DMSO at -80°C for 1 day prior to use. After thawing, viability was greater than 90%. A stainless steel mold consisting of 5 mm dia. x 10 mm long cylindrical prongs was placed into a row of a 48-well plate. To construct each agarose well, sterile, molten 2% agarose was added to wells fitted with the die. The agarose solidified at room temperature for 60 min, after which the mold was removed from the agarose. Two changes of culture medium were used to completely saturate the agarose well by the time of cell seeding. The medium was DMEM with 4.5 g/L-glucose and L-glutamine (Biowhittaker), 100 nM dexamethasone (Sigma), 1% Penicillin/Streptomycin/Fungizone (P/S/F) (Biowhittaker), 1% ITS+ (BD Scientific), 50 $\mu\text{g}/\text{mL}$ ascorbate-2-phosphate, 40 $\mu\text{g}/\text{mL}$ L-proline, and 100 $\mu\text{g}/\text{mL}$

sodium pyruvate (Fisher Scientific). To seed each construct, 5.5×10^6 cells were added in 100 μ l of culture medium. Constructs formed within 24 h in the agarose wells and were cultured in the same well until $t=10$ days, after which they were unconfined for the remainder of the study, as described previously [69]; $t=0$ was defined as 24 h after seeding.

Decellularization phase I

At $t=4$ weeks, self-assembled constructs ($n=6$ /group) were removed from culture and exposed to one of five decellularization treatments, for either 1 h or 8 h. The decellularization treatments included:

- 1) 1% SDS
- 2) 2% SDS
- 3) 2% TnBP
- 4) 2% Triton X-100
- 5) Hypotonic/Hypertonic Solution (half-time of each)
 - a. Hypotonic: 10 mM Tris HCl, 5 mM EDTA, 1 μ M PMSF
 - b. Hypertonic: 50 mM Tris HCl, 1 M NaCl, 10 mM EDTA, 1 μ M PMSF

All treatments included 0.5 mg/ml DNase Type I, 50 μ g/ml RNase, 0.02% EDTA, and 1% P/S/F, in PBS. Both 1 h control and 8 h control groups were exposed to this same solution without detergent treatments. These treatments were applied at 37°C with agitation. Following the 1 h or 8 h treatment, the constructs were washed for 2 h in PBS at 37°C with agitation. Additionally, an untreated control

was assessed immediately following construct removal from culture, without the treatment or wash steps.

Decellularization phase II

At $t=4$ weeks, self-assembled constructs ($n=6$ /group) were removed from culture and exposed to 2% SDS for 1, 2, 4, 6, or 8 h. As in phase I, all treatments included 0.5 mg/ml DNase Type I, 50 μ g/ml RNase, 0.02% EDTA, and 1% P/S/F, in PBS. These treatments were applied at 37°C with agitation. Following the SDS treatment, the constructs were washed for 2 h in PBS at 37°C with agitation. Additionally, an untreated control was assessed immediately following construct removal from culture, without the treatment or wash steps.

Histology

After freezing, samples were sectioned at 14 μ m. To determine construct cellularity, a hematoxylin & eosin (H&E) stain was used. A Safranin-O/fast green stain was used to examine GAG distribution,[187, 212] and picosirius-red was employed for collagen content.

Quantitative biochemistry

Samples were frozen overnight and lyophilized for 48 h, followed by re-suspension in 0.8 mL of 0.05 M acetic acid with 0.5 M NaCl and 0.1 mL of a 10 mg/mL pepsin solution (Sigma) at 4°C for 72 h. Next, 0.1 mL of 10x TBS was added along with 0.1 mL pancreatic elastase and mixed at 4°C overnight. A

Picogreen Cell Proliferation Assay Kit (Molecular Probes) was used to assess total DNA content. GAG content was quantified using the Blyscan Glycosaminoglycan Assay kit (Biocolor), based on 1,9-dimethylmethylene blue binding. After hydrolysis with 2 N NaOH for 20 min at 110°C, total collagen content was determined using a chloramine-T hydroxyproline assay [237].

Indentation testing

Samples were assessed with an indentation apparatus, as described previously [11]. A 0.7 g (0.007 N) mass was applied with a 1 mm flat-ended, porous indenter tip, and specimens crept until equilibrium, as described elsewhere [105]. For the constructs treated for 1 h with the hypotonic/hypertonic solution and 8 h with 1% SDS, 2% TnBP, or 2% Triton X-100, a 0.27 (0.0027 N) mass was applied instead to maintain equivalent strains. Strains generally ranged from 3-9%. Preliminary estimations of the aggregate modulus of the samples were obtained using the analytical solution for the axisymmetric Boussinesq problem with Papkovitch potential functions [99, 217]. The sample biomechanical properties, including aggregate modulus, Poisson's ratio, and permeability were then calculated using the linear biphasic theory [13].

Tensile testing

A uniaxial materials testing system (Instron Model 5565) was employed to determine tensile properties with a 50 N load cell, as described previously [15]. Briefly, samples were cut into a dog-bone shape with a 1-mm-long gauge length.

Samples were glued to paper tabs with cyanoacrylate glue outside of the gauge length. The 1-mm-long sections were pulled at a 1% constant strain rate. All samples broke within the gauge length. Stress-strain curves were created from the load-displacement curve and the cross-sectional area of each sample, and Young's modulus was calculated from each stress-strain curve.

Statistical analysis

All biomechanical and biochemical assessments were made using $n=6$. In phase I, the three control groups were compared using a single factor ANOVA. As no difference was noted, only the culture control was used in the final analysis. To compare treatment groups in both phases, a single factor ANOVA was used, and a Tukey's HSD *post hoc* test was used when warranted. Significance was defined as $p < 0.05$.

Results

Gross appearance and histology

In all groups, the construct diameter was approximately 6 mm at 4 wks. In phase I, treatment for 8 h with either 1% SDS or the hypotonic/hypertonic solution resulted in a significant decrease in construct thickness (Table 7-1). Additionally, treatment for 8 h with 1% SDS, 2% SDS, 2% Triton X-100, or the hypotonic/hypertonic solution resulted in a significant decrease in construct wet weight (Table 7-1). In phase II, treatment with 2% SDS for 6 h or 8h resulted in a significant decrease in construct thickness and wet weight (Table 7-2).

Figure 7-1 displays the histological results of phase I. Extensive staining for cell nuclei was observed in the H&E staining of the control group. Treatment with 1% SDS for 1 h reduced the number of cell nuclei, while treatment for 8 h eliminated all nuclei from the construct. The 2% SDS treatment had similar results. However, treatment with 2% TnBP or 2% Triton X-100, for either time point, had no effect on the number of nuclei. Both hypotonic/hypertonic treatments resulted in a slight reduction in number of cell nuclei. All decellularization treatments for 8 h resulted in a significant reduction or complete elimination of staining for GAGs. Additionally, 1 h treatment with the hypotonic/hypertonic solution reduced the GAG content. However, there were no apparent differences in GAG staining among the 1 h treatments with 1% SDS, 2% SDS, 2% TnBP, 2% Triton X-100, and the control. Finally, all constructs demonstrated extensive staining for collagen, although the 8 h decellularization treatments resulted in slight alterations in construct morphology.

Figure 7-2 displays the histological results of phase II. Extensive staining for cell nuclei was observed in the H&E staining of the control group. Increasing decellularization was observed with 2% SDS treatment from 1-4 h, while 6 or 8 h application times were required for complete histological decellularization. Treatment for 1 and 2 h resulted in maintenance of GAG and collagen staining, while the 4 h treatment resulted in decreased staining. However, treatment for 6 and 8 h resulted in no GAG staining and poor collagen staining.

Quantitative biochemistry

In phase I, several decellularization treatments resulted in a significant reduction in construct DNA (Figure 7-3). Treatment for 1 h with 2% SDS or the hypotonic/hypertonic solution, as well as 8 h treatment with 1 or 2% SDS or the hypotonic/hypertonic solution all resulted in a significant reduction of the DNA in the constructs. However, treatment with 2% TnBP or 2% Triton X-100 for either amount of time had no effect on construct DNA. In phase II, all application times resulted in a significant decrease in DNA content, although treatment for 8 h resulted in the greatest decrease (Figure 7-4).

For phase I, the effects of the decellularization agents on construct GAG content are found in Figure 7-5c. Treatment with 1% or 2% SDS for 1 h had no effect on GAG content, while all other treatments significantly reduced the GAG content of the constructs. Additionally, all 8 h treatments resulted in complete or nearly complete removal of GAG from the constructs. Finally, there were no significant changes in total collagen content following treatment with the decellularization agents (Figure 7-5d). For phase II, the effects of the decellularization agents on construct GAG content are found in Figure 7-6c. Treatment with 2% SDS for 1 or 2 h maintained GAG content, while 4 h treatment resulted in a significant decrease in GAG content. However, treatment for 6 or 8 h resulted in complete elimination of GAG. Treatment for 1, 2, 4, or 6 h did not significantly alter the collagen content, while treatment for 8 h resulted in a slight decrease in collagen content.

Biomechanical evaluation

For phase I, the effects of the various decellularization treatments on construct aggregate modulus are displayed in Figure 7-5a. Treatment for 1 h with 1% or 2% SDS as well as with 2% TnBP maintained the compressive stiffness. However, treatment for 8 h with 1% SDS, 2% TnBP, and 2% Triton X-100 significantly reduced the aggregate modulus. The groups treated for 8 h with either 2% SDS or the hypotonic/hypertonic solutions were too weak to be mechanically tested with creep indentation. Additionally, the effects of the various decellularization treatments on Poisson's ratio and permeability are displayed in Table 7-3. A significant decrease in Poisson's ratio was noted for the groups treated for 8 h with 1% SDS, 2% TnBP, and 2% Triton X-100. Finally, only treatment for 8 h with 1% SDS resulted in a significantly decreased permeability. For phase II, the effects of the various application times on construct aggregate modulus are displayed in Figure 7-6a. There was no significant difference in compressive stiffness with treatment for 1 and 2 h, while the 4 h treatment significantly reduced the stiffness. Additionally, the 6 and 8 h treatment resulted in constructs that were untestable in compression. As shown in Table 7-4, the 1, 2, and 4 h treatments did not result in significant changes in permeability and Poisson's ratio.

Figure 7-5b indicates the tensile properties of the constructs treated with the various agents in phase I. Treatment for 1 h with 1% SDS, 2% TnBP, or 2% Triton X-100 maintained the tensile stiffness. A 1 h treatment with 2% SDS actually increased the Young's modulus. However, 8 h treatments with 2% SDS,

2% TnBP, and 2% Triton X-100 significantly decreased the Young's modulus. Figure 7-6b displays the tensile properties of the constructs treated in phase II. Treatment with 2% SDS for 1 h resulted in a slight increase in tensile properties, although this was not significant. Treatment for 2 and 4 h maintained the tensile stiffness while treatment for 6 h resulted in reduced tensile stiffness. Constructs treated for 8 h were untestable in tension.

Discussion

To the best of our knowledge, this is the first study to decellularize hyaline articular cartilage tissue using a detergent-based approach, and this is the only study to decellularize musculoskeletal tissue engineered constructs. The objective of this study was to assess the effectiveness of multiple decellularization protocols on self-assembled articular cartilage constructs, and to determine an appropriate application time for the treatment. A two-phased approach was used. In phase I, a two-factor approach was employed, in which five different treatments were examined at two application times each. In phase II, the effects of multiple treatment times were examined.

The results of this study indicated that SDS, at concentrations of either 1% or 2%, is an effective treatment for tissue decellularization, thus confirming our hypothesis that cells could be significantly reduced from engineered constructs while maintaining the biomechanical properties. An ionic detergent, SDS typically is able to solubilize the nuclear and cytoplasmic cell membranes. Although all SDS treatments led to cell removal, treatment with 2% SDS appeared the most

promising, although application time also had significant effects. For instance, treatment with 2% SDS for 1 h resulted in a 33% decrease in cellularity, while maintaining both GAG and collagen content, as well as maintaining compressive stiffness. This treatment even resulted in an increase in tensile stiffness; a similar increase in tensile properties was observed in a study of ACL decellularization [242]. On the other hand, treatment with 2% SDS for 8 h led to complete histological decellularization, as well as a 46% decrease in DNA content. However, this treatment also resulted in loss of all GAG and compressive stiffness, as well as a decrease in tensile stiffness. Treatment with 2% SDS for 8 h also resulted in a significant decrease in construct WW, presumably as a result of the GAG loss, which would also decrease the tissue hydration. As 2% SDS resulted in the greatest decrease in DNA content as well as maintained or increased biomechanical and biochemical properties, it was selected for use in phase II.

Treatment with 2% SDS for 1 h resulted in tissue decellularization while maintaining construct functional properties. Although SDS at all application times led to decellularization, 6 or 8 h was required for complete histological decellularization. However, these time points resulted in complete removal of GAG as well as extremely poor compressive stiffness. However, the reduction in collagen content and tensile properties was less pronounced. On the other hand, as in phase I, treatment for 1 h resulted in a significant reduction in DNA content, while maintaining all biochemical and biomechanical properties, and even increasing tensile stiffness. The observed increase in tensile stiffness with a 1 h

application of SDS suggests an effect of the detergent on collagen fibers within the engineered construct. SDS is known to have a propensity to disrupt non-covalent bonds in proteins and confer negative charges on proteins that have been denatured. The application of SDS for 1 h followed by a wash step may have had a transient effect on collagen architecture, wherein collagen fibers unfold as described previously [166], and then return to their native conformations, reforming non-covalent bonds and strengthening interactions in the process. The putative mechanism may have led to the observed increased tensile stiffness at 1 h. With greater time in SDS, the effect is not observed, suggesting that any recovery undergone by collagen is counterbalanced by the detergent's aggregate effect on the rest of the tissue architecture.

It must be noted that although treatment with 2% SDS for 6 or 8 h resulted in complete histological decellularization, it did not result in complete elimination of DNA. It appeared that SDS treatment was effective at achieving complete lysis of cell membranes and nuclear membranes, as H&E staining did not reveal any indication of the presence of cell nuclei, while the DNase treatment was not completely effective in degrading the DNA following membrane lysis. It is possible that a higher DNase concentration is required to achieve more complete elimination of DNA. Additionally, as nucleases were only added during detergent treatment, it is possible that adding a nuclease during the wash step would enable the nucleases to more effectively destroy the remaining DNA.

However, the exact level of tissue decellularization requisite to eliminate an immune response, as well as the proper assessment of decellularization, is

currently unclear. For instance, a recent study by Gilbert et al. [84] demonstrated that several commercially available ECM scaffold materials contained measurable amounts of DNA; some even demonstrated histological staining for nuclear material. These products have all been used successfully clinically, so it is possible that the remaining DNA and nuclear material in the engineered cartilage constructs may result in a limited host response. Additionally, as it is believed that the joint space is relatively immune privileged, as reviewed previously [182], it is possible that complete decellularization of the tissue is not required. Furthermore, it is unclear if decellularization should be assessed histologically merely as elimination of cell nuclei, or if a more complete assessment involves quantifying the tissue's DNA content, as prior studies have utilized differing approaches. For example, Lumpkins et al. [141] found that 1% SDS treatment for 24 h resulted in complete removal of cell nuclei, although they did not assess the DNA content of the tissue. On the other hand, Dahl et al. [50] examined the effects of a hypotonic/hypertonic treatment and found that there was complete removal of cell nuclei, but no decrease in DNA content. To study this issue further, *in vivo* studies are warranted to determine if there is threshold of decellularization at which an immune response is eliminated.

Although it was less effective than the 2% concentration, 1% SDS displayed similar effects. For example, treatment for 1 h resulted in a 15% decrease in DNA content, while maintaining GAG and collagen content, as well as maintaining biomechanical properties. Additionally, treatment for 8 h resulted

in a 37% decrease in DNA content, loss of all GAG and compressive stiffness, as well as a decrease in tensile stiffness.

On the other hand, treatment with Triton X-100 and TnBP did not appear promising, as they had a minimal effect on tissue decellularization, and resulted in a slight decrease in GAG content. Several prior studies have indicated the ineffectiveness of Triton X-100, although it was used in this study as it is believed to have minimal effects on protein-protein interactions [85]. For example, Dahl et al. [50] examined the effects of 1% Triton X-100 on porcine carotid arteries, and found that this treatment resulted in similar cellularity to control and no decrease in DNA content. In another study on tendon decellularization, Cartmell and Dunn [39] examined the effect of 1% Triton X-100 for 24 h, and found that cell density remained similar to control. Contrary to our results, this study also demonstrated complete decellularization with 1% TnBP, although a 48 h treatment was required. Therefore, it is possible that TnBP treatment may result in decellularization of self-assembled constructs at longer application times, although the GAG loss after as little as 8 h prevents the use of longer application times.

Finally, although a hypotonic/hypertonic treatment has been an effective decellularization agent in this study as well as prior studies, it did not appear to be a viable treatment for self-assembled cartilage constructs, as it had severely detrimental effects on construct functional properties. For instance, treatment for as little as 1 h resulted in nearly complete loss of compressive and tensile stiffness, while constructs treated for 8 h were untestable mechanically.

Additionally, treatment at both application times resulted in nearly complete elimination of GAG content.

Based on these results, treatment with 2% SDS appears to be the most promising and should be examined further in future studies. *In vivo* studies should be performed to determine the immune response to the decellularized tissue. Additionally, the effects of different decellularization treatments on complement activation should be addressed in future *in vitro* studies. Furthermore, as this study aimed to reduce the cellularity, additional studies are needed to investigate the elimination of the Gal α 1,3 epitope, which plays a significant role in hyperacute rejection of xenografts [172]. Treatment for 1 or 2 h maintained biomechanical and biochemical properties, while simultaneously significantly reducing the DNA content of the tissue. Additionally, treatment for 6 or 8 h resulted in complete histological decellularization, but also resulted in elimination of GAG and compressive stiffness. Although the results of this study did not result in a completely decellularized construct with maintenance of biochemical and biomechanical properties, the results are promising and indicate the potential of a decellularized articular cartilage construct that could be used to treat damaged cartilage tissue without eliciting an immune response.

Table 7-1. Phase I Construct wet weight and thickness values

Treatment Group	Construct WW (mg)	Thickness (mm)
Control	14.8±1.1	0.49±0.03
1% SDS, 1 h	14.3±1.0	0.50±0.02
1% SDS, 8 h	8.8±1.2 ^a	0.38±0.04 ^a
2% SDS, 1 h	12.3±1.1	0.43±0.05
2% SDS, 8 h	9.3±2.6 ^a	0.47±0.08
2% TnBP, 1 h	15.2±1.1	0.53±0.06
2% TnBP, 8 h	12.2±1.2	0.49±0.04
2% Triton X-100, 1 h	13.7±1.2	0.47±0.05
2% Triton X-100, 8 h	11.2±1.7 ^a	0.47±0.08
Hypo/Hyper 1 h	15.0±3.0	0.40±0.09
Hypo/Hyper 8 h	7.0±1.3 ^a	0.35±0.04 ^a

^aSignificantly lower than control ($p < 0.05$)

Table 7-2. Phase II construct wet weight and thickness values

Treatment Group	Construct WW (mg)	Thickness (mm)
Control	19.9±3.3	0.73±0.14
1 h	16.0±4.1	0.73±0.16
2 h	15.8±3.6	0.66±0.10
4 h	14.8±2.5	0.56±0.09
6 h	9.3±1.9 ^a	0.53±0.07 ^a
8 h	10.7±1.8 ^a	0.53±0.08 ^a

^aSignificantly lower than control (p<0.05)

Table 7-3. Values for Poisson ratio and permeability from Phase I

Treatment Group	Poisson Ratio	Permeability ($\times 10^{-14}$ m ⁴ /Ns)
Control	0.30±0.07	14.3±3.9
1% SDS, 1 h	0.26±0.04	15.6±8.0
1% SDS, 8 h	0.07±0.09 ^a	2.0±1.6 ^a
2% SDS, 1 h	0.26±0.10	12.6±6.3
2% SDS, 8 h	Not testable	Not testable
2% TnBP, 1 h	0.24±0.13	5.5±3.1
2% TnBP, 8 h	0.04±0.03 ^a	7.3±7.5
2% Triton X-100, 1 h	0.16±0.11	4.3±2.6
2% Triton X-100, 8 h	0.04±0.04 ^a	5.1±4.7
Hypo/Hyper 1 h	0.14±0.14	14.9±6.6
Hypo/Hyper 8 h	Not testable	Not testable

^aSignificantly lower than control (p<0.05)

Table 7-4. Values of Poisson ratio and permeability from Phase II

Treatment Group	Poisson Ratio	Permeability ($\times 10^{-14}$ m ⁴ /Ns)
Control	0.13±0.07	32.0±18.2
1 h	0.09±0.08	27.0±15.2
2 h	0.08±0.08	15.5±4.4
4 h	0.09±0.09	66.3±77.3
6 h	Not testable	Not testable
8 h	Not testable	Not testable

^aSignificantly lower than control ($p < 0.05$)

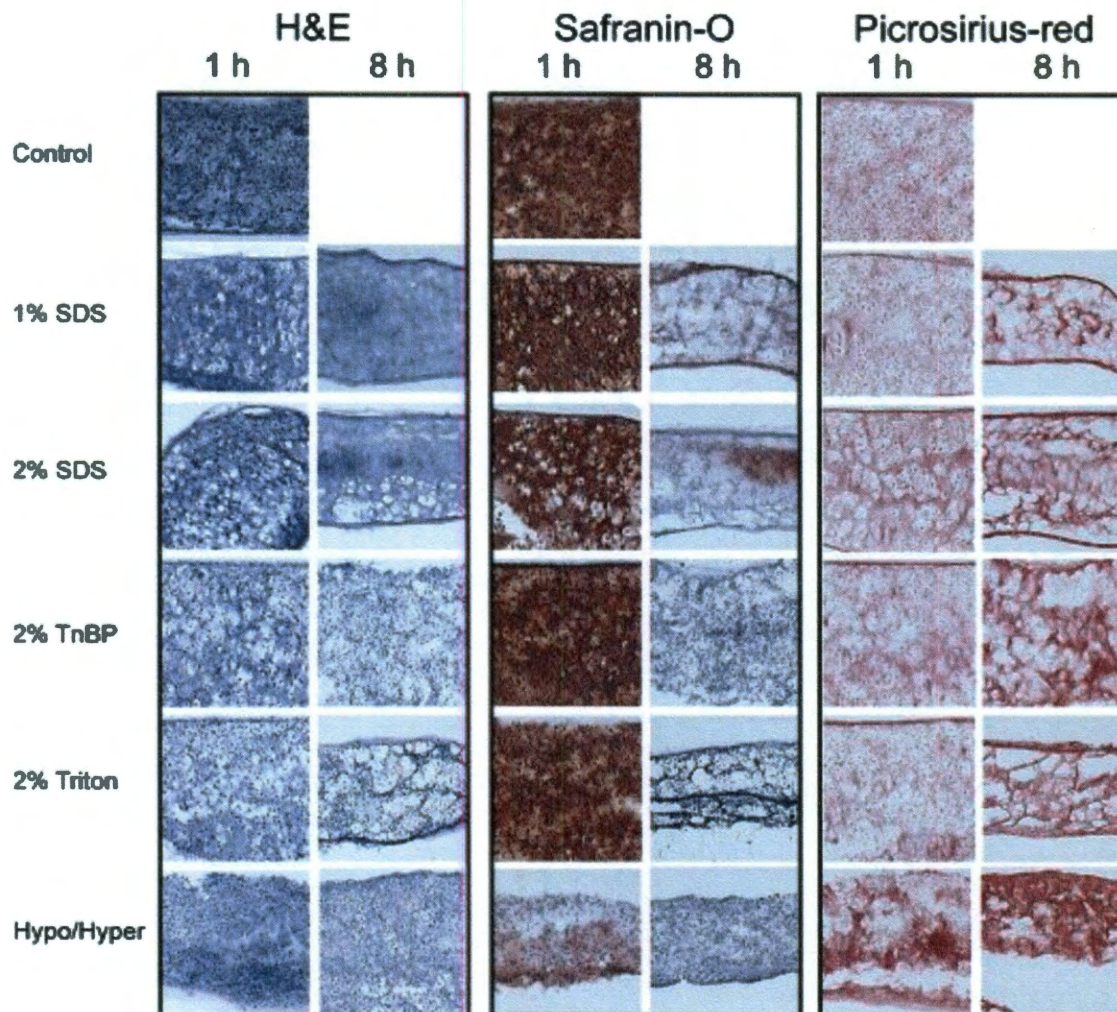


Figure 7-1. Histology for Phase I

Photomicrographs demonstrating construct cellularity, GAG content, and collagen content for various treatment groups in phase I. 10x original magnification. Treatment with 2% SDS for 1 h decreased cellularity while preserving GAG content, while treatment for 8 h eliminated all nuclei, but also eliminated all GAG.

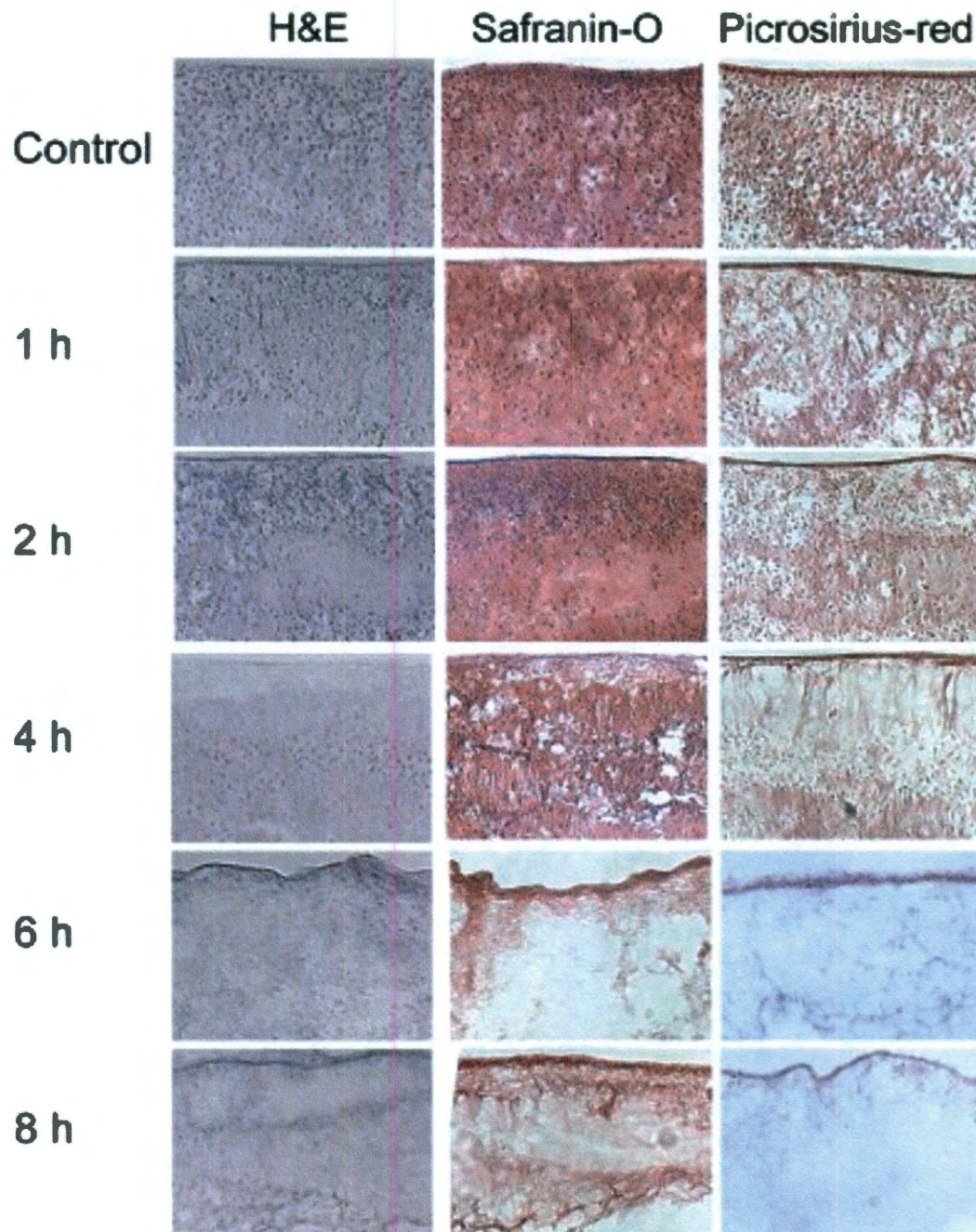


Figure 7-2. Histology for Phase II

Photomicrographs demonstrating construct cellularity, GAG content, and collagen content for treatment groups in phase II. 10x original magnification. Treatment with 2% SDS for 1, 2, and 4 h decreased cellularity while preserving GAG and collagen content, while treatment for 6 and 8 h eliminated all nuclei, but also eliminated GAG and reduced collagen.

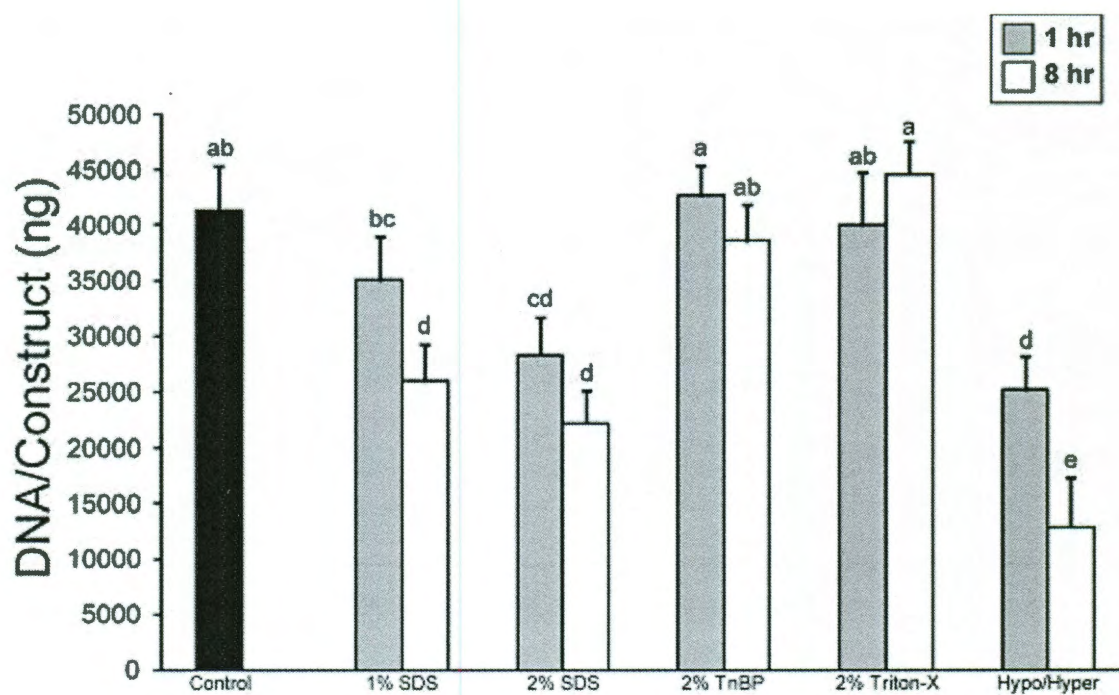


Figure 7-3. DNA content of constructs following decellularization in phase I
Treatment with 2% SDS or the hypotonic/hypertonic solutions at either application time significantly decreased construct DNA content. Columns and error bars represent means and standard deviations. Groups denoted by different letters are significantly different ($p < 0.05$).

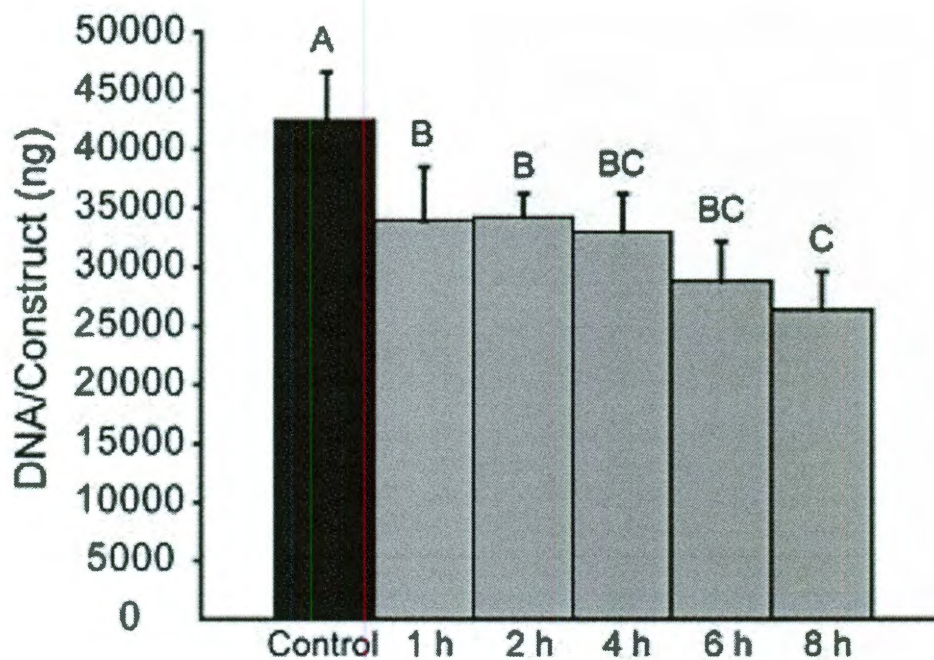


Figure 7-4. DNA content of constructs following decellularization in phase II
Treatment with 2% SDS at all application times significantly reduced DNA content, while treatment for 8 h resulted in the greatest reduction in DNA content. Columns and error bars represent means and standard deviations. Groups denoted by different letters are significantly different ($p < 0.05$).

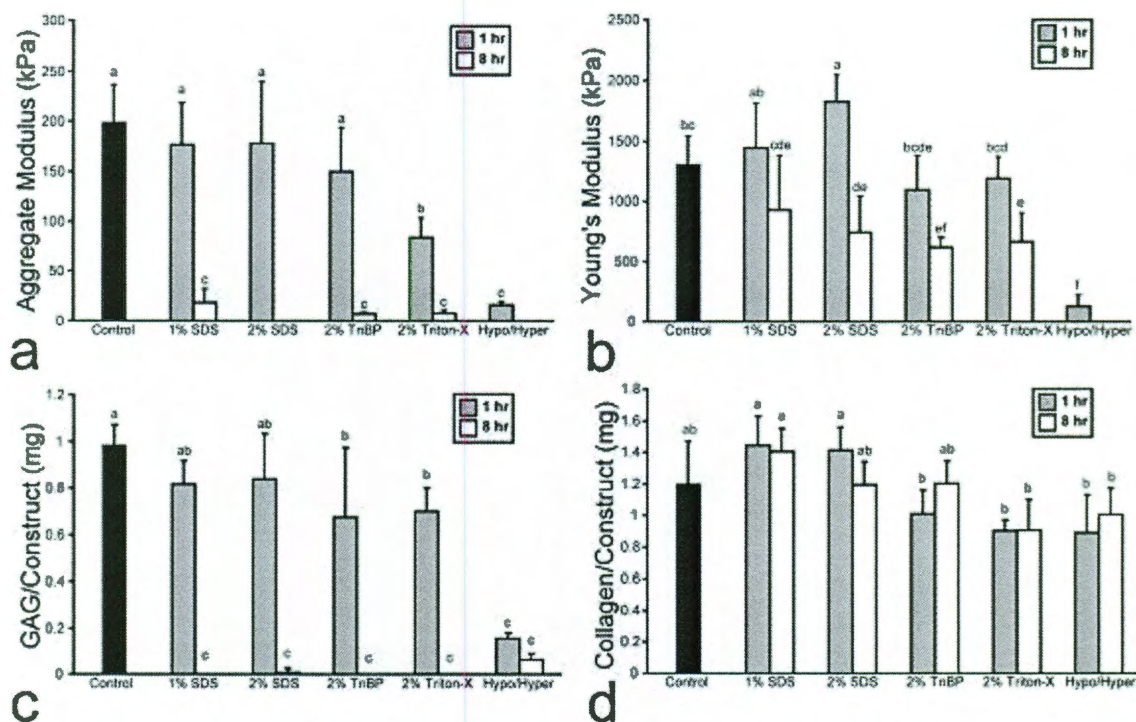


Figure 7-5. Construct properties following decellularization in phase I

(a) All 8 h treatments either significantly reduced compressive stiffness, or were untestable. Treatment for 1 h with 1% or 2% SDS, or 2% TnBP maintained compressive stiffness. (b) Treatment with 1% SDS for 1 h maintained tensile stiffness, while treatment with 2% SDS for 1 h increased tensile stiffness. (c) All 8 h treatments resulted in nearly complete GAG removal, while both 1% and 2% SDS for 1 h maintained GAG content. (d) Treatment with SDS or TnBP maintained collagen content, while treatment with Triton X-100 or the hypotonic/hypertonic combination significantly reduced total collagen content. Columns and error bars represent means and standard deviations. Groups denoted by different letters are significantly different ($p < 0.05$).

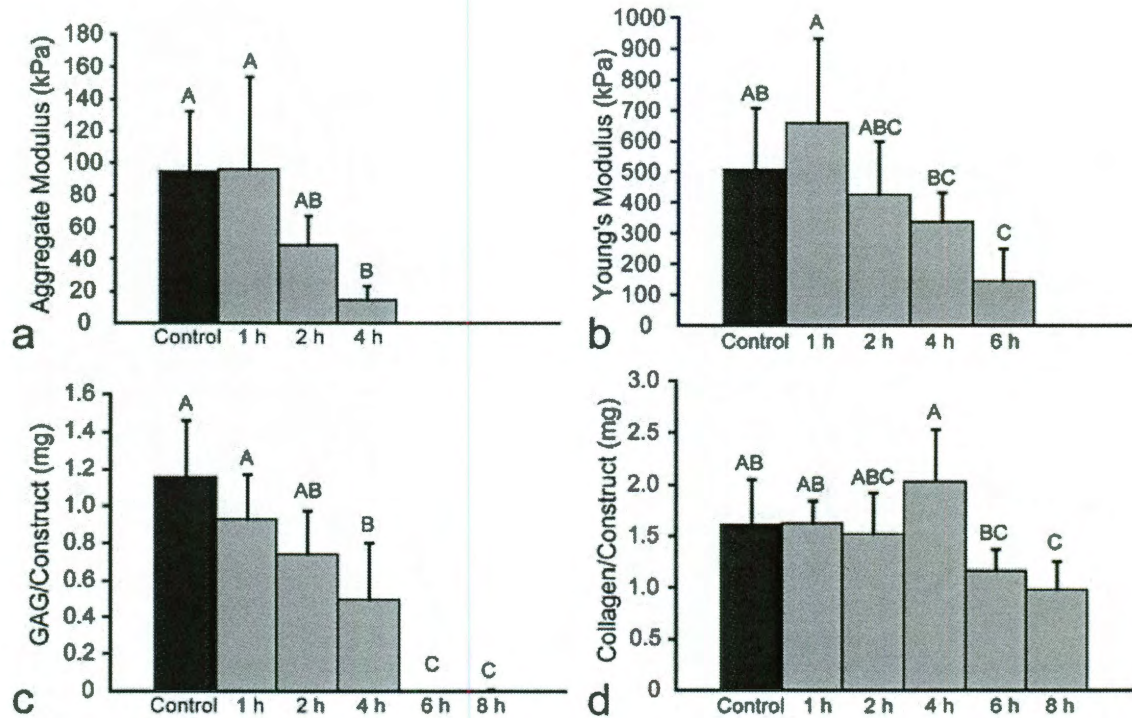


Figure 7-6. Construct properties following decellularization in phase II

(a) 2% SDS treatment for 1 or 2 h maintained compressive properties, while treatment for 6 or 8 h resulted in constructs that were untestable in compression. (b) Treatment for 1, 2, or 4 h maintained tensile stiffness, while 6 and 8 h treatments significantly reduced tensile stiffness. (c) Treatment for 1 or 2 h maintained GAG content, while treatment for 6 or 8 h resulted in near complete GAG removal. (d) Treatment for 1, 2, 4, or 6 h maintained collagen content, while treatment for 8 h resulted in a reduction in collagen content.

Chapter 8. Structure-function relationships in the immature knee joint^{*}

^{*} Published as **Eleswarapu SV⁺**, Responde DJ⁺, and Athanasiou KA, "Tensile properties, collagen content, and crosslinks of the immature knee joint," *PLoS ONE* 2011. ⁺ = Equal contribution.

Abstract

The major connective tissues of the knee joint act in concert during locomotion to provide joint stability, smooth articulation, shock absorption, and distribution of mechanical stresses. These functions are largely conferred by the intrinsic material properties of the tissues, which are in turn determined by biochemical composition. A thorough understanding of the structure-function relationships of the connective tissues of the knee joint is needed to provide design parameters for efforts in tissue engineering.

The objective of this study was to perform a comprehensive characterization of the tensile properties, collagen content, and pyridinoline crosslink abundance of condylar cartilage, patellar cartilage, medial and lateral menisci, cranial and caudal cruciate ligaments (analogous to anterior and posterior cruciate ligaments in humans, respectively), medial and lateral collateral ligaments, and patellar ligament from immature bovine calves. Tensile stiffness and strength were greatest in the menisci and patellar ligament, and lowest in the hyaline cartilages and cruciate ligaments; these tensile results reflected trends in collagen content. Pyridinoline crosslinks were found in every tissue despite the relative immaturity of the joints, and significant differences were observed among tissues. Notably, for the cruciate ligaments and patellar ligament, crosslink density appeared more important in determining tensile stiffness than collagen content.

To our knowledge, this study is the first to examine tensile properties, collagen content, and pyridinoline crosslink abundance in a direct head-to-head

comparison among all of the major connective tissues of the knee. This is also the first study to report results for pyridinoline crosslink density that suggest its preferential role over collagen in determining tensile stiffness for certain tissues.

Introduction

The major connective tissues of the knee joint act in concert during locomotion to provide joint stability, smooth articulation, shock absorption, and distribution of mechanical stresses [28, 123, 241]. These functions are largely conferred by the intrinsic material properties of the tissues, which are in turn determined by their biochemical compositions. Based on structure-function relationships, each connective tissue of the knee joint can be conceptualized along a continuum from hyaline to fibrocartilaginous to fibrous (Figure 8-1). These tissues have received considerable attention in both basic science and clinical literature, but much work remains to be done to elucidate the contributions of particular biochemical components to important mechanical parameters, especially with respect to applications in tissue engineering. Approaches in tissue engineering are guided heavily by the interplay of native tissue structures and their corresponding functional correlates. To better understand these relationships, this study examines the biochemical composition and tensile properties of the major connective tissues of the immature bovine knee joint.

The knee is a pivotal hinge joint that permits flexion, extension, and limited rotation through coordinated action of its hyaline, fibrocartilaginous, and fibrous connective tissues. Hyaline cartilage is found at the condylar surfaces of the

femur and tibia, as well as on the patella. Fibrocartilage comprises the medial and lateral menisci, which are crescent-shaped structures interposed between the femoral and tibial condyles. Fibrous tissue makes up the major ligaments of the knee joint, in particular the patellar ligament, the collateral ligaments, and the cruciate ligaments. The patellar ligament provides stability to the patella as it glides over the patellofemoral groove and femoral condyles. The medial and lateral collateral ligaments (MCL and LCL) are extracapsular ligaments that protect the medial and lateral sides of the knee from a contralateral outside or inside bending force, respectively. The anterior and posterior cruciate ligaments (ACL and PCL) are intracapsular ligaments that stabilize the knee during rotation and bending. Together, these tissues contribute significantly to normal knee function.

The connective tissues of the knee joint are known to derive their mechanical properties from their biochemical components, but precise structure-function relationships remain elusive beyond general notions of the role of the extracellular matrix (ECM). Structurally, each of these tissues is hypocellular and possesses an ECM rich in collagen, with varying amounts of glycosaminoglycans (GAGs) [7, 176]. In general, collagen is known to be largely responsible for the tensile integrity of these tissues, while GAGs, predominant in hyaline cartilage and sparse in fibrous tissues, contribute to compressive strength [181]. In addition to total collagen content, the amount of crosslinking present in the collagen network has been shown to play an important role in tissue tensile properties [24]. In examining tissue tensile properties, two important measures of

tensile integrity are Young's modulus and ultimate tensile strength (UTS). Young's modulus is a measure of a material's tensile stiffness, and the UTS is the maximum stress a material can withstand. Though collagen content and crosslinking are known to play a role in tensile mechanics, their precise structure-function relationships with respect to Young's modulus and UTS remain unclear. Pyridinoline crosslinks have been shown to correlate with both tensile strength and stiffness in articular cartilage [235], but there is a dearth of literature describing the contribution of pyridinoline crosslinks to the mechanical behavior of fibrocartilage or ligament tissues.

In humans, conditions afflicting the connective tissues of the knee, such as traumatic injury and osteoarthritis, contribute to substantial healthcare costs and work-related disability [1, 101, 139]. The field of tissue engineering aims to improve orthopaedic medicine by providing functional replacements for damaged or diseased joint tissues. Recent tissue engineering efforts have focused on major connective tissues such as hyaline cartilage [105, 148], meniscus [109, 230], tendon [36, 37], and ligament [98]. Although various approaches have been employed to engineer these tissues, it has been difficult to reproduce native collagen organization and attain native mechanical properties. Various types of mechanical [16, 71, 148, 168] and biochemical [88, 158] stimuli have been studied to improve construct properties, and both scaffold-free [105, 178, 203] and scaffold-based [47, 153] approaches have been investigated for connective tissue engineering applications. An additional consideration in these tissue engineering efforts has been the cell source used to produce constructs.

Comparisons of cell types have shown that immature cells exhibit increased biosynthesis [227], making them promising candidates for tissue engineering. Immature cells have been used to produce constructs with clinically relevant dimensions [105] and mechanical properties on par with native tissue. To make informed cell source choices, it is necessary to establish a comprehensive understanding of the physiology of immature joint tissues. Moreover, while studies on the knee joint are well represented in the literature, it is important to note that much of what is known about the structure-function relationships of these tissues comes from assessments of adult rather than immature joints, whether human or animal. Given the prevalence of knee injuries in the pediatric population [140], along with a greater push towards using immature tissues as cell sources for tissue engineering, a thorough elucidation of the biochemistry of immature knee joint tissues, not just adult tissues, is warranted. An understanding of immature joint physiology may also yield insight into tissue development by providing a reference to which adult tissues can be compared, as well as informing a general understanding of factors at play in pediatric joint injury. Additionally, because orthopaedic explant and tissue engineering studies are relying more readily on bovine tissues [16, 100, 105, 135, 192], it is imperative that a full assessment of the bovine joint be undertaken.

The objective of this study was to perform a comprehensive characterization of the tensile properties, collagen content, and pyridinoline crosslink abundance of the major connective tissues of the immature bovine knee joint. Tissues of interest were femoral condylar and patellar cartilage,

medial and lateral menisci, cranial and caudal cruciate ligaments (analogous to the ACL and PCL in humans, respectively), medial and lateral collateral ligaments, and patellar ligament. It was hypothesized that trends in tensile properties would reflect those in collagen content; that tensile properties and collagen content would be higher in fibrocartilaginous and ligamentous tissues than in hyaline tissues; and that pyridinoline crosslinks would be found in all tissues, in spite of the immaturity of the tissues. Results from this investigation reinforce the interplay of tissue biomechanics and biochemical content and provide design parameters for future efforts concerned with connective tissue engineering for joint repair.

Materials and methods

Tissue harvest and specimen preparation

Tissue specimens were harvested from the knee joints of 6 one-week-old male bovine calves (Research 87, Boston, MA), shortly after slaughter of the animals for commercial use in the food industry. To normalize variability among animals, each leg came from a different animal. Hyaline femoral condylar cartilage (CC), hyaline patellar cartilage (PC), medial meniscus (MM), lateral meniscus (LM), cranial cruciate ligament (CraCL), caudal cruciate ligament (CauCL), medial collateral ligament (MCL), lateral collateral ligament (LCL), and patellar ligament (PL) were taken. For CC and PC specimens, the cartilage was separated from subchondral bone with a scalpel. For MM and LM specimens, the femoral and tibial surfaces, as well as the inner 1/3 and outer 1/3 portions of the annulus,

were sliced away, leaving the approximate interior circumferential portion of the specimen for assessment. CraCL, CauCL, MCL, LCL, and PL were taken whole from their attachments.

From each freshly harvested specimen, a 3 mm dermal biopsy punch was used to obtain samples for histology, quantitative biochemistry, and high performance liquid chromatography (HPLC). The remainder of each specimen was then prepared for tensile testing. Tensile specimens were stored for a maximum of 24 h in phosphate buffered saline with protease inhibitors at 4°C and were allowed to equilibrate to room temperature prior to testing.

Histology

Samples were cryo-embedded and sectioned at 14 µm. Sections were fixed in formalin for 10 min and then stained with either picosirius red or safranin O/fast green as described previously [105]. Samples were dehydrated in an ascending series of ethanol and mounted with coverslips prior to imaging.

Quantitative biochemistry

Biochemistry samples were weighed wet, frozen, lyophilized for 48 h, and then digested in a phosphate buffer with 125 µg/mL papain (Sigma) for 18 h at 65°C. A chloramine-T hydroxyproline assay was employed to quantify total collagen content after 2 N NaOH hydrolysis for 20 min at 110°C [8]. Total collagen was normalized to tissue wet weight and tissue dry weight.

High performance liquid chromatography (HPLC)

HPLC was performed to quantify the abundance of pyridinoline crosslinks. Samples were weighed wet, digested in 800 μL of 6 N HCl at 100°C for 20 h, and then dried using a vacuum concentrator. Samples were re-suspended in 50 μL of an aqueous solution containing 10 nmol pyridoxine/mL and 2.4 μmol homoarginine/mL and then diluted fivefold with an aqueous solution of 0.5% HFBA acetonitrile in 10% acetonitrile. 10 μL of each sample was injected into a 25 mm C18 column (Shimadzu) and eluted using a solvent profile described previously [19]. To quantify the amount of crosslink in each sample, pyridinoline standards (Quidel) were employed to create a calibration curve.

Tensile testing

Each specimen was cut into a dog-bone shape with a 1-mm-long gauge length. Although this tissue preparation may limit comparison to an *in vivo* context, it was important to maintain consistent mechanical testing procedures across tissue types so that comparisons could be made between tissues without the risk of introducing confounding variables. The specimen was photographed alongside a ruler, and ImageJ software was used to determine the width and thickness. A uniaxial electromechanical materials testing system (Instron Model 5565) was employed to determine tensile properties with a 50 N (CC and PC only) or 5 kN load cell (all other tissues). CC and PC specimens were affixed with cyanoacrylate glue to paper tabs outside of the gauge length for gripping; all other specimens were gripped directly outside of the gauge length. MM and LM

specimens were tested in the circumferential direction. CraCL, CauCL, MCL, LCL, and PL specimens were tested in the longitudinal direction. Tensile tests were performed until failure within the gauge length at a strain rate of 1% of the gauge length per second. Force-displacement curves were generated, and stress-strain curves were calculated by normalizing data to specimen dimension. The apparent Young's modulus, a measure of specimen tensile stiffness, was determined by least squares fitting of the linear region of the stress-strain curve. The ultimate tensile strength (UTS) was determined as the maximum stress reached during a test.

Statistical analysis

All biochemical, HPLC, and tensile assessments were made using $n=5-6$. To compare among tissues, a single-factor analysis of variance was employed, and a Fisher least significant difference post hoc test was used when warranted. Significance was defined as $p<0.05$.

Results

Histology

Representative histology for hyaline cartilage, meniscus, and ligament are shown in Figure 8-2. Staining for collagen was observed in all tissues, though hyaline cartilage exhibited less extensive collagen staining compared to either meniscus or ligament. Extensive staining for GAG was observed in the hyaline cartilage

specimens, but was not qualitatively observed in meniscus or ligament specimens.

Collagen content

The collagen/wet weight for CC, PC, MM, LM, CraCL, CauCL, MCL, LCL, and PL were $6.7\pm 2.6\%$, $5.1\pm 1.4\%$, $22.7\pm 5.3\%$, $26.7\pm 7.5\%$, $4.6\pm 0.9\%$, $2.8\pm 1.2\%$, $19.4\pm 4.6\%$, $20.9\pm 0.3\%$, and $21.2\pm 3.5\%$, respectively (Figure 8-3A). Fibrocartilage tissues (MM and LM) had the highest collagen content; the fibrocartilage tissues averaged together had 4.1x the collagen content of the hyaline tissues and 6.7x the collagen content of the cruciate ligaments. Among just the fibrous tissues, the collateral ligaments (MCL and LCL) and PL had higher collagen content than the cruciate ligaments (CraCL and CauCL); in particular, the collateral ligaments averaged together had 5.4x the collagen content of the cruciate ligaments. The cruciate ligaments were not significantly different from the hyaline cartilage tissues (CC and PC) in collagen content. The collagen/dry weight for CC, PC, MM, LM, CraCL, CauCL, MCL, LCL, and PL were $45.6\pm 10.3\%$, $46.5\pm 16.2\%$, $91.6\pm 16.4\%$, $93.5\pm 10.6\%$, $72.6\pm 12.1\%$, $86.8\pm 10.7\%$, $70.8\pm 16.1\%$, $81.7\pm 9.3\%$, and $84.1\pm 11.6\%$, respectively (Figure 8-3B).

Pyridinoline crosslink content

Pyridinoline was resolved as one peak for all samples. Pyridinoline normalized to tissue wet weight (pyd/ww) for CC, PC, MM, LM, CraCL, CauCL, MCL, LCL, and PL were 0.303 ± 0.101 , 0.174 ± 0.049 , 0.498 ± 0.160 , 0.534 ± 0.115 , 0.374 ± 0.087 ,

0.565±0.204, 0.414±0.123, 0.422±0.067, and 0.585±0.069 nmol/mg, respectively (Figure 8-3C). Pyd/ww was highest in PL, while CauCL, LM, and MM samples trended higher compared to all other tissues. The hyaline cartilages (CC and PC) had the lowest pyd/ww. The fibrocartilage tissues averaged together had a pyd/ww 2.16x that of the hyaline cartilages, and all of the ligament tissues averaged together had a pyd/ww 1.98x that of the hyaline cartilages.

Pyridinoline normalized to collagen content (pyd/col) for CC, PC, MM, LM, CraCL, CauCL, MCL, LCL, and PL were 5.69±3.85, 3.68±1.59, 2.28±0.88, 2.17±0.92, 8.32±2.12, 16.08±4.53, 2.22±0.85, 2.02±0.34, and 2.80±0.42 nmol/mg, respectively (Figure 8-3D). Statistically, CauCL had the highest pyd/col and CraCL the second highest, followed by the hyaline cartilages. The collateral and patellar ligaments and both menisci were not statistically different from each other and were less than the cruciate ligaments and the hyaline cartilages. CauCL had a pyd/col 1.93x that of the CraCL, 3.43x that of the hyaline cartilages, 7.22x that of the fibrocartilage tissues, and 7.59x that of the collateral ligaments.

Tensile properties

The Young's moduli for CC, PC, MM, LM, CraCL, MCL, LCL, and PL were 8.4±4.1, 4.6±1.8, 25.9±7.0, 21.6±6.2, 2.1±1.0, 11.6±5.9, 13.2±5.8, 16.9±4.07, 27.5±2.8 MPa, respectively (Figure 8-4A). The UTS for CC, PC, MM, LM, CraCL, MCL, LCL, and PL were 7.0±2.2, 3.9±0.7, 15.1±4.5, 24.6±2.0, 1.4±0.6, 7.4±5.9, 10.1±6.4, 14.9±3.9, and 15.7±3.3 MPa, respectively (Figure 8-4B). MM, LM, and PL exhibited significantly higher stiffnesses (Young's moduli) and strengths

(UTS) compared to the other tissues, while CC, PC, CraCL, and CauCL were among the softest and weakest in tensile properties. Also of note, among the cruciate ligaments, CauCL was significantly stiffer and stronger than CraCL; Young's modulus and UTS for CauCL were both 5.4x the values for CraCL.

Discussion

This study examined the major connective tissues of the immature bovine knee joint, motivated by a need to understand the interplay of biomechanics and biochemistry in immature connective tissues, as well as to establish design parameters for *in vitro* tissue engineering efforts. In the present study, differences were found across tissue types with respect to histology, collagen content, pyridinoline crosslink abundance, and tensile properties. In addition to reinforcing orthopaedic structure-function relationships, to our knowledge, this study is the first to examine these parameters in a direct head-to-head comparison among all of the major connective tissues of the knee, the first to assess pyridinoline crosslink abundance in all the tissues of a bovine joint, and the first to report results for pyridinoline crosslink abundance that suggest its preferential role over collagen in determining stiffness for certain tissues.

In the present study, tissues of interest were first examined histologically for the presence of collagen and GAGs to infer qualitative structural differences underlying the biomechanical distinctions between these different tissues. Meniscus and ligament specimens appeared nearly identical, exhibiting extensive staining for collagen with no observable GAG staining (Figure 8-2).

Hyaline cartilage, by contrast, exhibited less collagen staining than either meniscus or ligament, but also significant GAG staining. These histological trends correspond to the notion of knee joint connective tissues spanning a continuum between hyaline tissue (high collagen, high GAG) and fibrous tissue (high collagen, low GAG) (Figure 8-1). These qualitative histological differences relate to the functional roles of these tissues: fibrous tissues (ligaments and tendons) and fibrocartilage tissues (menisci) experience tremendous tensile stresses during locomotion, while hyaline cartilage experiences a balance of both tensile and compressive stresses, though preferentially the latter.

Tissue tensile properties, especially in connective tissues, are derived in part from collagen content [181], as well as from other matrix components, such as elastin [214]; therefore, it was hypothesized that trends in tensile properties would reflect trends in collagen content. In this study, collagen content was quantified in each tissue and normalized to tissue wet weight (Figure 8-3A). It was found that the menisci had the highest collagen content, followed by the patellar ligament and the collateral ligaments. Collagen content was lowest in the hyaline cartilages and the cruciate ligaments. As expected, the tensile properties (Figure 8-4) appear to reflect the general trends observed in collagen content normalized to wet weight. In particular, it was found that the menisci and patellar ligament exhibited significantly higher stiffness (Young's moduli) and strength (UTS) values compared to the other tissues, while the hyaline cartilages and the cruciate ligaments were among the softest and weakest in tensile properties.

The differences in tensile properties among the ligament tissues (high in patellar ligament, medium in collateral ligaments, and low in cruciate ligaments) may reflect the anatomical development of these tissues, since the stiffer/stronger tissues are extracapsular ligaments, and the softer/weaker tissues are intracapsular ligaments. In particular, the patellar ligament arises from fibers of the quadriceps muscle attaching inferiorly to the tibial tuberosity, hence the term “patellar tendon” often used interchangeably with patellar ligament, given the tendinous origin; the cruciate ligaments develop posteriorly from the articular interzone; and the collateral ligaments form independently of the joint capsule (LCL) or from mesenchymal condensation in the joint capsule (MCL) [149]. Furthermore, of particular interest was the finding that CraCL is significantly softer and weaker than CauCL. Future studies should seek to examine whether this relationship is maintained in adult cows, as well as whether it is observed in humans (i.e., between the ACL and PCL). Taken together, the tensile data described above contribute important information about the tensile properties of immature tissues, especially in light of the increasing incidence of knee joint injuries among youths [140]. Additionally, these tensile properties may serve as important benchmarks to determine success criteria for *in vitro* engineering of the major knee joint connective tissues, all of which play important roles in mechanical function. Tissue engineering efforts aimed at recapitulating native tissue structures should strive to reproduce native tissue biomechanical properties, as well.

Crosslink analysis with HPLC showed that the different joint tissues had varying pyridinoline abundances that contributed to tensile stiffness. The data showed that the hyaline cartilages and the cruciate ligaments exhibited the highest pyridinoline levels (Figure 8-3). Both the patellar ligament and CauCL exhibited higher tensile stiffness values that paralleled pyridinoline content but not the amount of collagen. Although pyridinoline has been shown to correlate with tensile strength and stiffness in bovine articular cartilage [235], this is the first study to show that pyridinoline also contributes to the mechanical properties of other joint tissues. These results also corroborate structure-function relationships in other species. For example, a study of the rat tendon demonstrated that pyridinoline was a better indicator of ultimate stress than collagen content [40]. These structure-function relationships illustrate the importance of crosslinking in a variety of joint tissues.

Pyridinoline content is known to generally increase as tissues matures, but this study provides comprehensive, quantitative benchmarks that can be compared to adult tissue values. For instance, the observed pyridinoline abundances for condylar cartilage and meniscus fibrocartilage are approximately 50% and 70% of the mature values, respectively [76, 235]. These pyridinoline results can inform future tissue engineering efforts that aim to reproduce the biochemical composition of native tissues. Because engineered cartilage has shown less collagen crosslinking than native tissue, strategies such as increasing lysyl oxidase expression [61] may be needed to increase pyridinoline formation. Other stimuli such as TGF- β 1 have been shown to increase pyridinoline content

in articular cartilage [221] and could potentially be beneficial for enhancing crosslinking in engineered tissue as well. Considering the role of pyridinoline in tissue mechanics [235, 236] and the inherently mechanical nature of knee joint connective tissues, crosslinking should be a central focus of future tissue engineering approaches.

This study provides biochemical and biomechanical data describing hyaline, fibrocartilaginous, and fibrous tissues of the immature bovine knee joint. These data elucidate important structure-function relationships that can inform directed approaches for functional connective tissue engineering. In particular, future tissue engineering approaches should aim to incorporate methods for improving crosslinking, since crosslink abundance may be a more relevant predictor of tensile stiffness than collagen content for certain tissues, as evidenced by the relationships identified in the cruciate ligaments and patellar ligament. Future work may expand on this study by examining temporal development and maturation of the collagen network and tensile properties, or by making direct comparisons in pyridinoline crosslink abundance between immature and adult tissues. Finally, an assessment of these parameters in disease states such as osteoarthritis or traumatic injury models such as ligament rupture may shed light on predisposing factors.

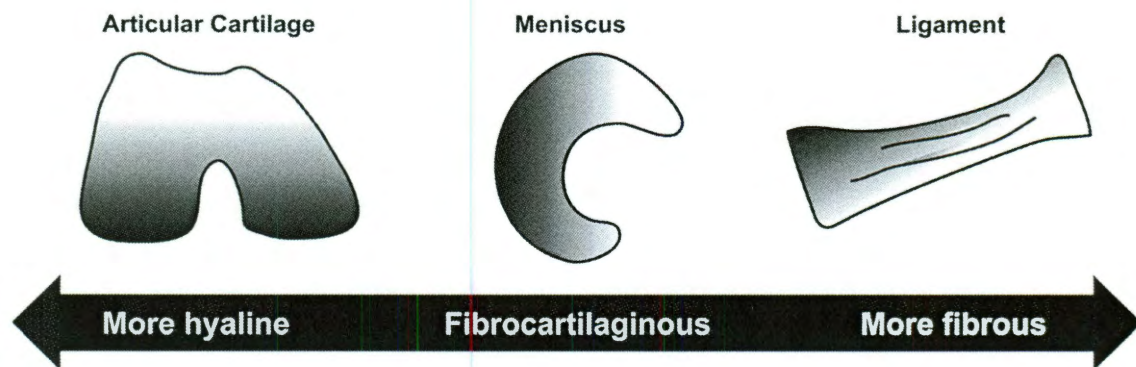


Figure 8-1. Continuum of knee joint connective tissues

Based on their structural compositions, the major connective tissues of the knee joint can be conceptualized along a continuum from hyaline (condylar and patellar cartilage), to fibrocartilaginous (meniscus), to fibrous (ligament).

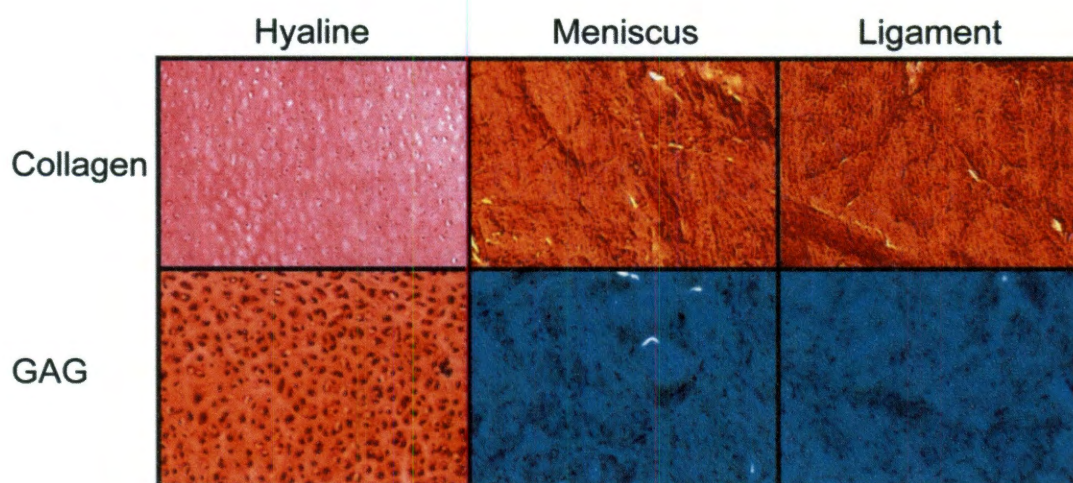


Figure 8-2. Histology of representative joint tissues

Picrosirius red staining for collagen showed that hyaline cartilage, meniscus, and ligament all had significant collagen content. The meniscus and ligament samples stained more intensely for collagen than hyaline cartilage. Safranin O/fast green staining for GAG showed that hyaline cartilage had significant GAG content; meniscus and ligament did not exhibit GAG staining.

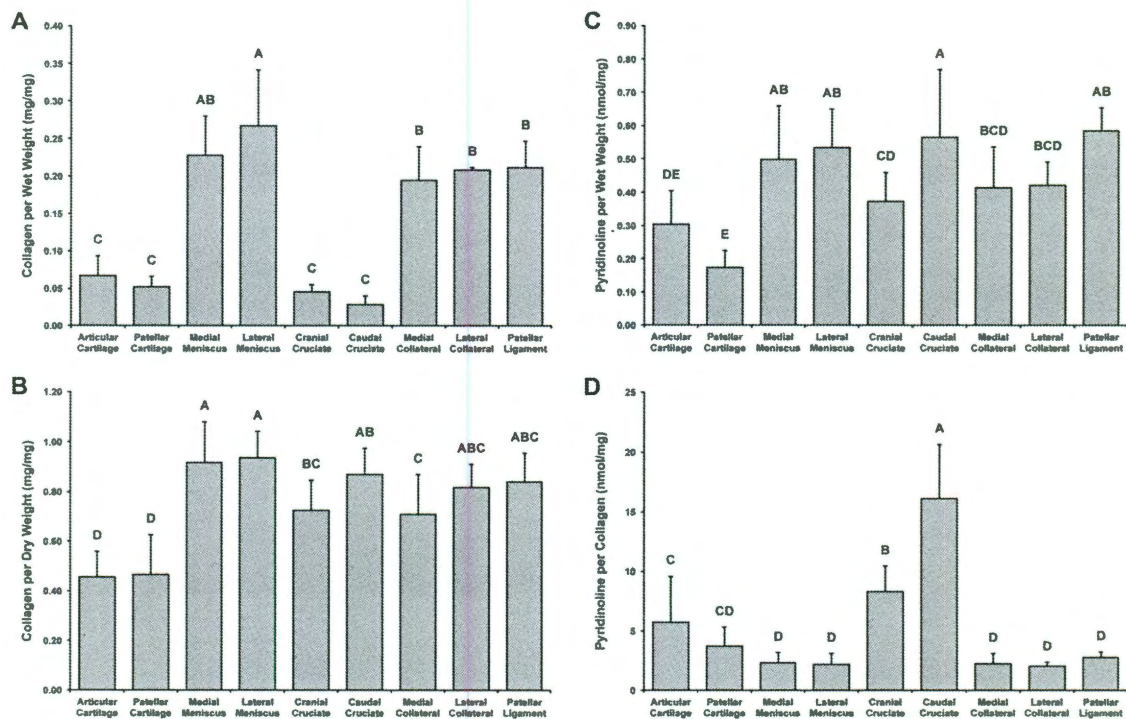


Figure 8-3. Collagen and pyridinoline content of joint tissues

(A) Collagen normalized to wet weight was significantly higher for the menisci, collateral ligaments, and patellar ligament. (B) Collagen normalized to dry weight was highest in the menisci and lowest in the hyaline cartilages. (C) Pyridinoline normalized to wet weight was highest for menisci, patellar ligament, and the caudal cruciate ligament. Crosslink content was lowest for patellar cartilage. (D) Pyridinoline normalized to collagen was highest for the hyaline cartilages and cruciate ligaments. Groups denoted by different letters are significantly different ($p < 0.05$).

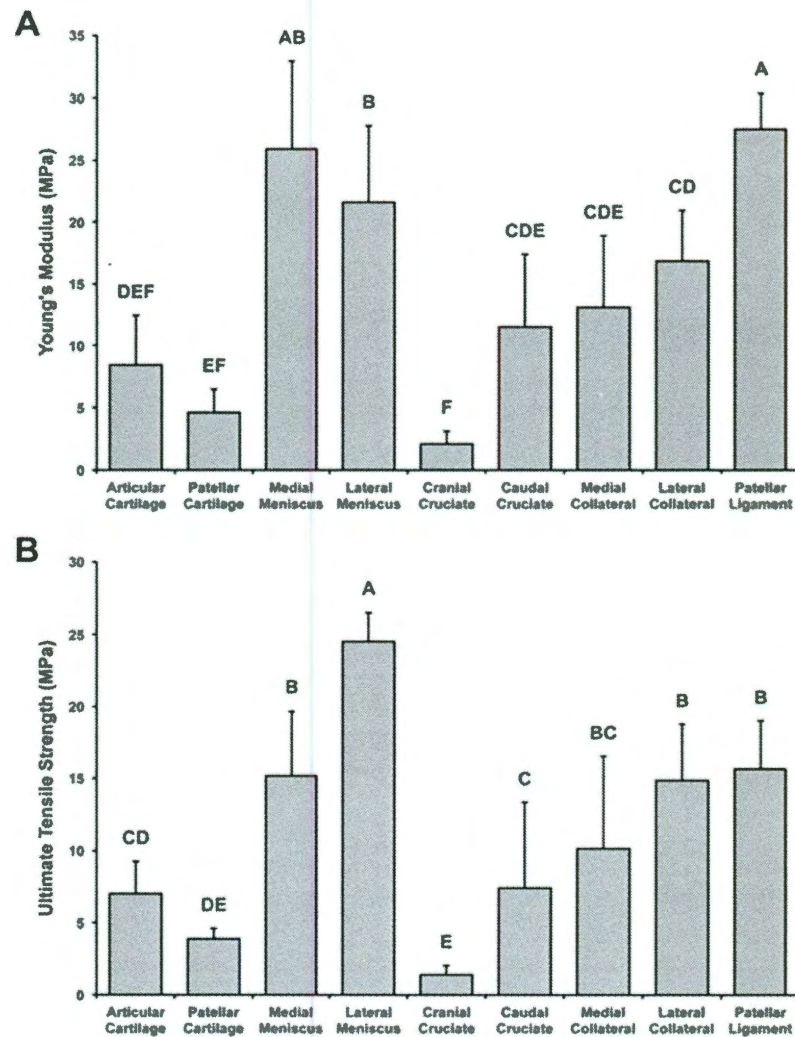


Figure 8-4. Tensile properties of joint tissues

(A) Young's modulus was highest for the menisci and patellar ligament and lowest for the cranial cruciate ligament. (B) Ultimate tensile strength was also higher for the patellar ligament and the menisci. Groups denoted by different letters are significantly different ($p < 0.05$).

Conclusions

Context

Damage to articular cartilage is irreversible and leads inescapably to significant physical debilitation. The clinical and economic consequences of osteoarthritis illuminate the urgency with which suitable replacements for cartilage are needed. Researchers in the field of tissue engineering have labored to develop methods for fabricating tissues *in vitro* that possess the biochemical and biomechanical properties of native, healthy cartilage. However, a biochemically and biomechanically robust engineered tissue continues to elude the field. Background information salient to this mission was reviewed in Chapter 1 of this thesis. Successful tissue engineering depends on a thorough understanding of tissue anatomy, physiology, and pathophysiology. The experiments described in this thesis were motivated by a need to improve overall understanding of cartilage physiology, as well as to develop strategies to enhance the functional engineering of articular cartilage. Towards this end, the global objective of this thesis was to use a multiscale approach to identify and manipulate physiologic and *in vitro* developmental milieus towards the functional repair of articular cartilage. The following sections will review some of the major results of the experiments described in this thesis.

Chondrocyte physiology

The first part of this thesis (Chapters 2 and 3) focused on probing cartilage phenotype at the single cell level. The motivation for this work was that a precise understanding of chondrocyte behavior is needed for future efforts in tissue

engineering. Because the chondrocyte is the sole cell type found within cartilage and is exclusively responsible for ECM biosynthesis, it is important to develop an understanding of how external variables, such as the cell's originating cartilage zone or bioactive agents like growth factors, can affect the chondrocyte's metabolism.

In Chapter 2, a single cell approach was proposed and implemented to examine single chondrocyte gene expression as a function of these external variables (Figure 2-1). In this approach, chondrocytes are exposed to a variety of physical or biochemical stimuli, and then examined for changes in gene expression to ascertain the immediate downstream effects of the particular stimuli. The experimental design of the study described in Chapter 1 was divided into two phases. In Phase I, chondrocytes were isolated from either the superficial or middle/deep zone of cartilage and then seeded for a short (3 hours) or long (18 hours) duration. At that point, the expression of key ECM genes was assessed using a real-time single cell RT-PCR assay developed especially for the study. Key objectives of Phase I were to quantify cell-to-cell variability, determine the validity of GAPDH as a housekeeping gene in single chondrocyte gene expression studies; and assess zone- and time-dependent differences in monolayer chondrocyte culture. Another objective was to determine the cartilage zone from which chondrocytes are more metabolically active at the transcriptional level, since it is important in tissue engineering to know whether a cell type is capable of recapitulating the ECM-rich architecture found *in vivo*. There were several major results from Phase I: single chondrocyte gene

expression follows a log-normal distribution; cell-to-cell variability could be quantified; GAPDH is a valid housekeeping gene for studies examining gene expression across different time scales within a subpopulation of chondrocytes, but cannot be used to compare expression across different zonal subpopulations; and modulators of catabolic activity, TIMP-1 and MMP-1, were expressed significantly between 3 and 18 hours. The middle/deep zone was determined to be more metabolically active than the superficial zone at the level of single cell gene transcription.

Based on the results of Phase I, the middle/deep zone was carried forward to Phase II of the study, in which the combinatorial effects of seeding time and growth factor exposure were evaluated. Important results emerged from Phase II. First, the GAPDH results from Phase I were corroborated: no difference was found in GAPDH within the middle/deep zone, even with growth factor treatment. Second, treatment of chondrocytes with IGF-I was found to increase the single cell expression of cartilage-specific genes in a time-dependent fashion: aggrecan and collagen type II were both expressed at super-significant levels ($p < 0.0001$) in response to IGF-I and overnight cell attachment in monolayer. Finally, it was shown that TIMP-1 expression could be modulated with growth factor treatment, and that collagen type I was not expressed in primary cells seeded in monolayer, suggesting that cartilage maintains its phenotype in monolayer before passaging. Altogether, the results from Chapter 2 demonstrate that chondrocyte metabolic activity can be influenced at the single cell level by growth factors, and that detectable changes happen even on short timescales.

In Chapter 3, the single cell approach and gene expression assay developed in the preceding chapter were adapted to examine chondrocyte mechanobiology. Chondrocytes from the superficial and middle/deep zone were seeded for 3 or 18 hours and exposed to TGF- β 1, IGF-I, or a combination of the two growth factors. Cell behavior was then evaluated using single cell unconfined creep compression, fluorescent staining for actin filaments, and gene expression of β -actin, an important component of the cell cytoskeleton. Instantaneous and relaxed moduli were determined for single chondrocytes from each zone, at each time point, and in the presence of each growth factor condition. It was found that growth factor treatment led to super-significant ($p < 0.0001$) increases in compressive moduli compared to controls, with no differences between the growth factors selected. Additionally, superficial zone cells had higher relaxed moduli than middle/deep zone cells. The interaction between zone and growth factor had a significant effect on compressive moduli, suggesting that the effects of growth factors on subcellular cytoskeleton organization cell subpopulation-dependent. The effects observed in compressive moduli were reflected in actin cytoskeleton fluorescent staining, which showed that growth factor treatment increased staining intensity super-significantly compared to controls. Intensity was shown to decrease over time. In terms of transcriptional changes at the single cell level, β -actin abundance was shown to vary in a time-dependent manner, but in general, there were no major differences in β -actin abundance; this result appears to indicate that whatever changes occur in the actin cytoskeleton as a result of growth factor treatment are not modulated at the gene

transcriptional level, but rather at the post-transcriptional, post-translational, or cell biophysical level.

The combined results from Chapters 2 and 3 of this thesis show that single cell behavior can be modulated and examined to yield important insights into chondrocyte metabolism and physiology. A single cell gene expression assay was developed and validated, single chondrocyte gene expression was detected and quantified, viscoelastic compressive properties of single chondrocytes were measured, and the effects of chondral zone, seeding time, and growth factors were assessed. The cumulative knowledge from the studies described in these chapters motivate future work on single chondrocyte physiology. For example, now that baseline ECM gene expression and compressive properties have been determined for single cells, it will be important to determine how cell mechanics can influence cell metabolism. Given that cartilage is a highly mechanical tissue, and that ECM synthesis by chondrocytes is hypothesized to result from complex mechanotransduction pathways, further studies should be undertaken in which cells are stimulated mechanically and then analyzed at the gene expression level. Furthermore, it is essential that any mechanobiological response in chondrocytes is assessed both in static and dynamic conditions, since cartilage homeostasis and health are highly dependent on dynamic deformation, while static compression of cartilage is typically associated with catabolic changes.

Cellular microenvironment and self-assembly

The second part of this thesis (Chapters 4, 5, and 6) examined chondrocytes at a higher level of complexity. Tissue engineered cartilage was used as a model system to evaluate the effects of modulating the cell microenvironment on ECM biosynthesis and tissue mechanics. This work was motivated both by observations described in the first two chapters of this thesis, as well as increasing evidence that intervention at the cell and ECM levels can have important consequences for tissue composition and function. The goal of the second part of this thesis was to produce tissues with greater biochemical and biomechanical properties by treating self-assembled cartilage constructs during *in vitro* development.

In Chapter 4, a Ca^{2+} -permeable, osmoregulatory channel called transient receptor potential vanilloid 4 (TRPV4) was evaluated for its role in tissue physiology. It was hypothesized that activation of TRPV4 would result in increased matrix production and enhanced biomechanical properties in self-assembled constructs. This study consisted of two phases. In Phase I, constructs were treated with a TRPV4 agonist, 4 α -PDD, during culture days 6-10, 10-14, or 14-18. The goals of this phase were to determine whether TRPV4 activation could produce tissue-level effects, and to identify whether the effects of TRPV4 activation are time-dependent. It was found that TRPV4 activation resulted in biochemical and biomechanical changes at the tissue-level, and that the beneficial effects occurred only as a result of treatment during days 10-14 of construct development. This underscored the importance of timing during *in vitro*

cartilage self-assembly and highlighted the fact that cell metabolism and responsiveness to stimuli vary during the course of tissue development. Based on the results of Phase I, the TRPV4 treatment regimen during culture days 10-14 was carried forward to Phase II of the study.

In Phase II, the effects of TRPV4 activation were compared to the effects of Na^+/K^+ pump inhibition, which has been shown in previous work to increase the tensile properties of self-assembled constructs. TRPV4 activation with 4α -PDD was compared to Na^+/K^+ pump inhibition with ouabain during days 10-14 of culture; the combination of these two agents was also assessed. It was found that 4α -PDD produced effects on self-assembled constructs that are comparable to those produced by ouabain: significant increases in both tensile properties and collagen content. The combination of both agents did not outperform each agent's individual use. While both agents showed the same net improvement in construct mechanical properties, it was clear from gross morphology and GAG data that the mechanisms for these improvements vary considerably between the two treatments. Notably, constructs treated with ouabain alone or the combination 4α -PDD and ouabain were significantly smaller and GAG-depleted compared to control constructs or constructs treated with 4α -PDD alone. Further work is necessary to determine how alterations in intracellular ion concentrations elicited by direct or indirect stimuli lead to changes in ECM synthesis and biomechanical properties. Future mechanistic studies on cell volume regulation and calcium transients *in situ* may provide some clues to the role of ion channel physiology during *in vitro* tissue development. Furthermore, it may be of interest

to study the effects of ion channel modulators in the presence of hyper-osmotic or hypo-osmotic loading, since ion channels are known to play a role in managing cell homeostasis in response to osmotic stress.

In light of the results with TRPV4 activation, Chapter 5 focused on a study in which osmotic loading was evaluated on self-assembled constructs during development. This study was motivated by work in the literature that has shown that osmotic stress affects cellular behavior and ECM biosynthesis in cells in monolayer or suspension. Osmotic stress is also known to play a role in native cartilage function, due to the attractive pull on water generated by the high density of fixed charges created by tightly-packed GAG in the tissue. It was hypothesized that osmotic loading would produce beneficial effects on construct biochemical and biomechanical properties. Constructs were subjected to static or dynamic application of hypo-osmotic or hyper-osmotic stress for 1 hour per day during culture days 10-14. It was found that the optimal loading regimen was static application of hyper-osmotic medium, which resulted in significant increases in GAG and collagen content, compressive stiffness, and tensile stiffness and strength. Dynamic osmotic loading had no effects on construct functional properties. These results suggest that osmotic loading may be an important component of future strategies in the functional tissue engineering of articular cartilage. Future work should aim to understand the precise physiological changes occurring at the cellular level *in situ* during osmotic loading of constructs. It is possible that cell volume changes produced *in situ*, with cells resident within an intact ECM, differ considerably from changes observed in cells

in monolayer or suspension. Confocal imaging techniques should be adapted to study the effects of osmotic loading and other changes in the cell microenvironment on tissue engineered constructs. It is possible that osmotic stress has an effect not just in terms of cell volume or ion channel-mediated homeostasis, but also at the level of MAPK signaling and gene expression. Further studies may be able to elucidate these changes by subjecting constructs to osmotic stimulation and then assessing changes at the cell and gene level immediately after stimulation, rather than weeks later at the gross tissue level.

Chapter 6 described a study in which self-assembled cartilage constructs were exposed to ribose, an agent known for its propensity to elicit non-enzymatic glycation of collagen. Glycation of collagen precipitates a cascade of biochemical reactions that lead ultimately to the formation of advanced glycation end-products (AGEs), which are known to crosslink the ECM and increase tissue stiffness. Crosslinking agents have been studied extensively in many tissues, but one impediment to adapting these agents in tissue engineering strategies is that they are often cytotoxic and produce significant inflammatory effects. Ribose is a particularly attractive solution because it avoids the negative effects of conventional crosslinking agents. The goal of the study described in Chapter 6 was to use ribose as both a biochemical and biophysical mediator of construct functional properties. Constructs were subjected to continuous 7-day treatment with ribose during culture weeks 1, 2, 3, or 4, or for the entire 4-week duration of culture. It was found that treatment with ribose produces beneficial effects on construct biomechanical properties, and that these effects are time-dependent,

having occurred with treatment during week 2, but not with treatment during the other weeks. Additionally, ribose treatment during week 1 appeared to have a deleterious effect on construct properties. These results emphasized the role of timing in construct development *in vitro*, corroborating the results from Chapter 4: based on the studies described in Chapters 4 and 6, it appears that week 2 of culture is an important time window for intervention with biochemical or biophysical stimuli. Furthermore, the effects of ribose may not be entirely crosslink-dependent, since construct biomechanical improvements were accompanied by increases in biochemical content. These results suggest that ribose has an important metabolic influence on cells *in situ*. Future work should aim to tease out the differential contributions of cell metabolism and ECM crosslinking to the tissue-level effects of ribose treatment. One possible method to make this comparison would be to quantify the levels of pentosidine, a molecule involved in glycation-mediated crosslinking, in constructs with and without ribose treatment. It will also be important to compare levels of pentosidine to levels of pyridinoline, the molecule involved in enzymatic crosslinking of collagen. Additionally, cell population gene expression in engineered constructs can be assessed in response to ribose exposure; if metabolic changes are responsible for tissue level increases in ECM, constructs may show increases in cartilage-specific ECM gene expression.

The combined results of the studies in Chapters 4, 5, and 6 show that modulating the cellular microenvironment in self-assembled constructs can produce tissue level improvements in construct biochemical and biomechanical

properties. Future investigations should aim to clarify whether these tissue level responses are manifestations of biochemical or biophysical changes. The techniques developed in these studies can be adapted in future tissue engineering strategies that combine them with other, more macroscopic tissue stimulation regimens (for example, direct compression or hydrostatic pressure). The combination of stimuli may produce additive or synergistic effects on tissue-level improvements in ECM production and tensile and compressive properties.

Improving clinical translatability

The third part of this thesis (Chapter 7 and 8) focused on improving the potential clinical translatability of *in vitro* cartilage repair strategies. These studies aimed to address the issue of clinical translatability from two directions. The first goal was to establish an optimal method for the decellularization of xenogenic cartilage. This goal was motivated by a need for methods to reduce the immunogenic potential of xenogenic tissues for future *in vivo* applications. Prior work has been performed to determine the feasibility of tissue decellularization to create non-immunogenic xenogenic tissue replacements for bladder, vasculature, heart valves, and other tissues; however, there has been a dearth of studies on cartilage decellularization. The second goal was to conduct a comprehensive characterization of the whole knee joint to establish benchmarks for future tissue repair strategies. This goal was motivated by the fact that future strategies in cartilage tissue engineering must incorporate important information about the other connective tissues resident in the healthy, intact joint. Furthermore, the

knowledge gained from a complete characterization of the major connective tissues of the knee will be particularly important in tailoring biochemical and biophysical stimuli within other tissue engineering strategies.

Chapter 7 described a study in which different decellularization treatments on self-assembled articular cartilage constructs were evaluated using a two-phased approach. In Phase I, five different decellularization treatments were examined: 1% SDS, 2% SDS, 2% tributyl phosphate, 2% Triton X-100, and hypotonic/hypertonic solutions. It was found that treatment with 2% SDS outperformed the other agents in terms of reduction in construct DNA content (i.e., biochemical decellularization) while maintaining construct functional properties. This treatment was carried forward to Phase II, in which 2% SDS treatment was evaluated over different application times (1, 2, 4, 6, or 8 hours). Complete histological decellularization was achieved with longer application of SDS, but GAG content was severely depleted and compressive properties were decreased after longer treatment. These results suggest that SDS treatment for 2-4 hours may be the most effective method for decellularizing cartilage while maintain construct properties. This study demonstrated that decellularization techniques can be adapted for xenogenic cartilage repair strategies. It further demonstrated that construct functional properties must be prioritized in future work on decellularization regimens. Future work should aim to minimize GAG loss and maintain compressive properties in constructs undergoing decellularization. One potential method is to use crosslinking agents to fix GAG within the tissue prior to decellularization. This may be accomplished by the use

of ribose, as suggested by Chapter 6 of this thesis, or by the use of an agent like periodate, a chemical that has been shown to fix GAG within glutaraldehyde-treated heart valves.

Chapter 8 presented a study in which a comprehensive characterization was undertaken of the tensile properties, collagen content, and pyridinoline crosslink abundance of the major connective tissues of immature bovine knee joint. This work was motivated by the need to develop a thorough understanding of the structure-function relationships of knee joint tissues, which can provide important insight into design parameters for efforts in tissue engineering. Condylar cartilage, patellar cartilage, medial and lateral menisci, cranial and caudal cruciate ligaments, medial and lateral collateral ligaments, and patellar ligament were harvested from immature bovine calves. Assessments included histology, quantification of collagen content, measurement of pyridinoline crosslink abundance, and uniaxial strain-to-failure testing. It was found that tensile stiffness and strength were greatest in the menisci and patellar ligaments, and lowest in the hyaline cartilages and cruciate ligaments; these trends reflected trends in collagen content, underscoring the importance of the collagen network in determining a tissue's response to tensile stress. Furthermore, pyridinoline crosslinks were found in every tissue despite the relative immaturity of the joints. It was found that the cruciate ligaments contained a high density of crosslinks, an interesting result given that the cruciate ligaments were also found to have a lower concentration of collagen compared to other, stiffer tissues. This study delivered important data on native joint tissue physiology and provides key

results that will inform future tissue engineering strategies. Further studies should undertake a similar characterization of the tensile properties, collagen content, and crosslink abundance of mature knee joint tissues to determine functional changes during the course of tissue maturation. It will be important in such future studies to examine the abundance of pentosidine crosslinks in addition to pyridinoline crosslinks, since pentosidine, as detailed in Chapter 6, can appear as a result of age-related stiffening of tissues.

The cumulative results presented in Chapters 7 and 8 provide important benchmarks for future work involving the translation of *in vitro* advances in cartilage repair to *in vivo* clinical therapies. The success of any of the strategies detailed in this thesis will ultimately depend on the ability of a biologic replacement to survive within the harsh physiologic environment of the native joint. This survival will be decided overwhelmingly by joint mechanics and the host immune response. Information from Chapters 7 and 8 provide a starting point for future translational studies. It will be important in the future to pursue *in vivo* studies to evaluate the technologies explored in this thesis. Animal studies can be performed to assess immune reactions as well as tissue survival in immobilized and, ultimately fully mobile joints. The strategies presented in this thesis can be used to optimize self-assembled constructs for use in such animal models.

Significance

The total body of work contained in this thesis contributes significantly both to a basic understanding of cartilage physiology as well as to evolving strategies for cartilage repair. This thesis examined tissue behavior at multiple levels of complexity: gene transcription, cytoskeletal architecture, ion channels, single cell mechanics, the extracellular matrix, intact tissue, and total joint physiology. This thesis also advanced the field of cartilage tissue engineering by presenting strategies for improving the biochemical and biomechanical properties of cartilage grown *in vitro* using a self-assembly process. Finally, a decellularization technique was optimized towards the future clinical translatability of the cartilage repair strategies developed in this thesis. The cumulative results of this thesis serve as an exciting contribution to the field of cartilage regeneration.

References

1. AAOS. *United States Bone and Joint Decade: The Burden of Musculoskeletal Disease in the United States*. Rosemount, IL: American Academy of Orthopaedic Surgeons, 2008, p. 247.
2. Aida Y, Maeno M, Suzuki N, Shiratsuchi H, Motohashi M, and Matsumura H. The effect of IL-1beta on the expression of matrix metalloproteinases and tissue inhibitors of matrix metalloproteinases in human chondrocytes. *Life Sci* 77: 3210-3221, 2005.
3. Aigner T, and McKenna L. Molecular pathology and pathobiology of osteoarthritic cartilage. *Cell Mol Life Sci* 59: 5-18, 2002.
4. Aigner T, Zien A, Gehrsitz A, Gebhard PM, and McKenna L. Anabolic and catabolic gene expression pattern analysis in normal versus osteoarthritic cartilage using complementary DNA-array technology. *Arthritis and rheumatism* 44: 2777-2789, 2001.
5. Akodu AK, Giwa SO, Akinbo SR, and Ahmed UA. Physiotherapy in the management of total knee arthroplasty: a review. *Nig Q J Hosp Med* 21: 99-105, 2011.
6. Alexopoulos LG, Haider MA, Vail TP, and Guilak F. Alterations in the mechanical properties of the human chondrocyte pericellular matrix with osteoarthritis. *J Biomech Eng* 125: 323-333, 2003.
7. Almarza AJ, and Athanasiou KA. Design characteristics for the tissue engineering of cartilaginous tissues. *Ann Biomed Eng* 32: 2-17, 2004.

8. Almarza AJ, and Athanasiou KA. Seeding techniques and scaffolding choice for tissue engineering of the temporomandibular joint disk. *Tissue Eng* 10: 1787-1795, 2004.
9. Archer CW, and Francis-West P. The chondrocyte. *Int J Biochem Cell Biol* 35: 401-404, 2003.
10. Asanbaeva A, Masuda K, Thonar EJ, Klisch SM, and Sah RL. Mechanisms of cartilage growth: modulation of balance between proteoglycan and collagen in vitro using chondroitinase ABC. *Arthritis Rheum* 56: 188-198, 2007.
11. Athanasiou KA, Agarwal A, and Dzida FJ. Comparative study of the intrinsic mechanical properties of the human acetabular and femoral head cartilage. *J Orthop Res* 12: 340-349, 1994.
12. Athanasiou KA, Agarwal A, Muffoletto A, Dzida FJ, Constantinides G, and Clem M. Biomechanical properties of hip cartilage in experimental animal models. *Clin Orthop Relat Res* 316: 254-266, 1995.
13. Athanasiou KA, Agarwal A, Muffoletto A, Dzida FJ, Constantinides G, and Clem M. Biomechanical properties of hip cartilage in experimental animal models. *Clin Orthop Relat Res* 254-266, 1995.
14. Athanasiou KA, Shah AR, Hernandez RJ, and LeBaron RG. Basic science of articular cartilage repair. *Clin Sports Med* 20: 223-247, 2001.
15. Aufderheide AC, and Athanasiou KA. Assessment of a bovine co-culture, scaffold-free method for growing meniscus-shaped constructs. *Tissue Eng* 13: 2195-2205, 2007.

16. Aufderheide AC, and Athanasiou KA. A direct compression stimulator for articular cartilage and meniscal explants. *Ann Biomed Eng* 34: 1463-1474, 2006.
17. Aydelotte MB, Greenhill RR, and Kuettner KE. Differences between sub-populations of cultured bovine articular chondrocytes. II. Proteoglycan metabolism. *Connect Tissue Res* 18: 223-234, 1988.
18. Aydelotte MB, and Kuettner KE. Differences between sub-populations of cultured bovine articular chondrocytes. I. Morphology and cartilage matrix production. *Connect Tissue Res* 18: 205-222, 1988.
19. Bank RA, Beekman B, Verzijl N, de Roos JA, Sakkee AN, and TeKoppele JM. Sensitive fluorimetric quantitation of pyridinium and pentosidine crosslinks in biological samples in a single high-performance liquid chromatographic run. *J Chromatogr B Biomed Sci Appl* 703: 37-44, 1997.
20. Barbour SA, and King W. The safe and effective use of allograft tissue--an update. *Am J Sports Med* 31: 791-797, 2003.
21. Basser PJ, Schneiderman R, Bank RA, Wachtel E, and Maroudas A. Mechanical properties of the collagen network in human articular cartilage as measured by osmotic stress technique. *Arch Biochem Biophys* 351: 207-219, 1998.
22. Bonassar LJ, Grodzinsky AJ, Frank EH, Davila SG, Bhaktav NR, and Trippel SB. The effect of dynamic compression on the response of articular cartilage to insulin-like growth factor-I. *J Orthop Res* 19: 11-17, 2001.

23. Bonassar LJ, Grodzinsky AJ, Srinivasan A, Davila SG, and Trippel SB. Mechanical and physicochemical regulation of the action of insulin-like growth factor-I on articular cartilage. *Arch Biochem Biophys* 379: 57-63, 2000.
24. Broom ND. Further insights into the structural principles governing the function of articular cartilage. *J Anat* 139 (Pt 2): 275-294, 1984.
25. Browning JA, Saunders K, Urban JP, and Wilkins RJ. The influence and interactions of hydrostatic and osmotic pressures on the intracellular milieu of chondrocytes. *Biorheology* 41: 299-308, 2004.
26. Brownlee M. Nonenzymatic glycosylation of macromolecules. Prospects of pharmacologic modulation. *Diabetes* 41 Suppl 2: 57-60, 1992.
27. Buckwalter JA. Articular cartilage: injuries and potential for healing. *J Orthop Sports Phys Ther* 28: 192-202, 1998.
28. Buckwalter JA. Articular cartilage: injuries and potential for healing. *J Orthop Sports Phys Ther* 28: 192-202, 1998.
29. Buckwalter JA, and Brown TD. Joint injury, repair, and remodeling: roles in post-traumatic osteoarthritis. *Clinical orthopaedics and related research* 7-16, 2004.
30. Buckwalter JA, Saltzman C, and Brown T. The impact of osteoarthritis: implications for research. *Clinical orthopaedics and related research* S6-15, 2004.

31. Buschmann MD, Gluzband YA, Grodzinsky AJ, and Hunziker EB. Mechanical compression modulates matrix biosynthesis in chondrocyte/agarose culture. *J Cell Sci* 108: 1497-1508, 1995.
32. Bush PG, and Hall AC. Passive osmotic properties of in situ human articular chondrocytes within non-degenerate and degenerate cartilage. *Journal of cellular physiology* 204: 309-319, 2005.
33. Bush PG, and Hall AC. Regulatory volume decrease (RVD) by isolated and in situ bovine articular chondrocytes. *Journal of cellular physiology* 187: 304-314, 2001.
34. Bustin SA. Absolute quantification of mRNA using real-time reverse transcription polymerase chain reaction assays. *J Mol Endocrinol* 25: 169-193, 2000.
35. Butler DL, Goldstein SA, and Guilak F. Functional tissue engineering: the role of biomechanics. *J Biomech Eng* 122: 570-575, 2000.
36. Butler DL, Juncosa-Melvin N, Boivin GP, Galloway MT, Shearn JT, Gooch C, and Awad H. Functional tissue engineering for tendon repair: A multidisciplinary strategy using mesenchymal stem cells, bioscaffolds, and mechanical stimulation. *J Orthop Res* 26: 1-9, 2008.
37. Calve S, Dennis RG, Kosnik PE, 2nd, Baar K, Grosh K, and Arruda EM. Engineering of functional tendon. *Tissue Eng* 10: 755-761, 2004.
38. Campbell CJ. The healing of cartilage defects. *Clinical orthopaedics and related research* 64: 45-63, 1969.

39. Cartmell JS, and Dunn MG. Effect of chemical treatments on tendon cellularity and mechanical properties. *J Biomed Mater Res* 49: 134-140, 2000.
40. Chan BP, Fu SC, Qin L, Rolf C, and Chan KM. Pyridinoline in relation to ultimate stress of the patellar tendon during healing: an animal study. *Journal of orthopaedic research : official publication of the Orthopaedic Research Society* 16: 597-603, 1998.
41. Chao PG, Tang Z, Angelini E, West AC, Costa KD, and Hung CT. Dynamic osmotic loading of chondrocytes using a novel microfluidic device. *Journal of biomechanics* 38: 1273-1281, 2005.
42. Chao PH, West AC, and Hung CT. Chondrocyte intracellular calcium, cytoskeletal organization, and gene expression responses to dynamic osmotic loading. *Am J Physiol Cell Physiol* 291: C718-725, 2006.
43. Chen RN, Ho HO, Tsai YT, and Sheu MT. Process development of an acellular dermal matrix (ADM) for biomedical applications. *Biomaterials* 25: 2679-2686, 2004.
44. Chen SS, Falcovitz YH, Schneiderman R, Maroudas A, and Sah RL. Depth-dependent compressive properties of normal aged human femoral head articular cartilage: relationship to fixed charge density. *Osteoarthritis Cartilage* 9: 561-569, 2001.
45. Choong PF, and Dowsey MM. Update in surgery for osteoarthritis of the knee. *Int J Rheum Dis* 14: 167-174, 2011.

46. Chowdhury TT, and Knight MM. Purinergic pathway suppresses the release of NO and stimulates proteoglycan synthesis in chondrocyte/agarose constructs subjected to dynamic compression. *Journal of cellular physiology* 209: 845-853, 2006.
47. Chu CR, Coutts RD, Yoshioka M, Harwood FL, Monosov AZ, and Amiel D. Articular cartilage repair using allogeneic perichondrocyte-seeded biodegradable porous polylactic acid (PLA): a tissue-engineering study. *J Biomed Mater Res* 29: 1147-1154, 1995.
48. Clark AL, Votta BJ, Kumar S, Liedtke W, and Guilak F. Chondroprotective role of the osmotically sensitive ion channel transient receptor potential vanilloid 4: age- and sex-dependent progression of osteoarthritis in Trpv4-deficient mice. *Arthritis and rheumatism* 62: 2973-2983, 2010.
49. Cooper JA. Effects of cytochalasin and phalloidin on actin. *J Cell Biol* 105: 1473-1478, 1987.
50. Dahl SL, Koh J, Prabhakar V, and Niklason LE. Decellularized native and engineered arterial scaffolds for transplantation. *Cell Transplant* 12: 659-666, 2003.
51. Darling EM, and Athanasiou KA. Biomechanical strategies for articular cartilage regeneration. *Ann Biomed Eng* 31: 1114-1124, 2003.
52. Darling EM, and Athanasiou KA. Growth factor impact on articular cartilage subpopulations. *Cell Tissue Res* 322: 463-473, 2005.
53. Darling EM, and Athanasiou KA. Rapid phenotypic changes in passaged articular chondrocyte subpopulations. *J Orthop Res* 23: 425-432, 2005.

54. Darling EM, Hu JC, and Athanasiou KA. Zonal and topographical differences in articular cartilage gene expression. *J Orthop Res* 22: 1182-1187, 2004.
55. De Mattei M, Pellati A, Pasello M, Ongaro A, Setti S, Massari L, Gemmati D, and Caruso A. Effects of physical stimulation with electromagnetic field and insulin growth factor-I treatment on proteoglycan synthesis of bovine articular cartilage. *Osteoarthritis Cartilage* 12: 793-800, 2004.
56. Dheda K, Huggett JF, Chang JS, Kim LU, Bustin SA, Johnson MA, Rook GA, and Zumla A. The implications of using an inappropriate reference gene for real-time reverse transcription PCR data normalization. *Anal Biochem* 344: 141-143, 2005.
57. Durrant LA, Archer CW, Benjamin M, and Ralphs JR. Organisation of the chondrocyte cytoskeleton and its response to changing mechanical conditions in organ culture. *J Anat* 194: 343-353, 1999.
58. Edlich M, Yellowley CE, Jacobs CR, and Donahue HJ. Cycle number and waveform of fluid flow affect bovine articular chondrocytes. *Biorheology* 41: 315-322, 2004.
59. Edlich M, Yellowley CE, Jacobs CR, and Donahue HJ. Oscillating fluid flow regulates cytosolic calcium concentration in bovine articular chondrocytes. *Journal of biomechanics* 34: 59-65, 2001.
60. Edwards RB, 3rd, Lu Y, Uthamanthil RK, Bogdanske JJ, Muir P, Athanasiou KA, and Markel MD. Comparison of mechanical debridement and radiofrequency energy for chondroplasty in an in vivo equine model of

- partial thickness cartilage injury. *Osteoarthritis Cartilage* 15: 169-178, 2007.
61. Elbjeirami WM, Yonter EO, Starcher BC, and West JL. Enhancing mechanical properties of tissue-engineered constructs via lysyl oxidase crosslinking activity. *J Biomed Mater Res A* 66: 513-521, 2003.
 62. Elder BD, and Athanasiou KA. Effects of confinement on the mechanical properties of self-assembled articular cartilage constructs in the direction orthogonal to the confinement surface. *J Orthop Res* 26: 238-246, 2008.
 63. Elder BD, and Athanasiou KA. Effects of Temporal Hydrostatic Pressure on Tissue-Engineered Bovine Articular Cartilage Constructs. *Tissue Eng Part A* 15: 1151-1158, 2008.
 64. Elder BD, and Athanasiou KA. Effects of temporal hydrostatic pressure on tissue-engineered bovine articular cartilage constructs. *Tissue engineering Part A* 15: 1151-1158, 2009.
 65. Elder BD, and Athanasiou KA. Hydrostatic pressure in articular cartilage tissue engineering: from chondrocytes to tissue regeneration. *Tissue Eng Part B Rev* 15: 43-53, 2009.
 66. Elder BD, and Athanasiou KA. Paradigms of tissue engineering with applications to cartilage regeneration. In: *Musculoskeletal Tissue Regeneration: Biological Materials and Methods*, edited by Pietrzak WS. Totowa, NJ: Humana Press, 2008.

67. Elder BD, and Athanasiou KA. Synergistic and additive effects of hydrostatic pressure and growth factors on tissue formation. *PLoS ONE* 3: e2341, 2008.
68. Elder BD, and Athanasiou KA. Systematic assessment of growth factor treatment on biochemical and biomechanical properties of engineered articular cartilage constructs. *Osteoarthritis Cartilage* 17: 114-123 2009.
69. Elder BD, and Athanasiou KA. Systematic assessment of growth factor treatment on biochemical and biomechanical properties of engineered articular cartilage constructs. *Osteoarthritis Cartilage* 2008.
70. Elder BD, Mohan A, and Athanasiou KA. Beneficial effects of exogenous crosslinking agents on self-assembled tissue engineered cartilage construct biomechanical properties. *J Mech Med Biol* 11: 433-443, 2011.
71. Elder SH, Sanders SW, McCulley WR, Marr ML, Shim JW, and Hasty KA. Chondrocyte response to cyclic hydrostatic pressure in alginate versus pellet culture. *J Orthop Res* 24: 740-747, 2006.
72. Erickson GR, Alexopoulos LG, and Guilak F. Hyper-osmotic stress induces volume change and calcium transients in chondrocytes by transmembrane, phospholipid, and G-protein pathways. *Journal of biomechanics* 34: 1527-1535, 2001.
73. Erickson GR, Northrup DL, and Guilak F. Hypo-osmotic stress induces calcium-dependent actin reorganization in articular chondrocytes. *Osteoarthritis and cartilage / OARS, Osteoarthritis Research Society* 11: 187-197, 2003.

74. Eyre D. Collagen of articular cartilage. *Arthritis Res* 4: 30-35, 2002.
75. Eyre DR, Dickson IR, and Van Ness K. Collagen cross-linking in human bone and articular cartilage. Age-related changes in the content of mature hydroxypyridinium residues. *Biochem J* 252: 495-500, 1988.
76. Eyre DR, Koob TJ, and Van Ness KP. Quantitation of hydroxypyridinium crosslinks in collagen by high-performance liquid chromatography. *Anal Biochem* 137: 380-388, 1984.
77. Fermor B, Weinberg JB, Pisetsky DS, Misukonis MA, Banés AJ, and Guilak F. The effects of static and intermittent compression on nitric oxide production in articular cartilage explants. *Journal of orthopaedic research : official publication of the Orthopaedic Research Society* 19: 729-737, 2001.
78. Finan JD, Chalut KJ, Wax A, and Guilak F. Nonlinear osmotic properties of the cell nucleus. *Annals of biomedical engineering* 37: 477-491, 2009.
79. Finan JD, and Guilak F. The effects of osmotic stress on the structure and function of the cell nucleus. *Journal of cellular biochemistry* 109: 460-467, 2010.
80. Finan JD, Leddy HA, and Guilak F. Osmotic stress alters chromatin condensation and nucleocytoplasmic transport. *Biochemical and biophysical research communications* 408: 230-235, 2011.
81. Frazer A, Bunning RA, Thavarajah M, Seid JM, and Russell RG. Studies on type II collagen and aggrecan production in human articular chondrocytes in vitro and effects of transforming growth factor-beta and interleukin-1beta. *Osteoarthritis Cartilage* 2: 235-245, 1994.

82. Galâera P, Vivien D, Pronost S, Bonaventure J, Râedini F, Loyau G, Pujol JP, and Laboratoire de Biochimie du Tissu Conjonctif CHUCdNCF. Transforming growth factor-beta 1 (TGF-beta 1) up-regulation of collagen type II in primary cultures of rabbit articular chondrocytes (RAC) involves increased mRNA levels without affecting mRNA stability and procollagen processing. *J Cell Physiol* 153: 596-606, 1992.
83. Gelse K, von der Mark K, Aigner T, Park J, and Schneider H. Articular cartilage repair by gene therapy using growth factor-producing mesenchymal cells. *Arthritis and rheumatism* 48: 430-441, 2003.
84. Gilbert TW, Freundb SJ, and Badylak SF. Quantification of DNA in Biologic Scaffold Materials. *J Surg Res* 2008.
85. Gilbert TW, Sellaro TL, and Badylak SF. Decellularization of tissues and organs. *Biomaterials* 27: 3675-3683, 2006.
86. Girton TS, Oegema TR, and Tranquillo RT. Exploiting glycation to stiffen and strengthen tissue equivalents for tissue engineering. *J Biomed Mater Res* 46: 87-92, 1999.
87. Gooch KJ, Blunk T, Courter DL, Sieminski AL, Bursac PM, Vunjak-Novakovic G, and Freed LE. IGF-I and mechanical environment interact to modulate engineered cartilage development. *Biochem Biophys Res Commun* 286: 909-915, 2001.
88. Gooch KJ, Blunk T, Courter DL, Sieminski AL, Vunjak-Novakovic G, and Freed LE. Bone morphogenetic proteins-2, -12, and -13 modulate in vitro development of engineered cartilage. *Tissue Eng* 8: 591-601, 2002.

89. Guilak F, Fermor B, Keefe FJ, Kraus VB, Olson SA, Pisetsky DS, Setton LA, and Weinberg JB. The role of biomechanics and inflammation in cartilage injury and repair. *Clin Orthop Relat Res* 17-26, 2004.
90. Guilak F, Leddy HA, and Liedtke W. Transient receptor potential vanilloid 4: The sixth sense of the musculoskeletal system? *Annals of the New York Academy of Sciences* 1192: 404-409, 2010.
91. Guilak F, Ratcliffe A, Lane N, Rosenwasser MP, and Mow VC. Mechanical and biochemical changes in the superficial zone of articular cartilage in canine experimental osteoarthritis. *Journal of orthopaedic research : official publication of the Orthopaedic Research Society* 12: 474-484, 1994.
92. Hall AC. Differential effects of hydrostatic pressure on cation transport pathways of isolated articular chondrocytes. *Journal of cellular physiology* 178: 197-204, 1999.
93. Hall AC, Horwitz ER, and Wilkins RJ. The cellular physiology of articular cartilage. *Exp Physiol* 81: 535-545, 1996.
94. Hall AC, Urban JP, and Gohl KA. The effects of hydrostatic pressure on matrix synthesis in articular cartilage. *J Orthop Res* 9: 1-10, 1991.
95. Hall BK, and Miyake T. Divide, accumulate, differentiate: cell condensation in skeletal development revisited. *Int J Dev Biol* 39: 881-893, 1995.
96. Han E, Chen SS, Klisch SM, and Sah RL. Contribution of proteoglycan osmotic swelling pressure to the compressive properties of articular cartilage. *Biophysical journal* 101: 916-924, 2011.

97. Han SH, McCool BA, Murchison D, Nahm SS, Parrish AR, and Griffith WH. Single-cell RT-PCR detects shifts in mRNA expression profiles of basal forebrain neurons during aging. *Brain Res Mol Brain Res* 98: 67-80, 2002.
98. Hayami JW, Surrao DC, Waldman SD, and Amsden BG. Design and characterization of a biodegradable composite scaffold for ligament tissue engineering. *J Biomed Mater Res A* 92: 1407-1420, 2010.
99. Hayes WC, Keer LM, Herrmann G, and Mockros LF. A mathematical analysis for indentation tests of articular cartilage. *J Biomech* 5: 541-551, 1972.
100. Hoben GM, and Athanasiou KA. Creating a spectrum of fibrocartilages through different cell sources and biochemical stimuli. *Biotechnol Bioeng* 100: 587-598, 2008.
101. Hootman JM, and Helmick CG. Projections of US prevalence of arthritis and associated activity limitations. *Arthritis Rheum* 54: 226-229, 2006.
102. Hopewell B, and Urban JP. Adaptation of articular chondrocytes to changes in osmolality. *Biorheology* 40: 73-77, 2003.
103. Howard EW, Benton R, Ahern-Moore J, and Tomasek JJ. Cellular contraction of collagen lattices is inhibited by nonenzymatic glycation. *Experimental cell research* 228: 132-137, 1996.
104. Howard TH, and Meyer WH. Chemotactic peptide modulation of actin assembly and locomotion in neutrophils. *J Cell Biol* 98: 1265-1271, 1984.
105. Hu JC, and Athanasiou KA. A self-assembling process in articular cartilage tissue engineering. *Tissue Eng* 12: 969-979, 2006.

106. Hu JC, and Athanasiou KA. Structure and function of articular cartilage. In: *Handbook of Histology Methods for Bone and Cartilage*, edited by An YH, and Martin KL. Totowa, N.J.: Humana Press Inc., 2003.
107. Hu K, Xu L, Cao L, Flahiff CM, Brussiau J, Ho K, Setton LA, Youn I, Guilak F, Olsen BR, and Li Y. Pathogenesis of osteoarthritis-like changes in the joints of mice deficient in type IX collagen. *Arthritis Rheum* 54: 2891-2900, 2006.
108. Huang CY, and Gu WY. Effects of tension-compression nonlinearity on solute transport in charged hydrated fibrous tissues under dynamic unconfined compression. *Journal of Biomechanical Engineering* 129: 423-429, 2007.
109. Huey DJ, and Athanasiou KA. Maturation growth of self-assembled, functional menisci as a result of TGF-beta1 and enzymatic chondroitinase-ABC stimulation. *Biomaterials* 32: 2052-2058.
110. Huey DJ, and Athanasiou KA. Maturation growth of self-assembled, functional menisci as a result of TGF-beta1 and enzymatic chondroitinase-ABC stimulation. *Biomaterials* 32: 2052-2058, 2011.
111. Huggett J, Dheda K, Bustin S, and Zumla A. Real-time RT-PCR normalisation; strategies and considerations. *Genes Immun* 6: 279-284, 2005.
112. Hung CT. Transient receptor potential vanilloid 4 channel as an important modulator of chondrocyte mechanotransduction of osmotic loading. *Arthritis and rheumatism* 62: 2850-2851, 2010.

113. Hung CT, LeRoux MA, Palmer GD, Chao PH, Lo S, and Valhmu WB. Disparate aggrecan gene expression in chondrocytes subjected to hypotonic and hypertonic loading in 2D and 3D culture. *Biorheology* 40: 61-72, 2003.
114. Hunter CJ, Mouw JK, and Levenston ME. Dynamic compression of chondrocyte-seeded fibrin gels: effects on matrix accumulation and mechanical stiffness. *Osteoarthritis and cartilage / OARS, Osteoarthritis Research Society* 12: 117-130, 2004.
115. Hunter W. Of the structure and disease of articulating cartilages. 1743. *Clinical orthopaedics and related research* 3-6, 1995.
116. Hunziker EB. Articular cartilage repair: are the intrinsic biological constraints undermining this process insuperable? *Osteoarthritis and cartilage / OARS, Osteoarthritis Research Society* 7: 15-28, 1999.
117. Idowu BD, Knight MM, Bader DL, and Lee DA. Confocal analysis of cytoskeletal organisation within isolated chondrocyte sub-populations cultured in agarose. *Histochem J* 32: 165-174, 2000.
118. Kempson GE, Muir H, Pollard C, and Tuke M. The tensile properties of the cartilage of human femoral condyles related to the content of collagen and glycosaminoglycans. *Biochim Biophys Acta* 297: 456-472, 1973.
119. King GL, and Brownlee M. The cellular and molecular mechanisms of diabetic complications. *Endocrinol Metab Clin North Am* 25: 255-270, 1996.

120. Knowles GC, and McCulloch CA. Simultaneous localization and quantification of relative G and F actin content: optimization of fluorescence labeling methods. *J Histochem Cytochem* 40: 1605-1612, 1992.
121. Koay EJ, Shieh AC, and Athanasiou KA. Creep indentation of single cells. *J Biomech Eng* 125: 334-341, 2003.
122. Komar AA, Gross SR, Barth-Baus D, Strachan R, Hensold JO, Goss Kinzy T, and Merrick WC. Novel characteristics of the biological properties of the yeast *Saccharomyces cerevisiae* eukaryotic initiation factor 2A. *J Biol Chem* 280: 15601-15611, 2005.
123. Kurosawa H, Fukubayashi T, and Nakajima H. Load-bearing mode of the knee joint: physical behavior of the knee joint with or without menisci. *Clinical orthopaedics and related research* 283-290, 1980.
124. Lai WM, Mow VC, and Zhu W. Constitutive modeling of articular cartilage and biomacromolecular solutions. *Journal of Biomechanical Engineering* 115: 474-480, 1993.
125. Lambolez F, Azogui O, Joret AM, Garcia C, von Boehmer H, Di Santo J, Ezine S, and Rocha B. Characterization of T cell differentiation in the murine gut. *J Exp Med* 195: 437-449, 2002.
126. Langelier E, Suetterlin R, Hoemann CD, Aebi U, and Buschmann MD. The chondrocyte cytoskeleton in mature articular cartilage: structure and distribution of actin, tubulin, and vimentin filaments. *J Histochem Cytochem* 48: 1307-1320, 2000.

127. Lee JH, Fitzgerald JB, Dimicco MA, and Grodzinsky AJ. Mechanical injury of cartilage explants causes specific time-dependent changes in chondrocyte gene expression. *Arthritis Rheum* 52: 2386-2395, 2005.
128. Lee JW, Hee Kim Y, Boong Park H, Xu LH, Cance WG, Block JA, and Scully SP. The C-terminal domain of focal adhesion kinase reduces the tumor cell invasiveness in chondrosarcoma cell lines. *J Orthop Res* 21: 1071-1080, 2003.
129. Leipzig ND, and Athanasiou KA. Cartilage regeneration. In: *The encyclopedia of biomaterials and bioengineering*, edited by Wnek G, and Bowlin G. New York: Marcel Dekker Inc, 2004, p. 283-291.
130. Leipzig ND, and Athanasiou KA. Unconfined creep compression of chondrocytes. *J Biomech* 38: 77-85, 2005.
131. Leipzig ND, Eleswarapu SV, and Athanasiou KA. The effects of TGF-beta1 and IGF-I on the biomechanics and cytoskeleton of single chondrocytes. *Osteoarthritis Cartilage* 14: 1227-1236, 2006.
132. Leipzig ND, Eleswarapu SV, and Athanasiou KA. Growth factor effects on the biomechanical properties of single chondrocytes. *Osteoarthritis Cartilage* Submitted: 2006.
133. Lichtenstein N, Geiger B, and Kam Z. Quantitative analysis of cytoskeletal organization by digital fluorescent microscopy. *Cytometry A* 54: 8-18, 2003.
134. Likhitpanichkul M, Guo XE, and Mow VC. The effect of matrix tension-compression nonlinearity and fixed negative charges on chondrocyte responses in cartilage. *Mol Cell Biomech* 2: 191-204, 2005.

135. Lim JJ, Scott L, Jr., and Temenoff JS. Aggregation of bovine anterior cruciate ligament fibroblasts or marrow stromal cells promotes aggrecan production. *Biotechnology and bioengineering* 108: 151-162, 2011.
136. Lima EG, Bian L, Ng KW, Mauck RL, Byers BA, Tuan RS, Ateshian GA, and Hung CT. The beneficial effect of delayed compressive loading on tissue-engineered cartilage constructs cultured with TGF-beta3. *Osteoarthritis and cartilage / OARS, Osteoarthritis Research Society* 15: 1025-1033, 2007.
137. Lima EG, Tan AR, Tai T, Marra KG, DeFail A, Ateshian GA, and Hung CT. Genipin enhances the mechanical properties of tissue-engineered cartilage and protects against inflammatory degradation when used as a medium supplement. *J Biomed Mater Res Part A* 91: 692-700, 2009.
138. Loeser RF. Growth factor regulation of chondrocyte integrins. Differential effects of insulin-like growth factor 1 and transforming growth factor beta on alpha 1 beta 1 integrin expression and chondrocyte adhesion to type VI collagen. *Arthritis Rheum* 40: 270-276, 1997.
139. Lohmander LS, Englund PM, Dahl LL, and Roos EM. The long-term consequence of anterior cruciate ligament and meniscus injuries: osteoarthritis. *The American journal of sports medicine* 35: 1756-1769, 2007.
140. Louw QA, Manilall J, and Grimmer KA. Epidemiology of knee injuries among adolescents: a systematic review. *Br J Sports Med* 42: 2-10, 2008.

141. Lumpkins SB, Pierre N, and McFetridge PS. A mechanical evaluation of three decellularization methods in the design of a xenogeneic scaffold for tissue engineering the temporomandibular joint disc. *Acta Biomater* 4: 808-816, 2008.
142. Madry H, Zurakowski D, and Trippel SB. Overexpression of human insulin-like growth factor-I promotes new tissue formation in an ex vivo model of articular chondrocyte transplantation. *Gene Ther* 8: 1443-1449, 2001.
143. Malesud CJ, Killeen W, Hering TM, and Purchio AF. Enhanced sulfated-proteoglycan core protein synthesis by incubation of rabbit chondrocytes with recombinant transforming growth factor-beta 1. *J Cell Physiol* 149: 152-159, 1991.
144. Mankin HJ, and Lippiello L. Biochemical and metabolic abnormalities in articular cartilage from osteo-arthritic human hips. *The Journal of bone and joint surgery American volume* 52: 424-434, 1970.
145. Mankin HJ, and Lippiello L. The glycosaminoglycans of normal and arthritic cartilage. *The Journal of clinical investigation* 50: 1712-1719, 1971.
146. Mauck RL, Byers BA, Yuan X, and Tuan RS. Regulation of cartilaginous ECM gene transcription by chondrocytes and MSCs in 3D culture in response to dynamic loading. *Biomechanics and modeling in mechanobiology* 6: 113-125, 2007.

147. Mauck RL, Nicoll SB, Seyhan SL, Ateshian GA, and Hung CT. Synergistic action of growth factors and dynamic loading for articular cartilage tissue engineering. *Tissue Eng* 9: 597-611, 2003.
148. Mauck RL, Soltz MA, Wang CC, Wong DD, Chao PH, Valhmu WB, Hung CT, and Ateshian GA. Functional tissue engineering of articular cartilage through dynamic loading of chondrocyte-seeded agarose gels. *J Biomech Eng* 122: 252-260, 2000.
149. Merida-Velasco JA, Sanchez-Montesinos I, Espin-Ferra J, Merida-Velasco JR, Rodriguez-Vazquez JF, and Jimenez-Collado J. Development of the human knee joint ligaments. *The Anatomical record* 248: 259-268, 1997.
150. Mierisch CM, Anderson PC, Balian G, and Diduch DR. Treatment with insulin-like growth factor-1 increases chondrogenesis by periosteum in vitro. *Connect Tissue Res* 43: 559-568, 2002.
151. Minns RJ, and Steven FS. The collagen fibril organization in human articular cartilage. *J Anat* 123: 437-457, 1977.
152. Monnier VM, Kohn RR, and Cerami A. Accelerated age-related browning of human collagen in diabetes mellitus. *Proceedings of the National Academy of Sciences of the United States of America* 81: 583-587, 1984.
153. Moutos FT, Freed LE, and Guilak F. A biomimetic three-dimensional woven composite scaffold for functional tissue engineering of cartilage. *Nat Mater* 6: 162-167, 2007.
154. Mouw JK, Imler SM, and Levenston ME. Ion-channel regulation of chondrocyte matrix synthesis in 3D culture under static and dynamic

- compression. *Biomechanics and modeling in mechanobiology* 6: 33-41, 2007.
155. Mow VC, Kuei SC, Lai WM, and Armstrong CG. Biphasic creep and stress relaxation of articular cartilage in compression? Theory and experiments. *J Biomech Eng* 102: 73-84, 1980.
156. Muramatsu S, Wakabayashi M, Ohno T, Amano K, Ooishi R, Sugahara T, Shiojiri S, Tashiro K, Suzuki Y, Nishimura R, Kuhara S, Sugano S, Yoneda T, and Matsuda A. Functional gene screening system identified TRPV4 as a regulator of chondrogenic differentiation. *The Journal of biological chemistry* 282: 32158-32167, 2007.
157. Nagai R, Ikeda K, Kawasaki Y, Sano H, Yoshida M, Araki T, Ueda S, and Horiuchi S. Conversion of Amadori product of Maillard reaction to Nepsilon-(carboxymethyl)lysine in alkaline condition. *FEBS Lett* 425: 355-360, 1998.
158. Natoli R, Revell CM, and Athanasiou K. Chondroitinase ABC Treatment Results in Increased Tensile Properties of Self-Assembled Tissue Engineered Articular Cartilage. *Tissue Eng Part A* 15: 3119-3128, 2009.
159. Natoli RM, Responde DJ, Lu BY, and Athanasiou KA. Effects of multiple chondroitinase ABC applications on tissue engineered articular cartilage *Journal of Orthopaedic Research* 10.1002/jor.20821, 2009.
160. Natoli RM, Skaalure S, Bijlani S, Chen KX, Hu J, and Athanasiou KA. Intracellular Na(+) and Ca(2+) modulation increases the tensile properties

- of developing engineered articular cartilage. *Arthritis and rheumatism* 62: 1097-1107, 2010.
161. Ng KW, Mauck RL, Statman LY, Lin EY, Ateshian GA, and Hung CT. Dynamic deformational loading results in selective application of mechanical stimulation in a layered, tissue-engineered cartilage construct. *Biorheology* 43: 497-507, 2006.
162. Nixon AJ, Lillich JT, Burton-Wurster N, Lust G, and Mohammed HO. Differentiated cellular function in fetal chondrocytes cultured with insulin-like growth factor-I and transforming growth factor-beta. *J Orthop Res* 16: 531-541, 1998.
163. Ofek G, Revell CM, Hu JC, Allison DD, Grande-Allen KJ, and Athanasiou KA. Matrix development in self-assembly of articular cartilage. *PLoS ONE* 3: e2795, 2008.
164. Ong KL, Lau E, Suggs J, Kurtz SM, and Manley MT. Risk of subsequent revision after primary and revision total joint arthroplasty. *Clin Orthop Relat Res* 468: 3070-3076, 2010.
165. Oswald ES, Ahmed HS, Kramer SP, Bulinski JC, Ateshian GA, and Hung CT. Effects of Hypertonic (NaCl) Two-Dimensional and Three-Dimensional Culture Conditions on the Properties of Cartilage Tissue Engineered from an Expanded Mature Bovine Chondrocyte Source. *Tissue engineering Part C, Methods* 2011.
166. Otzen DE. Protein unfolding in detergents: effect of micelle structure, ionic strength, pH, and temperature. *Biophys J* 83: 2219-2230, 2002.

167. Palmer GD, Chao Ph PH, Raia F, Mauck RL, Valhmu WB, and Hung CT. Time-dependent aggrecan gene expression of articular chondrocytes in response to hyperosmotic loading. *Osteoarthritis and cartilage / OARS, Osteoarthritis Research Society* 9: 761-770, 2001.
168. Pei M, Solchaga LA, Seidel J, Zeng L, Vunjak-Novakovic G, Caplan AI, and Freed LE. Bioreactors mediate the effectiveness of tissue engineering scaffolds. *Faseb J* 16: 1691-1694, 2002.
169. Pfaffl MW. A new mathematical model for relative quantification in real-time RT-PCR. *Nucleic Acids Res* 29: 2002-2007, 2001.
170. Phan MN, Leddy HA, Votta BJ, Kumar S, Levy DS, Lipshutz DB, Lee SH, Liedtke W, and Guilak F. Functional characterization of TRPV4 as an osmotically sensitive ion channel in porcine articular chondrocytes. *Arthritis and rheumatism* 60: 3028-3037, 2009.
171. Plaas AH, Sandy JD, and Kimura JH. Biosynthesis of cartilage proteoglycan and link protein by articular chondrocytes from immature and mature rabbits. *The Journal of biological chemistry* 263: 7560-7566, 1988.
172. Platt JL, Fischel RJ, Matas AJ, Reif SA, Bolman RM, and Bach FH. Immunopathology of hyperacute xenograft rejection in a swine-to-primate model. *Transplantation* 52: 214-220, 1991.
173. Pritchard S, and Guilak F. The role of F-actin in hypo-osmotically induced cell volume change and calcium signaling in anulus fibrosus cells. *Annals of biomedical engineering* 32: 103-111, 2004.

174. Qi WN, and Scully SP. Effect of type II collagen in chondrocyte response to TGF-beta 1 regulation. *Exp Cell Res* 241: 142-150, 1998.
175. Quinn TM, Grodzinsky AJ, Buschmann MD, Kim YJ, and Hunziker EB. Mechanical compression alters proteoglycan deposition and matrix deformation around individual cells in cartilage explants. *J Cell Sci* 111: 573-583, 1998.
176. Ralphs JR, and Benjamin M. The joint capsule: structure, composition, ageing and disease. *Journal of anatomy* 184 (Pt 3): 503-509, 1994.
177. Rao JY, Hurst RE, Bales WD, Jones PL, Bass RA, Archer LT, Bell PB, and Hemstreet GP, 3rd. Cellular F-actin levels as a marker for cellular transformation: relationship to cell division and differentiation. *Cancer Res* 50: 2215-2220, 1990.
178. Reginato AM, Iozzo RV, and Jimenez SA. Formation of nodular structures resembling mature articular cartilage in long-term primary cultures of human fetal epiphyseal chondrocytes on a hydrogel substrate. *Arthritis Rheum* 37: 1338-1349, 1994.
179. Reginster JY. The prevalence and burden of arthritis. *Rheumatology (Oxford)* 41 Supp 1: 3-6, 2002.
180. Reginster JY, and Khaltsev NG. Introduction and WHO perspective on the global burden of musculoskeletal conditions. *Rheumatology (Oxford)* 41 Supp 1: 1-2, 2002.

181. Responde DJ, Natoli RM, and Athanasiou KA. Collagens of articular cartilage: structure, function, and importance in tissue engineering. *Critical reviews in biomedical engineering* 35: 363-411, 2007.
182. Revell CM, and Athanasiou KA. Success rates and immunologic responses of autogenic, allogenic, and xenogenic treatments to repair articular cartilage defects. *Tissue Eng Part B (In press)* 2009.
183. Revell CM, Reynolds CE, and Athanasiou KA. Effects of Initial Cell Seeding in Self Assembly of Articular Cartilage. *Ann Biomed Eng* 36: 1441-1448, 2008.
184. Roos EM, and Lohmander LS. The Knee injury and Osteoarthritis Outcome Score (KOOS): from joint injury to osteoarthritis. *Health Qual Life Outcomes* 1: 64, 2003.
185. Rosario DJ, Reilly GC, Ali Salah E, Glover M, Bullock AJ, and Macneil S. Decellularization and sterilization of porcine urinary bladder matrix for tissue engineering in the lower urinary tract. *Regen Med* 3: 145-156, 2008.
186. Rosen DM, Stempien SA, Thompson AY, and Seyedin SM. Transforming growth factor-beta modulates the expression of osteoblast and chondroblast phenotypes in vitro. *J Cell Physiol* 134: 337-346, 1988.
187. Rosenberg L. Chemical basis for the histological use of safranin O in the study of articular cartilage. *J Bone Joint Surg Am* 69-82, 1971.
188. Roughley PJ, and Lee ER. Cartilage proteoglycans: structure and potential functions. *Microsc Res Tech* 28: 385-397, 1994.

189. Roy R, Boskey A, and Bonassar LJ. Processing of type I collagen gels using nonenzymatic glycation. *Journal of biomedical materials research Part A* 93: 843-851, 2010.
190. Roy R, Boskey AL, and Bonassar LJ. Non-enzymatic glycation of chondrocyte-seeded collagen gels for cartilage tissue engineering. *Journal of orthopaedic research : official publication of the Orthopaedic Research Society* 26: 1434-1439, 2008.
191. Sah RL, Kim YJ, Doong JY, Grodzinsky AJ, Plaas AH, and Sandy JD. Biosynthetic response of cartilage explants to dynamic compression. *J Orthop Res* 7: 619-636, 1989.
192. Sah RL, Trippel SB, and Grodzinsky AJ. Differential effects of serum, insulin-like growth factor-I, and fibroblast growth factor-2 on the maintenance of cartilage physical properties during long-term culture. *J Orthop Res* 14: 44-52, 1996.
193. Salminen H, Perala M, Lorenzo P, Saxne T, Heinegard D, Saamanen AM, and Vuorio E. Up-regulation of cartilage oligomeric matrix protein at the onset of articular cartilage degeneration in a transgenic mouse model of osteoarthritis. *Arthritis Rheum* 43: 1742-1748, 2000.
194. Sanchez JC, Danks TA, and Wilkins RJ. Mechanisms involved in the increase in intracellular calcium following hypotonic shock in bovine articular chondrocytes. *Gen Physiol Biophys* 22: 487-500, 2003.

195. Sanchez JC, and Wilkins RJ. Changes in intracellular calcium concentration in response to hypertonicity in bovine articular chondrocytes. *Comp Biochem Physiol A Mol Integr Physiol* 137: 173-182, 2004.
196. Sanchez JC, and Wilkins RJ. Effects of hypotonic shock on intracellular pH in bovine articular chondrocytes. *Comp Biochem Physiol A Mol Integr Physiol* 135: 575-583, 2003.
197. Schnabel M, Marlovits S, Eckhoff G, Fichtel I, Gotzen L, Vecsei V, and Schlegel J. Dedifferentiation-associated changes in morphology and gene expression in primary human articular chondrocytes in cell culture. *Osteoarthritis Cartilage* 10: 62-70, 2002.
198. Schneiderbauer MM, Dutton CM, and Scully SP. Signaling "cross-talk" between TGF-beta1 and ECM signals in chondrocytic cells. *Cell Signal* 16: 1133-1140, 2004.
199. Schumacher BL, Block JA, Schmid TM, Aydelotte MB, and Kuettner KE. A novel proteoglycan synthesized and secreted by chondrocytes of the superficial zone of articular cartilage. *Arch Biochem Biophys* 311: 144-152, 1994.
200. Schwartz MH, Leo PH, and Lewis JL. A microstructural model for the elastic response of articular cartilage. *J Biomech* 27: 865-873, 1994.
201. Scott CC, Luttge A, and Athanasiou KA. Development and validation of vertical scanning interferometry as a novel method for acquiring chondrocyte geometry. *J Biomed Mater Res A* 72: 83-90, 2005.

202. Segal S, and Foley J. The metabolism of D-ribose in man. *The Journal of clinical investigation* 37: 719-735, 1958.
203. Sekiya I, Vuoristo JT, Larson BL, and Prockop DJ. In vitro cartilage formation by human adult stem cells from bone marrow stroma defines the sequence of cellular and molecular events during chondrogenesis. *Proc Natl Acad Sci U S A* 99: 4397-4402, 2002.
204. Shakibaei M, John T, De Souza P, Rahmanzadeh R, and Merker HJ. Signal transduction by beta1 integrin receptors in human chondrocytes in vitro: collaboration with the insulin-like growth factor-I receptor. *Biochem J* 342: 615-623, 1999.
205. Sharif M, Saxne T, Shepstone L, Kirwan JR, Elson CJ, Heinegard D, and Dieppe PA. Relationship between serum cartilage oligomeric matrix protein levels and disease progression in osteoarthritis of the knee joint. *Br J Rheumatol* 34: 306-310, 1995.
206. Shieh AC, and Athanasiou KA. Biomechanics of single chondrocytes and osteoarthritis. *Crit Rev Biomed Eng* 30: 307-343, 2002.
207. Shieh AC, and Athanasiou KA. Biomechanics of single zonal chondrocytes. *J Biomech* 39: 1595-1602, 2006.
208. Shieh AC, and Athanasiou KA. Biomechanics of single zonal chondrocytes. *J Biomech* 2005.
209. Shieh AC, and Athanasiou KA. Biomechanics of single zonal chondrocytes. *J Biomech* In Press, 2006.

210. Shieh AC, and Athanasiou KA. Dynamic compression of single cells. *Osteoarthritis Cartilage* 15: 328-334, 2007.
211. Shieh AC, Koay EJ, and Athanasiou KA. Strain-dependent recovery behavior of single chondrocytes. *Biomech Model Mechanobiol* 5: 172-179, 2006.
212. Shimizu M, Minakuchi K, Kaji S, and Koga J. Chondrocyte migration to fibronectin, type I collagen, and type II collagen. *Cell Struct Funct* 22: 309-315, 1997.
213. Shin D, and Athanasiou K. Cytoindentation for obtaining cell biomechanical properties. *J Orthop Res* 17: 880-890, 1999.
214. Smith KD, Vaughan-Thomas A, Spiller DG, Innes JF, Clegg PD, and Comerford EJ. The organisation of elastin and fibrillins 1 and 2 in the cruciate ligament complex. *Journal of anatomy* 218: 600-607, 2011.
215. Smith RL, Lin J, Trindade MC, Shida J, Kajiyama G, Vu T, Hoffman AR, van der Meulen MC, Goodman SB, Schurman DJ, and Carter DR. Time-dependent effects of intermittent hydrostatic pressure on articular chondrocyte type II collagen and aggrecan mRNA expression. *J Rehabil Res Dev* 37: 153-161, 2000.
216. Smith RL, Rusk SF, Ellison BE, Wessells P, Tsuchiya K, Carter DR, Caler WE, Sandell LJ, and Schurman DJ. In vitro stimulation of articular chondrocyte mRNA and extracellular matrix synthesis by hydrostatic pressure. *J Orthop Res* 14: 53-60, 1996.

217. Sneddon I. The relaxation between load and penetration in the axisymmetric Boussinesq problem for a punch of arbitrary profile. *Int J Eng Sci* 47-57, 1965.
218. Soltz MA, and Ateshian GA. Interstitial fluid pressurization during confined compression cyclical loading of articular cartilage. *Annals of biomedical engineering* 28: 150-159, 2000.
219. Soohoo NF, Tang EY, Krenek L, Eagan M, and McGlynn E. Variations in the quality of care delivered to patients undergoing total knee replacement at 3 affiliated hospitals. *Orthopedics* 34: 356, 2011.
220. Stapleton TW, Ingram J, Katta J, Knight R, Korossis S, Fisher J, and Ingham E. Development and characterization of an acellular porcine medial meniscus for use in tissue engineering. *Tissue Eng Part A* 14: 505-518, 2008.
221. Tanimori S, Fukubayashi K, and Kiriata M. Synthesis of the spirosuccinimide moiety of Asperparaline A. *Biosci Biotechnol Biochem* 64: 1758-1760, 2000.
222. Tew SR, Peffers MJ, McKay TR, Lowe ET, Khan WS, Hardingham TE, and Clegg PD. Hyperosmolarity regulates SOX9 mRNA posttranscriptionally in human articular chondrocytes. *Am J Physiol Cell Physiol* 297: C898-906, 2009.
223. Tew SR, Vasieva O, Peffers MJ, and Clegg PD. Post-transcriptional gene regulation following exposure of osteoarthritic human articular

- chondrocytes to hyperosmotic conditions. *Osteoarthritis and cartilage / OARS, Osteoarthritis Research Society* 19: 1036-1046, 2011.
224. Trickey TR, Lee M, and Guilak T. Viscoelastic properties of chondrocytes from normal and osteoarthritic human cartilage. *J Orthop Res* 18: 891-898, 2000.
225. Trickey WR, Vail TP, and Guilak F. The role of the cytoskeleton in the viscoelastic properties of human articular chondrocytes. *J Orthop Res* 22: 131-139, 2004.
226. Urban JP, Hall AC, and Gohl KA. Regulation of matrix synthesis rates by the ionic and osmotic environment of articular chondrocytes. *Journal of cellular physiology* 154: 262-270, 1993.
227. Van Eijk F, Saris DB, Riesle J, Willems WJ, Van Blitterswijk CA, Verbout AJ, and Dhert WJ. Tissue engineering of ligaments: a comparison of bone marrow stromal cells, anterior cruciate ligament, and skin fibroblasts as cell source. *Tissue Eng* 10: 893-903, 2004.
228. van Susante JL, Buma P, van Beuningen HM, van den Berg WB, and Veth RP. Responsiveness of bovine chondrocytes to growth factors in medium with different serum concentrations. *J Orthop Res* 18: 68-77, 2000.
229. Vunjak-Novakovic G, Martin I, Obradovic B, Treppo S, Grodzinsky AJ, Langer R, and Freed LE. Bioreactor cultivation conditions modulate the composition and mechanical properties of tissue-engineered cartilage. *J Orthop Res* 17: 130-138, 1999.

230. Walsh CJ, Goodman D, Caplan AI, and Goldberg VM. Meniscus regeneration in a rabbit partial meniscectomy model. *Tissue Eng* 5: 327-337, 1999.
231. Wang L, Almqvist KF, Veys EM, and Verbruggen G. Control of extracellular matrix homeostasis of normal cartilage by a TGFbeta autocrine pathway. Validation of flow cytometry as a tool to study chondrocyte metabolism in vitro. *Osteoarthritis Cartilage* 10: 188-198, 2002.
232. Wang N, Butler JP, and Ingber DE. Mechanotransduction across the cell surface and through the cytoskeleton. *Science* 260: 1124-1127, 1993.
233. Wang N, and Ingber DE. Control of cytoskeletal mechanics by extracellular matrix, cell shape, and mechanical tension. *Biophys J* 66: 2181-2189, 1994.
234. Wilkins RJ, Browning JA, and Urban JP. Chondrocyte regulation by mechanical load. *Biorheology* 37: 67-74, 2000.
235. Williamson AK, Chen AC, Masuda K, Thonar EJ, and Sah RL. Tensile mechanical properties of bovine articular cartilage: variations with growth and relationships to collagen network components. *J Orthop Res* 21: 872-880, 2003.
236. Williamson AK, Masuda K, Thonar EJ, and Sah RL. Growth of immature articular cartilage in vitro: correlated variation in tensile biomechanical and collagen network properties. *Tissue Eng* 9: 625-634, 2003.

237. Woessner JF, Jr. The determination of hydroxyproline in tissue and protein samples containing small proportions of this imino acid. *Arch Biochem Biophys* 93: 440-447, 1961.
238. Woessner JF, Jr. The determination of hydroxyproline in tissue and protein samples containing small proportions of this imino acid. *Archives of biochemistry and biophysics* 93: 440-447, 1961.
239. Wong M, Wuethrich P, Buschmann MD, Egli P, and Hunziker E. Chondrocyte biosynthesis correlates with local tissue strain in statically compressed adult articular cartilage. *J Orthop Res* 15: 189-196, 1997.
240. Wong M, Wuethrich P, Egli P, and Hunziker E. Zone-specific cell biosynthetic activity in mature bovine articular cartilage: a new method using confocal microscopic stereology and quantitative autoradiography. *J Orthop Res* 14: 424-432, 1996.
241. Woo SL, Debski RE, Zeminski J, Abramowitch SD, Saw SS, and Fenwick JA. Injury and repair of ligaments and tendons. *Annu Rev Biomed Eng* 2: 83-118, 2000.
242. Woods T, and Gratzer PF. Effectiveness of three extraction techniques in the development of a decellularized bone-anterior cruciate ligament-bone graft. *Biomaterials* 26: 7339-7349, 2005.
243. Wu JZ, and Herzog W. Elastic anisotropy of articular cartilage is associated with the microstructures of collagen fibers and chondrocytes. *J Biomech* 35: 931-942, 2002.

244. Yaeger PC, Masi TL, de Ortiz JL, Binette F, Tubo R, and McPherson JM. Synergistic action of transforming growth factor-beta and insulin-like growth factor-I induces expression of type II collagen and aggrecan genes in adult human articular chondrocytes. *Exp Cell Res* 237: 318-325, 1997.
245. Yellowley CE, Hancox JC, and Donahue HJ. Effects of cell swelling on intracellular calcium and membrane currents in bovine articular chondrocytes. *Journal of cellular biochemistry* 86: 290-301, 2002.
246. Yellowley CE, Jacobs CR, and Donahue HJ. Mechanisms contributing to fluid-flow-induced Ca²⁺ mobilization in articular chondrocytes. *Journal of cellular physiology* 180: 402-408, 1999.
247. Zanasi S. Innovations in total knee replacement: new trends in operative treatment and changes in peri-operative management. *Eur Orthop Traumatol* 2: 21-31, 2011.
248. Zaucke F, Dinser R, Maurer P, and Paulsson M. Cartilage oligomeric matrix protein (COMP) and collagen IX are sensitive markers for the differentiation state of articular primary chondrocytes. *Biochem J* 358: 17-24, 2001.